EPA-600/2-77-132
July 1977

Environmental Protection Technology Series

GENERATION OF FUMES SIMULATING PARTICULATE AIR POLLUTANTS

Industrial Environmental Research Laboratory
Office of Research and Development
U.S. Environmental Protection Agency
Research Triangle Park, North Carolina 27711

RESEARCH REPORTING SERIES

Research reports of the Office of Research and Development, U.S. Environmental Protection Agency, have been grouped into five series. These five broad categories were established to facilitate further development and application of environmental technology. Elimination of traditional grouping was consciously planned to foster technology transfer and a maximum interface in related fields. The five series are:

1. Environmental Health Effects Research
2. Environmental Protection Technology
3. Ecological Research
4. Environmental Monitoring
5. Socioeconomic Environmental Studies

This report has been assigned to the ENVIRONMENTAL PROTECTION TECHNOLOGY series. This series describes research performed to develop and demonstrate instrumentation, equipment, and methodology to repair or prevent environmental degradation from point and non-point sources of pollution. This work provides the new or improved technology required for the control and treatment of pollution sources to meet environmental quality standards.

EPA REVIEW NOTICE

This report has been reviewed by the U.S. Environmental Protection Agency, and approved for publication. Approval does not signify that the contents necessarily reflect the views and policy of the Agency, nor does mention of trade names or commercial products constitute endorsement or recommendation for use.

This document is available to the public through the National Technical Information Service, Springfield, Virginia 22161.

EPA-600/2-77-132
July 1977

GENERATION OF FUMES SIMULATING PARTICULATE AIR POLLUTANTS

by

J.W. Carroz, F.K. Odencrantz, and W.G. Finnegan

Research Department
Naval Weapons Center
China Lake, California 93555

EPA Interagency Agreement IAG-D5-0669
Program Element No. 1AB012
ROAP No. 21ADM-031

EPA Project Officer: Dennis C. Drehmel

Industrial Environmental Research Laboratory
Office of Energy, Minerals, and Industry
Research Triangle Park, N.C. 27711

Prepared for

U.S. ENVIRONMENTAL PROTECTION AGENCY
Office of Research and Development
Washington, D.C. 20460

DISCLAIMER

This report has been reviewed by the Industrial & Environmental Research Laboratory, U.S. Environmental Protection Agency, and approved for publication. Approval does not signify that the contents necessarily reflect the views and policies of the U.S. Environmental Protection Agency, nor does mention of trade names or commercial products constitute endorsement or recommendation for use.

FOREWORD

This project was undertaken to develop techniques for generation of large quantities of reproducible, stable, inorganic, fine solid particle aerosol fumes which are required for testing industrial pollution control apparatus. Aerosols were generated to simulate the effluents from combustion of pulverized coal, zinc smelters, and arc and basic oxygen furnaces.

This work was performed at Naval Weapons Center and funded by the Environmental Protection Agency under Interagency Agreement EPA-1AG-D5-0669.

ABSTRACT

This project supported the EPA stationary industrial pollution control program. Techniques were developed for generating large quantities of reproducible, stable, inorganic, solid particulate, fine particle aerosol fumes. The aerosols were generated by burning flammable solutions containing appropriate soluble compounds (nitrates, for example) of the desired elements. In the flame these compounds decomposed to oxides. Particle size determinations were made using scanning and transmission electron microscope (SEM and TEM) photographic analysis of captured particles and Whitby and Royco aerosol analyzers. Particle sizes from 0.0075 to 10 micrometers and concentrations up to 10^{10} particles per cm^3 were measured. Particle compositions were determined by X-ray diffraction, SEM X-ray non-dispersive and cyclotron excitation analyses. A dynamic aerosol diluter was designed to reduce the aerosol particle concentrations by a factor as large as 38,700 so that the Whitby and Royco aerosol analyzers would not become saturated. The generated aerosol flow rates were as high as 42 m^3 per minute (148 cfm); the particle loadings were as high as 16.8 g per m^3 @ STP. For most aerosols the aerosol particle and condensation nuclei concentrations were of the order of 10^9 particles per cm^3. The aerosol volume median diameters varied from less than 0.015 to greater than 4.7 μm and were primarily a function of the solution ingredients.

The particle counts of the Whitby and Royco were compared. In the overlap range of these instruments, the ratio of the Whitby counts to those of the Royco varied from 0.68 to 343! For a coal fly ash simulation aerosol, the particle counts of the EAA and Royco were compared with cascade impactor (Lundgren and Celesco) measurements.

Particle loadings (g/m^3) were determined from the instrument particle counts and also from the generation rates. A comparison of the loadings shows that for some of the generated aerosols the loadings measured by the Whitby were significantly higher than the loadings determined from the generation rates.

Electron microscopic pictures (SEM and TEM) of precipitated particles show that many of the larger particles (20 μm) are hollow and that the smaller particles (0.01 μm) are in chain aggregates.

Special aerosols were generated to simulate the fine particulate effluents generated by combustion of pulverized coal (electricity generation) electric arc and basic oxygen furnaces (iron and steel production) and zinc smelters. Methods were developed to vary the sulfur dioxide concentration and the particle resistivities. The generation technique can be used to generate aerosols of many different oxides and chlorides.

This work was funded by Interagency Agreement EPA-1AG-D5-0669 between NWC and the EPA. It began in January 1975 and ended May 1977.

CONTENTS

FIGURES

FIGURES (continued)

FIGURES (Continued)

TABLES

TABLES (continued)

ACKNOWLEDGMENT

The cascade impactor measurements by Dr. Raymond L. Chuan; constructive criticism of a preliminary diluter design by Professor Kenneth T. Whitby; advice on the simulation of industrial effluents by Drs. Dennis C. Drehmel and James H. Abbott; guidance on particle measurements by Dr. Edward E. Hindman II, and the leadership of Dr. Pierre St.-Amand are gratefully acknowledged.

SECTION 1

INTRODUCTION

Particles smaller than 5 μm (fine particles) can penetrate the human nasal cavity and enter the lungs. Fine particles remain airborne for long periods because they are too small to rapidly settle to the ground. Thus, the potential hazard of these particles as an air pollutant is greater than that of larger particles.

Pollution abatement equipment is available for collecting large particles (D>5μ). Conventional technology can be used to control primary fine particle emissions (Drehmel, 1976a). When the resistivity of the particles is about 10^{10} ohm-cm, some electrostatic precipitators collect 90% of the particles at all size ranges. The collection efficiency of electrostatic precipitators, however, depends on the particle electrical resistivity. Since electrostatic precipitators are the most common particulate control devices in power production and since western low sulfur coals produce a significantly higher resistivity fly ash, the low sulfur coals will make it more difficult to conform to particulate emission standards for utility boilers with standard equipment (Drehmel, (1976b). Fabric filters can collect 95% of the particles at all size ranges and do not depend on particle resistivity. There are possibilities for improvements in all precipitators and filters. Emerging technology should improve the collection and reduce operating costs.

The Environmental Protection Agency needs stable sources of well-characterized solid particulate, fine particle aerosols (fumes) for laboratory pilot plant tests of pollution abatement equipment. To provide this, we have conducted a research program on the continuous generation of inorganic solid, fine particulate aerosols (fumes). These aerosols are intended to simulate the fine particulate effluents generated by combustion of pulverized coal for electricity generation, electric arc and basic oxygen furnaces, and zinc smelters. Only the fine particle (D<3μm) portion of the effluents were to be simulated. For coal fly ash simulation aerosols, the particle electrical resistivity was to be variable over a wide range.

The aerosols were generated by burning flammable solutions containing appropriate soluble compounds (nitrates, for example) of the desired elements. In the flame these compounds decomposed to oxides. Particle size determinations were made using scanning and transmission electron microscope (SEM and TEM) photographic analysis of captured particles and Whitby and Royco aerosol analyzers. Particle sizes from 0.0075 to 10 micrometers and concentrations up to 10^{16} particles per cubic meter could be measured. Particle compositions were determined by X-ray diffraction, SEM X-ray non-dispersive and cyclotron excitation analyses.

This work was funded by Interagency Agreement EPA-1AG-D5-0669 between NWC and the EPA. It began in January 1975 and ended April 1977.

SECTION 2

CONCLUSIONS AND RECOMMENDATIONS

The program objective of developing reproducible stable sources of well-characterized solid particulate, fine particle aerosols for laboratory pilot plant tests of pollution abatement equipment was accomplished. The materials and the techniques used in this simulation aerosol project are flexible; many thousand different aerosols can be made by choosing ingredients, dissolving them in a flammable solvent, and burning them in the aerosol generation apparatus. It will be possible to generate aerosols with a wide variety of properties to meet specific test requirements.

The most useful aerosols are those comprised of a single compound because all of the particles have many of the same properties (density, resistivity, etc.) and this will simplify test analyses. By using several different simple aerosols in separate tests, it should be possible to discover and determine the basic principles and parameters concerning pollution abatement equipment. Because of analytical difficulties, using complex aerosols comprised of a variety of chemical compounds will not yield conclusive results.

The analysis of the results showed that for some aerosols the particle mass loadings determined from the Whitby Aerosol Analyzer (EAA) were significantly higher than the particle loadings determined from the generation rates. This finding is important if EAA counts are to be used to determine aerosol particle mass loadings.

SECTION 3

CHARACTERISTICS OF EFFLUENTS

COAL FLY ASH

The characteristics of pulverized coal fly-ash and other coal fly-ash vary widely. The type of coal, the plant and the pollution control devices all affect the characteristics of the fly ash samples collected. Most analyses to determine the characteristics of fly ash have been conducted with samples of ash collected by pollution control devices. This material usually contains coarse particles. There is a need for more analysis of samples containing only the fine particles.

Table 1 (Vandegrift et al., 1971) shows the characteristics of pulverized coal fly-ash. Note the great variability in properties of different ashes. The characteristics of the fine particles may not be the same as those shown in Table 1 where 75% of the mass is larger than 5 μm.

Luke (1961) characterized a fly ash sample taken from a hopper of an electrostatic precipitator. The ash contained 79% glass, 6% magnetite-hematite and 4% carbon particles. His X-ray diffraction results showed magnetite (Fe_3O_4) the most abundant crystalline component, hematite (Fe_2O_3) second, and quartz (SiO_2) third. Trace amounts of mullite ($3Al_2O_3 \cdot 2SiO_2$), calcite ($CaCO_3$) and anhydrite ($CaSO_4$) were found.

Harvey (1971) measured the fly ash from boiler number 10 of the TVA plant in Paducah, Kentucky. He separated the ash into non-magnetic and magnetic fractions. An X-ray diffraction analysis of the non-magnetic fraction (48% of ash) was high in quartz, medium in lime and low in portlandite ($Ca(OH)_2$) and anhydrite. The analysis of the magnetic fraction was high in magnetite, medium in hematite and low in periclase (MgO). The chemical analysis of the fly ash showed 39% SiO_2, 16% Al_2O_3, 32% Fe_2O_3, 11% CaO, 2% others.

Yakowitz et al. (1972) analyzed fly ash particles taken from the area of an electric power plant in Minneapolis, Minnesota, by means of combined electron microscopy and X-ray micro-analysis. For the most part, the fly ash consisted of nearly spherical particles ranging in size from 0.5 to 3 μm or more in diameter. The elements in the ash particles were silicon, aluminum, calcium, iron, potassium, magnesium and titanium, listed in decreasing order of abundance within the particles. The spherical particles did not vary significantly in composition as a function of size.

TABLE 1. PULVERIZED COAL COMBUSTION EFFLUENT (ELECTRICITY GENERATION), reprinted with permission from Vandegrift, 1971, p. 53.

Particle size (wt.% < size, μm) - 15<3, 25<5, 42<10, 65<20, 81<40

Solids loading (g/m^3) - 2.3 - 12.8 (mean 7.6)

Chemical composition (Wt.%) -

SiO_2	17-64	(average 43)
Fe_2O_3	2-36	(15)
Al_2O_3	9-58	(24)
CaO	0.1-22	(4)
MgO	0.1-5	(1.0)
Na_2O	0.3-4	(0.9)

Bulk density - .48-.8 (g/cm^3)

Particle density - 0.6-3.0 (average 2.3)

Electrical resistivity - 10^8-10^{13} ohm.cm

Moisture content - 0.23 wt.%

Carrier Gas

Temperature - 121-157°C

Moisture content - 5.9-8.0 Vol.%

Chemical composition (Vol.%) -

CO_2	12.5-14.9
O_2	4.2-6.6
N_2	Balance
CO	5-69 ppm
NO_x	161-526 ppm
SO_2	1080-1780 ppm
SO_3	3-66ppm

X-ray diffraction results of Cavin et al. (1974) revealed the mineral content of the fly ash they measured to be primarily mullite with the presence of hematite, magnetite, quartz and gypsum.

Davison et al. (1974) measured the elemental composition of several size fractions of fly ash. Two types of fly ash are represented; (a) fly ash retained in a cyctonic precipitation system, and (b) airborne fly ash collected in the ducting about 3 m from the base of the stack with an Anderson stack sampler. Table 2 shows the results of these measurements.

Sem (1975) measured the size distribution of airborne particles from 1.0 to less than 0.01 μm diameter at the Nucla, Colorado, power plant. The results of Sem are shown in modified form in Figure 1 with his permission. In Sem (1975), the volume distribution is reported as $\mu m^3/m^3$ since a considerable unknown fraction of the volume was above 1 μm. Figure 1 shows the volume distribution of only the submicron particles upstream of the baghouse as measured on November 12, 1975.

Shen et al. (1977) characterized the emissions from a coal-fired power plant with an electrostatic precipitator. They found about 35% by mass of the particulates emitted were less than 3 μm (measured with an Anderson stack cascade impactor). The major elements emitted were Fe, Ti, Si, S, K, Ca. These emissions do not contain as much aluminum as the airborne fly ash measured by Davison (see Table 2).

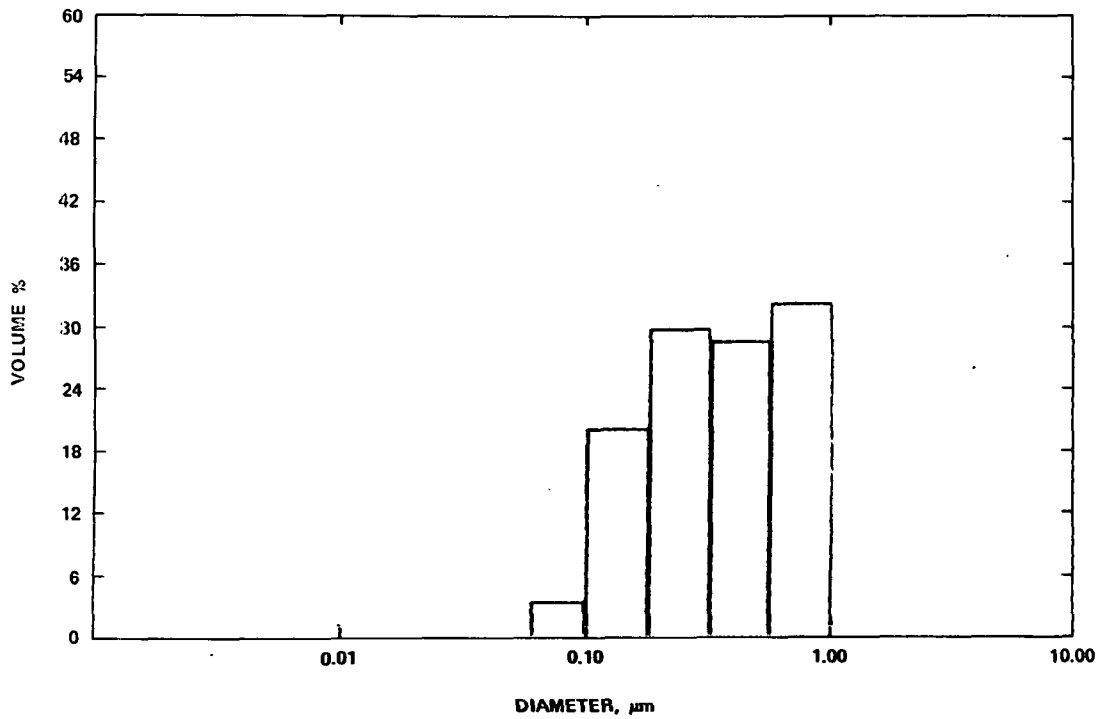

Figure 1. Airborne fly ash volume distribution of the submicron particles upstream of the baghouse at the Nucla Power Plant.

TABLE 2. ELEMENTAL COMPOSITION, reprinted with permission from Environmental Science & Technology, 1974 by Davison. Copyright by the American Chemical Society.

A. Fly Ash Retained in Plant

Sieved fractions

Particle diameter, μm	Fe,wt.%	Si,wt.%	Mg,wt.%	C,wt.%	S,wt.%	Al,wt.%
>74	...	...	...	...	...	...
44-74	18	18	0.39	11	1.3	9.4
Aerodynamically sized fractions						
>40	50	3.0	0.02	0.12	<0.01	1.3
30-40	18	14	0.31	0.21	0.01	6.9
20-30	...	...	...	0.63	...	...
15-20	...	...	...	2.5	...	...
10-15	6.6	19	0.16	6.6	4.4	9.8
5-10	8.6	26	0.39	5.5	7.8	13
<5	...	...	...	...	...	...
B. Airborne Fly Ash						
>11.3	13	34	0.89	0.66	8.3	19.7
7.3-11.3	...	...	...	0.70	...	...
4.7-7.3	12	27	0.95	0.62	7.9	16.2
3.3-4.7	...	...	...	0.57	...	...
2.06-3.3	17	35	1.4	0.81	25	21.0
1.06-2.06	...	...	...	0.61	...	...
0.65-1.06	15	23	0.19	...	48.8	9.8

OTHER EFFLUENTS

Table 3 (Vandegrift et al., 1971) shows that the characteristics of the fumes from electric arc furnaces vary a great deal. The mass median diameters of several electric arc furnace fumes have been measured (unknown author, 1974); these diameters ranged from 0.3 to 5.4 μm.

Table 4 (Vandegrift et al., 1971) shows the characteristics of the fumes from basic oxygen furnaces. The number median diameter of the fume is 0.012. At a solids loading of 10 g/m^3, there would be $3x10^{18}$ particles/m^3 (using a particle density of 3.44 g/cm^3)!

Harris and Drehmel (1973) measured the solids loading of various sized aerosol particles of zinc smelters using a Brink impactor. Table 5 shows their results. Table 6 (Vandegrift et al., 1971) shows the characteristics of the fumes from zinc smelters.

TABLE 3. ELECTRIC ARC FURNACE EFFLUENT (NO OXYGEN LANCE), reprinted with permission from Vandegrift, 1971, p. 123 and 126.

Particle size (wt%<size, μm) - highly variable, generaly 60<5, BAHCO analysis: 68<5, 84<10, 95<20, 99<40

Solids loading (g/m^3) - 0.2 to 5.

Chemical composition (wt %) - dependent on nature of charge

Fe_2O_3	19-44	ZnO	0-44
FeO	4-10	CuO	0-1
Cr_2O_3	0-12	NiO	0-3
SiO_2	2-9	PbO	0-4
Al_2O_3	1-13	C	2-4
CaO	5-22	Alkalies	1-11
MgO	2-15	S	0-1
MnO	3-12	P	0-1

Particle density (g/cm^3) - 3.8-3.9

Electrical properties (ohm·cm) - $6x10^5$ - $6.6x10^{13}$

Carrier Gas

Temperature - 100-1650°C depending on use of cooling techniques

Moisture content - 0.045 g/g dry gas

Chemical composition (Vol. %) - mainly CO_2, CO, O_2, and N_2 - composition varies with operating practice.

TABLE 4. BASIC OXYGEN FURNACE EFFLUENT, reprinted with permission from Vandegrift, 1971, p. 123 & 126.

Particle size (wt %<size, μm) - 85-95<1 (number median diameter 0.012, mass median diameter 0.095)

Solids loading (g/m^3) - 4.6 to 23

Chemical composition (wt %) -

Fe_2O_3	90
FeO	1.5
MnO	0.4-1.5
SiO_2	1.3-2.0
Al_2O_3	0.2
CaO	3-5
MgO	0.6-1.1

Particle density - 3.44 (g/m^3)

Carrier Gas

Temperature - 290-1650°C depending on utilization of waste heat

Chemical composition (Vol. %) -

	Before combustion with aspirated air	After combustion with aspirated air
CO_2	5-16	0.7-13.5
CO	74-91	0-0.3
N_2	3-8	74-78.9
O_2	- - -	balance

TABLE 5. ZINC ROASTER & SINTERING MACHINE CONDITIONS AT PRECIPITATOR, reprinted with permission from Harris and Drehmel, 1973.

Particle Size μm	Roaster g/m^3	g/m^3	Sintering Machine g/m^3
	Test 1	Test 2	Test 3
>3.1	0	0	0.1747
1.8-3.1	0.0032	0	0.2817
1.25-1.8	0.0032	0.0016	0.6594
0.62-1.25	0.0708	0.0142	0.9820
0.38-0.62	0.1904	0.0960	0.6279
<0.38	0.0551	0.0730	0.6720

TABLE 6. ZINC ROASTER & SINTER MACHINE EFFLUENT, reprinted with permission from Vandegrift, 1971, p. 263-265.

Particle size (wt%<size μm) - Roaster: 14<5, 31<10, 70<20

Sinter Machine: 100<10

Solids loading (g/m^3) - Roaster: 12 - 150

Sinter Machine: 0.9 - 10

Chemical composition (wt%) - Sinter Machine: ZnO 5 - 25

PbO 30 - 55

CdO 2 - 15

The chemical compositions given by Vandegrift were assumed to be for oxides.

Carrier Gas

Temperature - 160 - 482°C

Chemical composition (Vol. %) - SO_2 0.7 - 13

O_2, N_2, CO_2 and H_2O Balance

SECTION 4

METHOD OF GENERATION

Solution-burning aerosol generators used for weather modification field experiments (Carroz, 1972) have been modified to dispense metal oxides. Flammable solutions of appropriate chemicals were made. The solutions were put into a heavy walled, stainless steel tank, pressurized with nitrogen gas, and, using standard industrial nozzles of the proper type and size, atomized into aerosol droplets. The aerosol droplets were burned to produce predominantly submicron particles of metal oxides by high temperature decomposition and/or vaporization of the chemicals. The hot gaseous products of combustion, together with excess air, greatly reduce agglomeration of the aerosol particles.

HARDWARE

Figures 2 and 3 and Photographs 1 and 2 show the aerosol generator and stacks. The larger diameter stack shown in Figure 2 was used for pulverized coal effluent simulation. The smaller diameter stack (Figure 3) was used for the other simulations. For some aerosols, a reducer was used at the top of the stack to decrease the draft and to increase the particle loadings. The gas line pressurizes the pressure tank at 1.4 MPa (200 psi). Several sizes of pressure tanks have been used, as small as 1 liter and as large as 38 liters. The tanks were fabricated from No. 316 stainless steel. The valve located between the tank and the nozzle was used to turn the flow on and off. The nozzle is an industrial solid cone nozzle with a 30^{o} spray angle. The flow rate of solution through the nozzle is about 5.9×10^{-6} cubic meters per second (A Delavan Corp. Type WDB 4.0, 30^{o}, stainless steel nozzle is satisfactory). The flow rate depends on the solution being sprayed.

The flame cone (see Figure 2) consists of a perforated metal cone, 0.60 m high, with a 0.26 m diameter at the top and a 25 mm diameter at the bottom. The cone is perforated with several 25 mm diameter holes. The flameholder consists of a 0.25 m diameter, 0.50 m high sheet metal stove pipe.

The large diameter stack is 0.425 m in diameter and is 3.05 m high. Ambient air is used to cool the combustion products coming out of the flame holder. Jets of air were used to insure adequate mixing of the generated aerosol fume and ambient air. There are four jets evenly spaced at the bottom edge of the stack. The 1 mm inside diameter jets are about 45^{o} from the horizontal plane; they were supplied with air at 210 KPa (30 psi). The small diameter stack is 0.25 m in diameter and 3.5 m high. It does not require air jets. When the reducer was used, the diameter was reduced to 0.15 m.

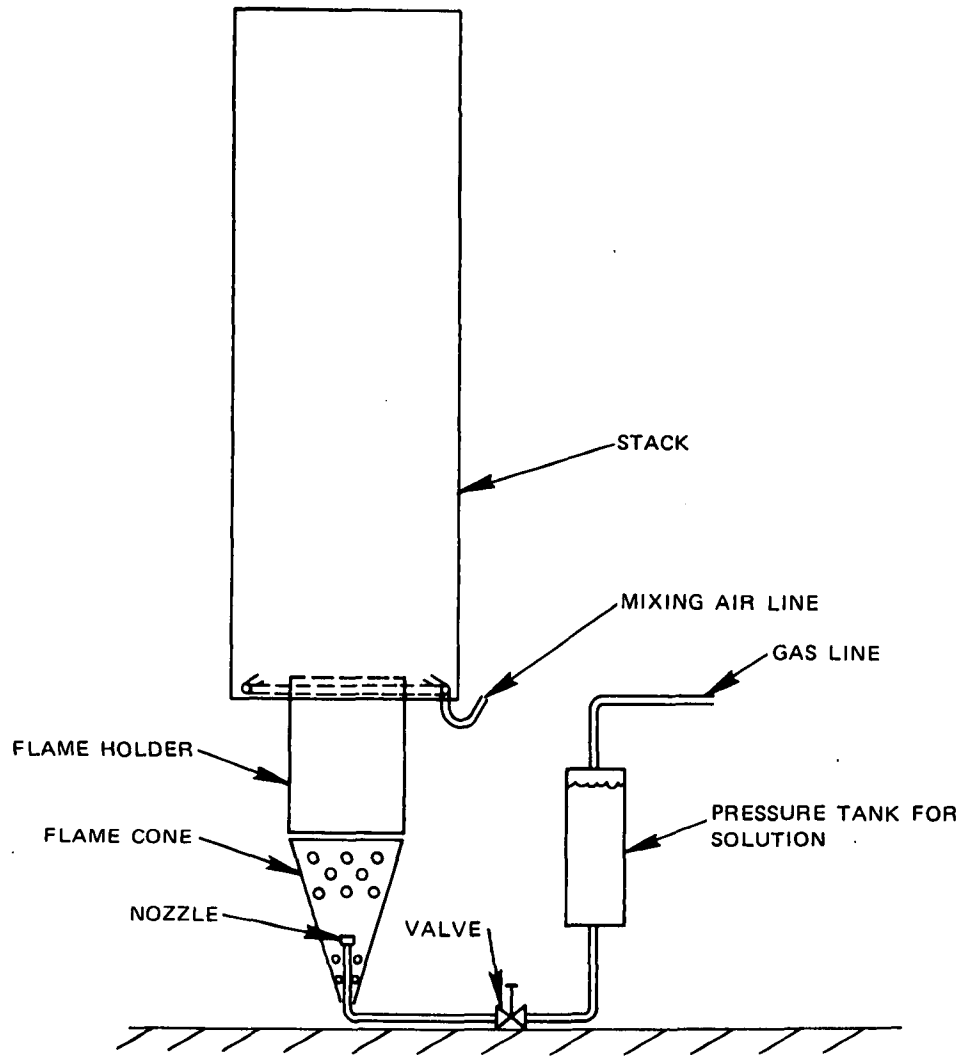

Figure 2. Generator set-up for coal fly ash simulation aerosol. The larger diameter stack reduces the exit aerosol temperature.

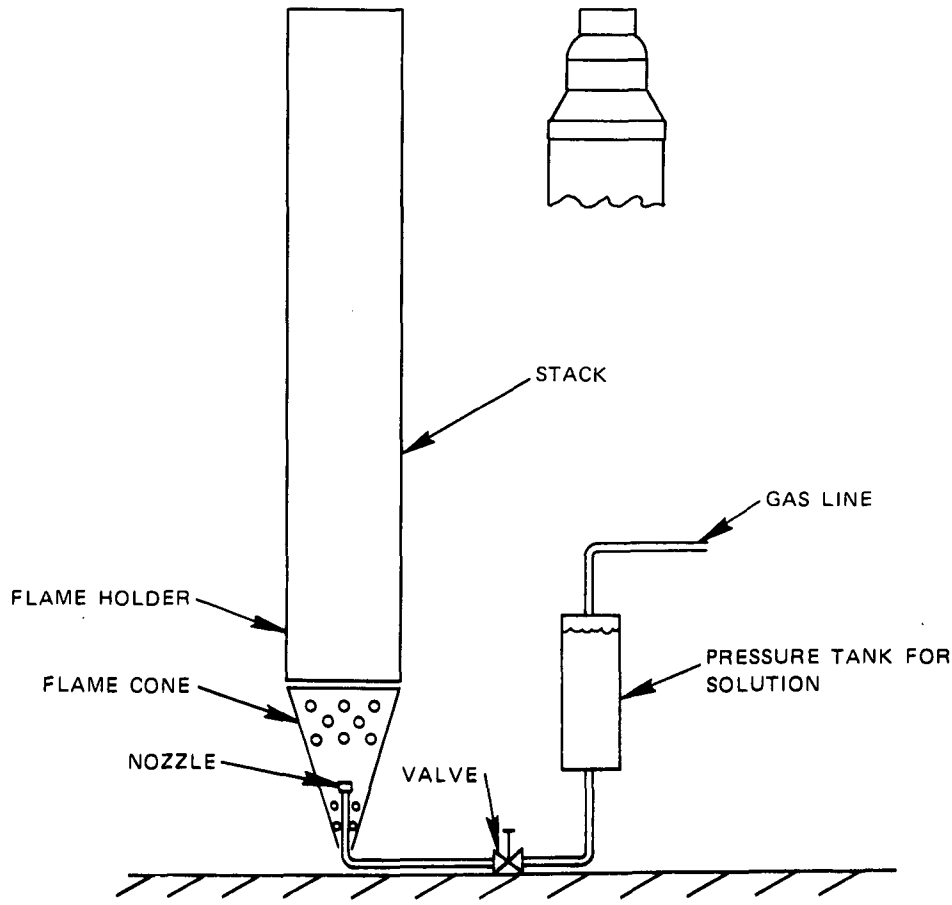

Figure 3. Generator set-up for producing simulation aerosols. Reducer is sometimes used at top of stack to increase solids loading.

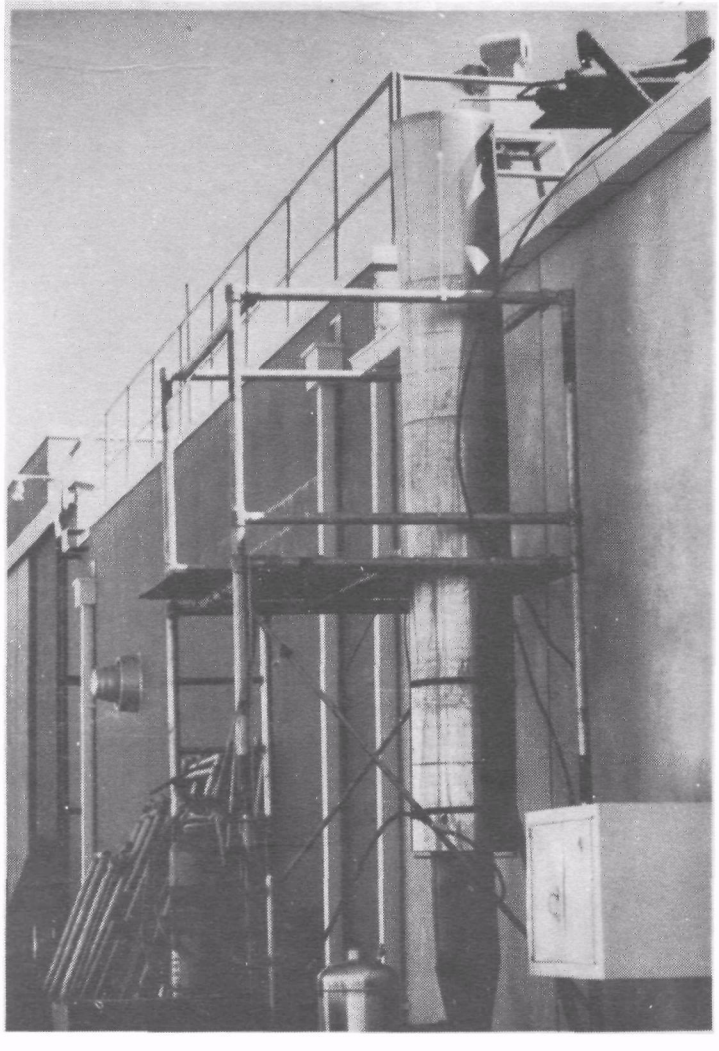

Photograph 1. Aerosol Generator and Stack for Coal Fly Ash Simulation Aerosol.

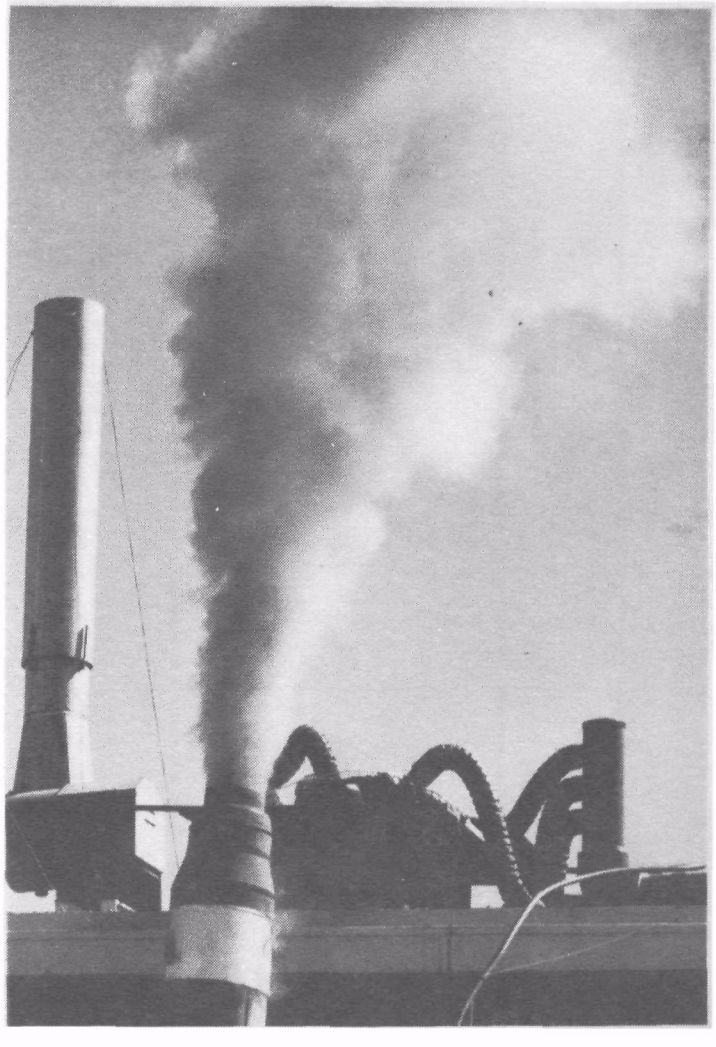

Photograph 2. Basic Oxygen Furnace Simulation Aerosol Exiting from Stack Reducer.

SOLUTIONS FOR SIMULATION AEROSOLS

The basic solution for generating simulated fly ash aerosol contains: 200 g of hydrated aluminum nitrate ($Al(NO_3)\cdot 9H_2O$); 91.7 g of hydrated ferric nitrate ($Fe(NO_3)_3\cdot 9H_2O$); and 112 g of dimethyl diethoxysilane ($(CH_3)_2Si(OC_2H_5)_2$) per liter of ethanol. Up to 80 g per liter of lithium nitrate ($LiNO_3$) can be added to the basic solution to generate aerosol particles with a higher electrical conductivity. Hydrated lithium perchlorate ($LiClO_4\cdot 3H_2O$) is also compatible with the basic solution and was also used to raise the particle conductivity. Carbon disulfide (CS_2) can also be added to the basic solution. Burning 30 ml of CS_2 per liter of ethanol results in about 2300 PPM of SO_2 in the aerosol.

When the solution for simulated fly ash is burned in air, the reactants and reaction products are:

$$Al(NO_3)_3\cdot 9H_2O + Fe(NO_3)_3\cdot 9H_2O + (CH_3)_2Si(OC_2H_5)_2 + C_2H_6O + (\text{excess})O_2 \xrightarrow{\Delta}$$
$$Al_2O_3\cdot XH_2O + Fe_2O_3 + Fe_3O_4 + SiO_2 + CO_2 + H_2O + N_2$$

The basic solution for generating simulated electric arc furnace effluent contains: 115 g of hydrated ferric nitrate ($Fe(NO_3)_3\cdot 9H_2O$); 47.5 g of hydrated chromic nitrate ($Cr(NO_3)_3\cdot 9H_2O$); 43.5 g of hydrated magnesium nitrate ($Mg(NO_3)_2\cdot 4H_2O$); and 33 g of aqueous manganese nitrate solution (51% $Mn(NO_3)_2$) per liter of ethanol.

There are two basic solutions for generating simulated basic oxygen furnace effluent. The first yields a high solids loading (6 g/m^3) of hematite particles (Fe_2O_3); the second yields a solids loading of 1.8 g/m^3 of primarily magnetite particles (Fe_3O_4). The first solution contains 293 ml (427g) of iron pentacarbonyl ($Fe(CO)_5$) in 700 ml of acetone (CH_3COCH_3). The second contains 379 g of hydrated ferric nitrate ($Fe(NO_3)_3\cdot 9H_2O$) and 16.5 g of hydrated calcium nitrate ($Ca(NO_3)_2\cdot 4H_2O$) per liter of ethanol.

The basic solution for generating simulated zinc smelter effluent contains 159 g of (73% pure) zinc nitrate ($Zn(NO_3)_2\cdot xH_2O$); 60 g of hydrated cadmium nitrate ($Cd(NO_3)_2\cdot 4H_2O$); 14.9 g vanadium oxide sulfate ($VOSO_4\cdot xH_2O$) and 20 ml of water per liter of methanol.

An Operating Procedure in Appendix A gives some additional details about the solutions.

SAFETY

$Fe(CO)_5$ is considered very toxic (Brakhnova, 1975). CdO, CS_2 and CH_3OH are also toxic; $(CH_3)_2Si(OC_2H_5)_2$ is probably toxic. Most heavy metals can be toxic; when they exist as fine particle aerosols their potential hazard is increased.

The Operating Procedure in Appendix A should be followed for safe operation.

SECTION 5

AEROSOL SAMPLING SYSTEM

GENERAL

The generated aerosol was sampled at the top of the stack. For particle size measurements, the aerosol was diluted continuously at the top of the stack, piped down to the laboratory (located just inside the building beside the generator) and simultaneously measured with electrical and optical particle counters and a condensation nuclei counter.

A water-cooled nickel plated 0.14 x 0.16 m rectangular brass plate was used to precipitate aerosol particles for X-ray diffraction analysis. After capture, a part of the sample was immediately sealed in a glass capillary tube to await analysis. For SEM and TEM analysis the aerosol particles from the top of the stack were collected on grids with a thermal impactor.

The fume velocity in the stack was measured with a specially designed balance (see Photograph 3); the temperature was measured with a thermocouple.

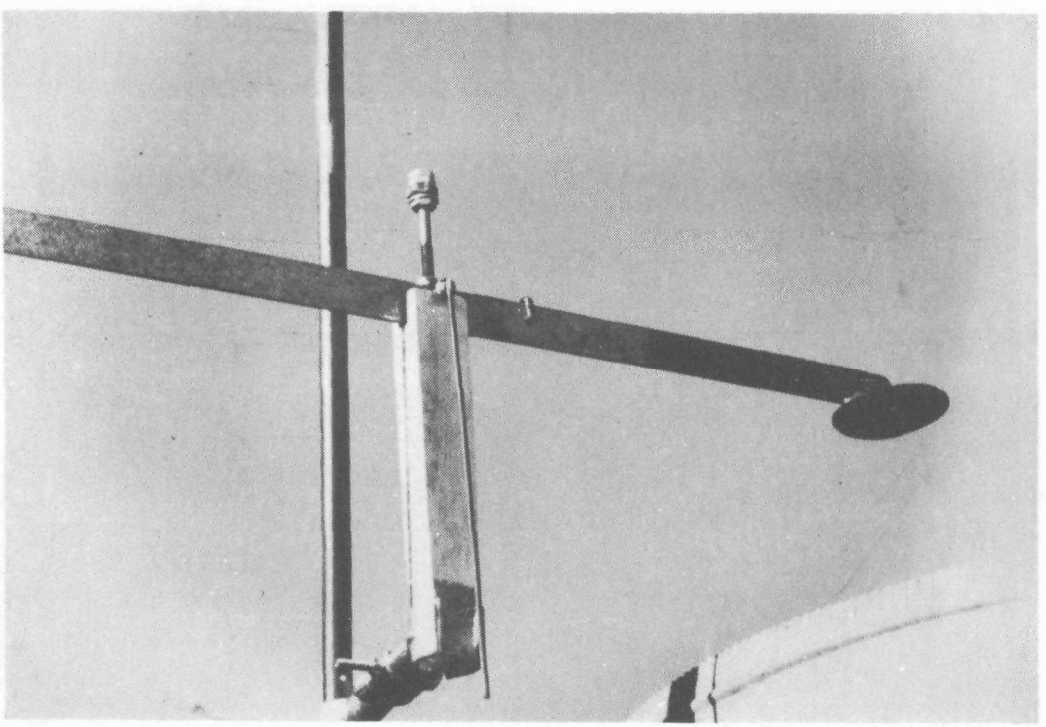

Photograph 3. Balance in position for measuring the fume velocity in the stack. The stack is in the bottom right hand corner of the picture.

DILUTER

A relatively simple diluter system was used to reduce the aerosol particle concentration so that electrical aerosol analyzers and optical particle counters could operate without saturating. The diluter system dilutes an aerosol in increments. The system has three diluter stages in series; one or more stages can be used by connecting a sample line leading to the instruments to the outlet of any of the three stages (see Figure 4 and Photograph 4). The system was calibrated by generating several aerosols with different particle concentrations. With the proper aerosol particle concentration in the stack, measurements were made with the particle counters using x dilution stages and using (x-1) stages. The aerosol particle concentration with (x-1) diluter stages divided by the particle concentration with x stages is equal to the aerosol dilution caused by stage x. The dilution was then computed for many different particle sizes between 0.03 to 5 μm. Table 7 shows the results of the measurements with 1 and 2 stages. The dilution by stage 1 is 16, by stage 2, 16 and by stage 3, 27. Therefore, if only the first stage is used, the dilution is 16. If the first two stages are used, the dilution is 256 and if all three stages are used the dilution is 6900.

TABLE 7. DILUTER CALIBRATION, STAGE 2

Solution: 75g $Al(NO_3)_3 \cdot 9H_2O$ dissolved in 10 ℓ of ethanol

	Average Electrical Aerosol Analyzer Measurements, Number of Particles with Diameters between D_x and D_y					
Diameter (μm)	0.03	.06	.1	.15	.3	.6
ΔN_1 (#/cm^3) 1 stage	1.6E4*	5.4E3	3.8E3	5.6E3	8.2E2	
ΔN_2 (#/cm^3) 2 stages	1.4E3	3.5E2	2.8E2	3.9E2	5.3E1	
N_1/N_2	11	15	14	14	15	

	Average Royco Measurements, Number of Particles with Diameters Greater than D_x							
Diameter (μm)	.8	1.	1.2	1.5	2.	3.	4.	5.
N_1 (#/cm^3) 1 stage	95	73	54	40	28	19	11	6.5
N_2 (#/cm^3) 2 stages	6.6	4.6	3.4	2.3	1.6	1.0	0.56	0.44
N_1/N_2	14	16	16	17	17	19	18	15

*Expodential notation, 1.6E4 is 1.6×10^4

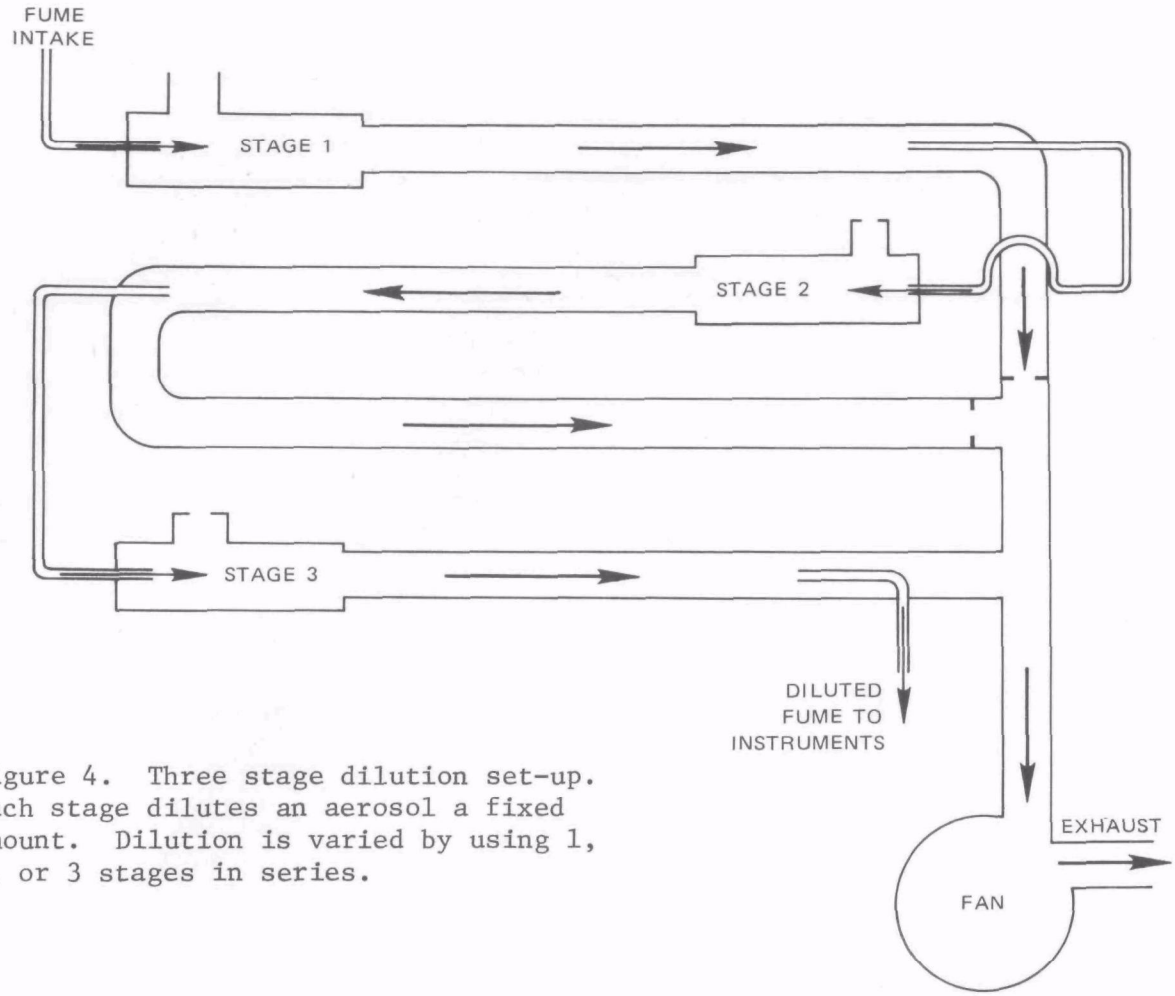

Figure 4. Three stage dilution set-up. Each stage dilutes an aerosol a fixed amount. Dilution is varied by using 1, 2, or 3 stages in series.

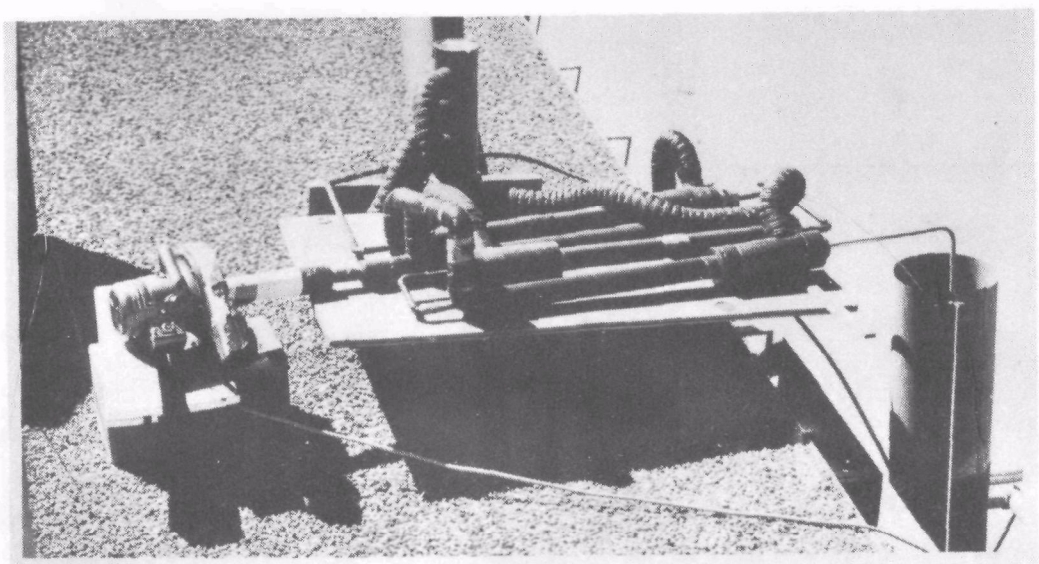

Photograph 4. Aerosol dilution apparatus

Using particle counting instruments to measure the dilution is more reliable than measuring the volumes of fume and air being mixed. Because of the small pressure differences between stages, it is difficult to accurately measure the gas flow rates without disturbing them. Accurately determining the dilution of each stage is important because the total dilution is the product of the dilution of each stage and any errors are multiplied.

Three different aerosols were used to measure the dilution of the three stages. The stage 1 dilution was determined with an aerosol generated by burning a solution of 0.05 g of zinc nitrate and 0.1 g of aluminum nitrate per liter of ethanol. The stage 2 dilution was determined by burning a solution of 7.5 g of aluminum nitrate per liter of ethanol and stage 3 by burning a solution of 200 g of aluminum nitrate and 91.6 g of ferric nitrate per liter of ethanol. The 0.42 m stack was used; the aerosol temperature at the diluter intake was between 170 and 250°C for the various tests.

Concentrated aerosol enters the first dilution stage (see Figure 5) through a 11 mm inside diameter stainless steel sample probe. The sampling is close to isokinetic; the small differences in stack velocity and probe velocity should not be significant for particles smaller than 10 μm diameter. A streamlined reducer (reducer B shown in Figure 5) is attached to the end of the tube to reduce the velocity through the tube. Reducers are used to adjust the amount of dilution and to adjust the velocities for nearly isokinetic sampling. Aerosol enters the diluter because the pressure at B is less than at A. Ambient air enters the diluter at C and passes through a sintered porous bronze tube D before coming into contact with the aerosol. This uniform flow prevents any severe impaction or turbulence. Restrictions at the inlet to C are used to adjust the pressure at B so that the aerosol flows from one stage to the next. E is a mixer composed of two disks, each with six holes. The disks are oriented to produce maximum turbulent mixing.

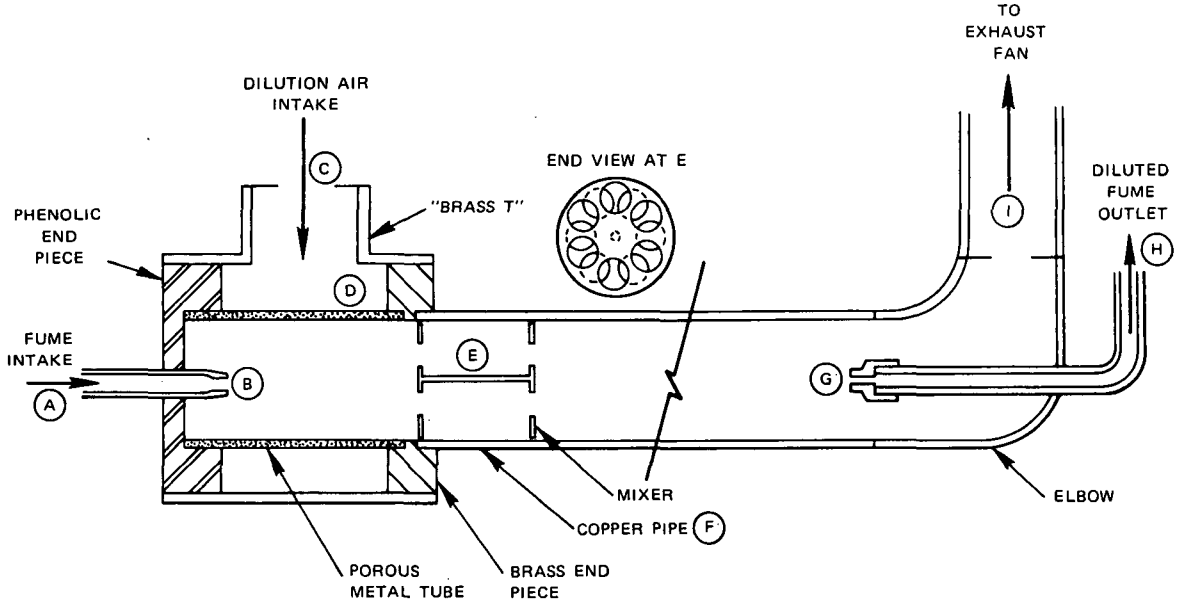

Figure 5. Diluter, Stage #1.

The copper mixing pipe, F, extends from the downstream disk to the diluted aerosol sampling point, G. A streamlined reducer (shown at G in Figure 5) is attached to the copper tube located on the diluter centerline where the diluted aerosol exits. The diluted aerosol (position H in Figure 5) is drawn either into the next dilution stage or to the measuring instruments. The remaining diluted aerosol leaves the diluter stage at I and is exhausted into the atmosphere by a fan common to all stages. Filtered air from the laboratory is used for the aerosol dilution. There is no contamination of this air by the generated aerosol. The air flow is adjusted by an orifice located downstream of I. Stages 1, 2, and 3 have different sized orifices, designed so that the vacuum from one fan maintains the proper pressures in all three diluters. The feed line from the diluter to the instruments is connected at H on stage 3, or on stage 2 or 1 if less dilution is required. (See Appendix A for a more detailed description of the diluter.)

INSTRUMENTS

The instruments received a continuous supply of fresh aerosol from the feed line. The concentrated aerosol was rapidly diluted near the sample point at the top of the stack. This diminished the rate of particle coagulation. The diluted aerosol was transported to the laboratory through 6.86 m of 13.3 mm I.D. copper tubing. The aerosol passed through a Thermo-Systems Model 3012 Krypton 85 aerosol neutralizer prior to entering the copper feed line to the instruments. The flow rate through the copper tubing was about 22 liters per minute; half of this flow passed into the instruments. Short lengths (~2cm) of plastic tubing connected the copper lines to the instruments, thus essentially all the surfaces in contact with the aerosol were metal. The only exception was a 1 m long rubber tube which connected the condensation nuclei counter to the sample line. Three instruments were used simultaneously (see Photograph 5): an Environment I, Rich 100, condensation nuclei monitor (CNC), a Model 3000 Whitby Electrical Aerosol Analyzer (EAA)*, a Model 200 Royco Optical Particle Counter (Royco). The CNC detects very small particles (to about 20Å in diameter) over a wide concentration range (from about 100 particles/cm^3 to 10^7 particles/cm^3). The EAA measures an equivalent sphere diameter based on electrical charge and mobility. The Royco measures the equivalent light scattering diameters of latex spheres. The Royco did not have a sheath air inlet system to prevent aerosol recirculation in the sensing zone. The Whitby-Cantrell Electrical Aerosol Analyzer Constants, adjusted to the Model 3000, were used to obtain aerosol particle size distributions from the currents measured with the EAA (see Appendix C). The original EAA Model 3000 data reduction constants are also shown in Appendix C. The EAA can measure particles in the size range 0.0075 to 0.6 μm; the Royco measures particles in the size range of 0.3 to 10 μm.

*Note: Throughout this paper "EAA" is an acronym for the Model 3000 Whitby Electrical Aerosol Analyzer and not for the Model 3030 Electrical Aerosol Analyzer as it usually is. Although both the Model 3000 and 3030 instruments operate on the same basic principle, there are important differences in design and presumably, also in performance (personal communication, B. Y. H. Liu to G. J. Sem).

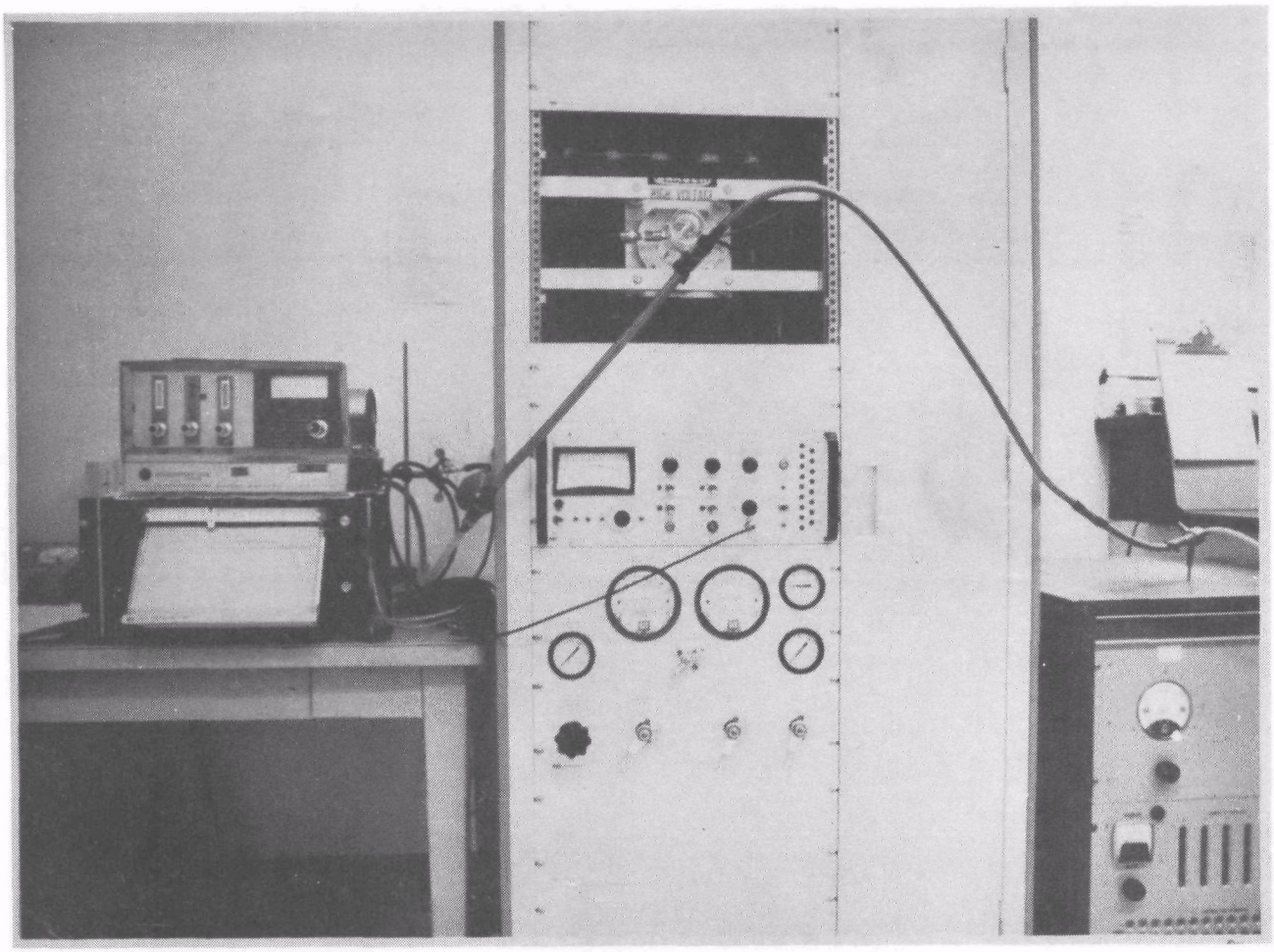

Photograph 5. Instruments, at the left an Environment I condensation nuclei counter (CNC) on top of a voltage recorder used to record the Model 3000 Whitby Electrical Aerosol Analyzer (EAA) in the center and at the right a Model 200 Royco Optical Particle Counter.

Aerosol generation times of 5 to 30 minutes were used and the particle counts measured during this time were averaged for each size range. Care was taken to achieve the proper dilution of the generated aerosol so that the particle concentrations of the smaller particles were not high enough to cause instrument saturation and also that the particle concentrations of the larger particles were significantly above the background counts. Laboratory air was used to dilute the generated aerosols. On most days the background (laboratory air without generated aerosol) particle counts were less than 10% of the diluted generated aerosol particle counts. Because the laboratory is located in the desert, the air is almost always very dry and there was no problem of water condensation even when only one diluter stage was used.

The instruments measured diluted aerosol particles that were generated 9 seconds prior to entering these instruments.

SIZE DISTRIBUTIONS

Most size distributions are plotted as, N(D), the total number of particles per cm^3 with diameters greater than D vs. particle diameter, D. The outputs from the ROYCO optical particle counter are plotted in this format without modification. The outputs from the electrical aerosol analyzer (EAA) are added to the ROYCO count at D=0.6 μm to calculate N(D) for D's smaller than 0.6 μm. At particle sizes between 0.3 and 0.6 μm the outputs from both instruments are shown. Some of the size distributions are plotted as $\Delta N/\Delta \log D$.

Aerosol particle volumes were calculated assuming that the particle counts, ΔN_i, in each size interval (D_i to D_{i+1}) are the numbers of single spherical particles of diameter equal to the geometric diameter of the size interval (square root of $D_i D_{i+1}$). Thus the volume of particles, ΔV, counted in size interval D_i, D_{i+1} is

$$\Delta V = \frac{\Pi}{6} \Delta N (D_i D_{i+1})^{3/2}$$

The volume distributions are plotted as volume %. The EAA counts are used for sizes smaller than 0.6 μm; Royco counts are used for the larger sizes.

SECTION 6

RESULTS

Measurements, Observations and Comparisons

THE PARTICLES

The aerosol particles were measured approximately 9 seconds after generation. They remain suspended in air while they are sized and counted by the EAA and Royco instruments. They do not, however, remain as single spherical particles, even though most of them probably formed as single, "nearly" spherical particles. Most of the single particles quickly coagulate with other particles. Fuchs (1964, pp. 288-315) offers a good introduction to the theory of coagulation of aerosols. Readers not familiar with the subject can better understand our experimental results by studying this or similar works.

Several of the generated aerosols were precipitated and photographed. The larger particles (D>10 μm) were sampled by letting them impact a glass slide coated with adhesive; the smaller particles were thermally precipitated onto SEM and TEM grids.

Photograph 6a shows a 25 μm diameter zinc oxide particle covered with smaller particles which coagulated with it. Photograph 6b shows a 20 μm diameter hollow iron oxide (probably Fe_3O_4) particle. Photograph 6c shows a close up of the surface of an iron oxide particle with some smaller captured particles. Photograph 6d shows another hollow particle captured while generating the electric arc furnace simulation aerosol. Photograph 7a shows a large number of iron oxide particles several of which have holes showing that they are hollow; possibly all of these particles are hollow. Further evidence of large hollow particles was noted by observing the behavior of particles which precipitated onto the stack. After a test when the stack cooled, there was often a slight draft; particles dislodged by rapping the stack floated up and out of the stack. After one test where MgO aerosol had been generated, particles, later identified as clusters of three to six 50 μm diameter particles, were observed floating up. The air velocity was less than 0.2 m/s. This indicates a maximum particle density of 2.5 g/cm^3 which is only 68% of the density of MgO.

When calcium nitrate solutions were burned, the captured particles appeared to have "wet" smooth surfaces. We were not able to identify the chemical composition with X-ray diffraction analysis. Photograph 7b shows one of these hydrated particles.

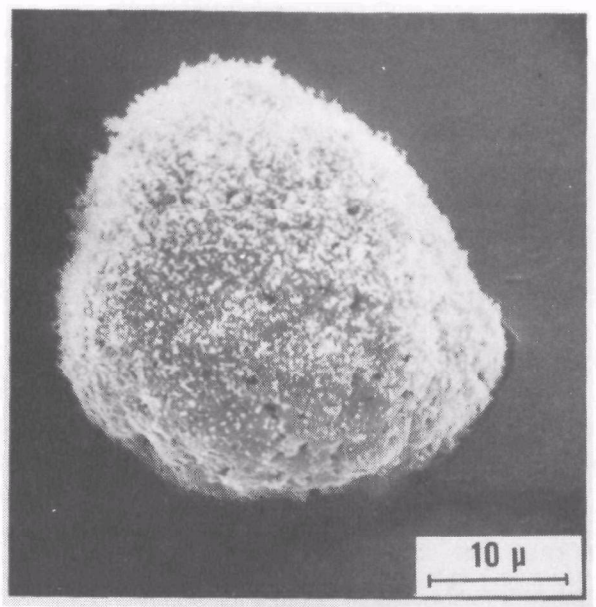

Photograph 6a. Zinc oxide particle coated with submicron particles.

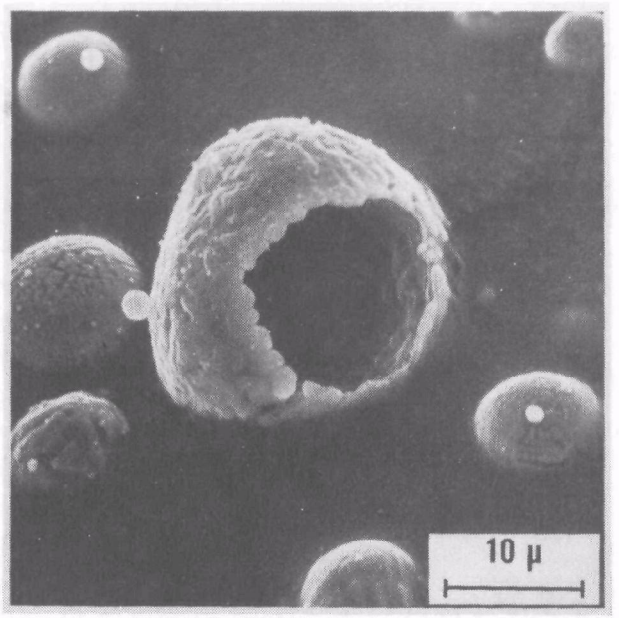

Photograph 6b. Iron oxide particles from basic oxygen furnace simulation aerosol BB.

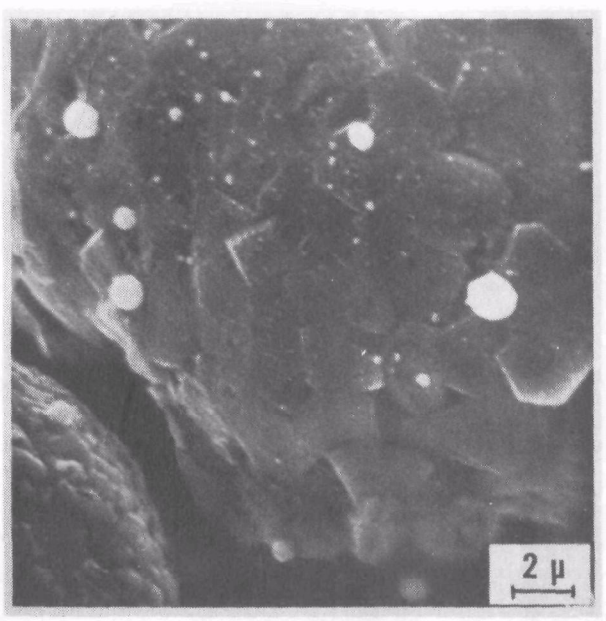

Photograph 6c. Iron oxide particle surface.

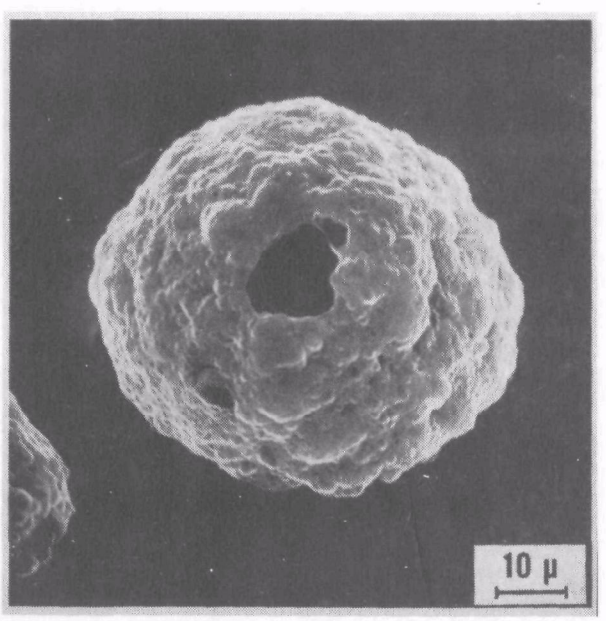

Photograph 6d. Hollow particle from the electric arc furnace simulation aerosol.

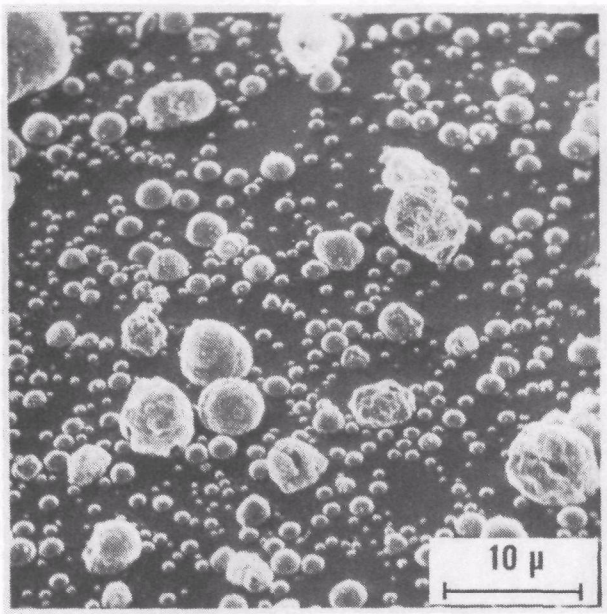

Photograph 7a. A large number of iron oxide particle several of which have holes showing that they are hollow.

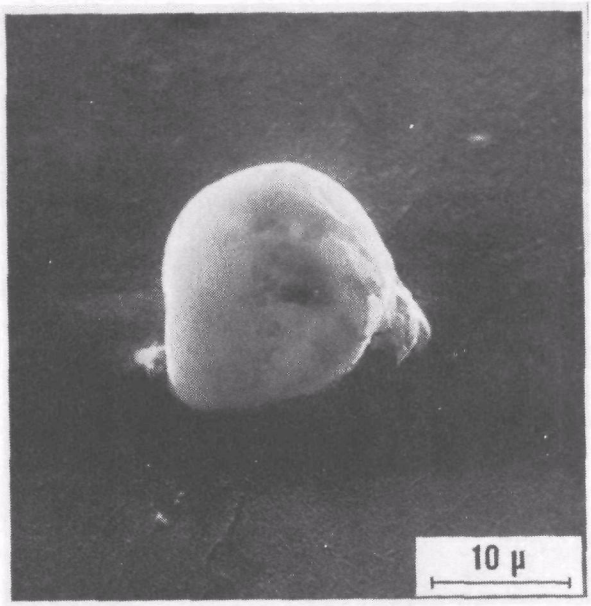

Photograph 7b. A hydrated particle containing an unidentified calcium compound.

The smaller particles are seldom seen as single spheres. Photograph 8a shows a single 0.2 μm particle with several particles of about 0.01 μ diameter coagulated with it. Photograph 8b shows a wide spectrum of particle sizes and aggregates. The particles on these plates were captured from the coal fly ash simulation aerosol. Photographs 8c an 8d show particles captured from the electric arc furnace simulation aerosol; they are primarily chain aggregates of 0.01 to 0.02 μm particles. For most of the aerosols generated, the bulk of the aerosol mass appears to exist as chain aggregates. The aggregates form from the very high concentrations ($>10^9$ particles per cm^3) of 0.01 to 0.02 μm particles. The Royco and EAA are calibrated with spherical particles with specific physical properties. Consequently, the indicated particle size ranges may be biased to various degrees by different aerosols. The Royco and EAA counts are, in reality, a measurement corresponding to the number of spheres of a standard material that could produce an equivalent signal. The aggregated particles have non-ideal shapes and it is difficult, if not impossible, to calculate their electrical, aerodynamic and optical properties.

PARTICLE COUNTS

The size distributions of 26 different aerosols were measured simultaneously by the EAA and Royco instruments. In many of these tests the CNC instrument was used also. There are some interesting disagreements between the instrument counts. The particle counts were used to compute aerosol volume concentrations and these were compared with concentrations determined from the solutions and burn times. Again there were some interesting disagreements.

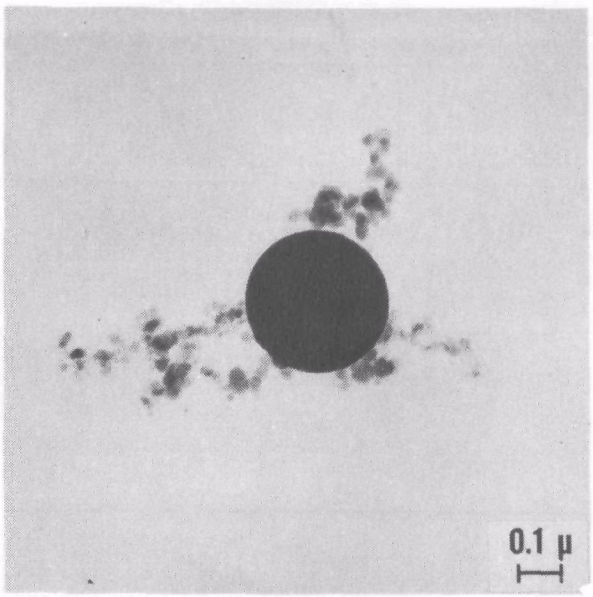

Photograph 8a. Few of the submicron particles were seen as single spheres.

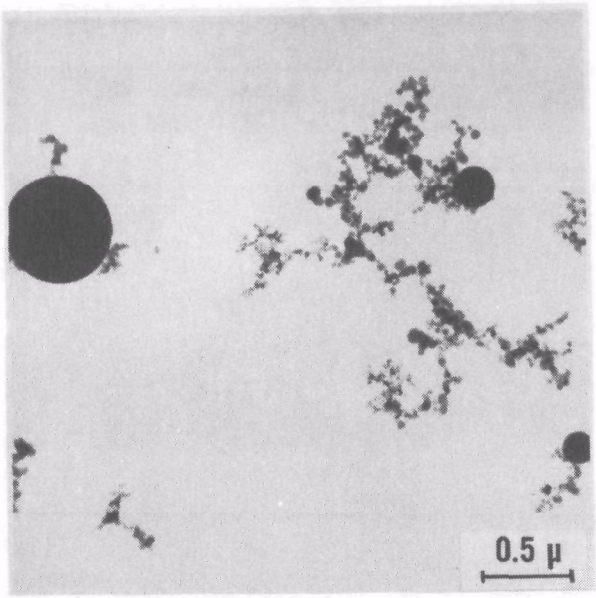

Photograph 8b. Particles from the coal fly ash simulation aerosol.

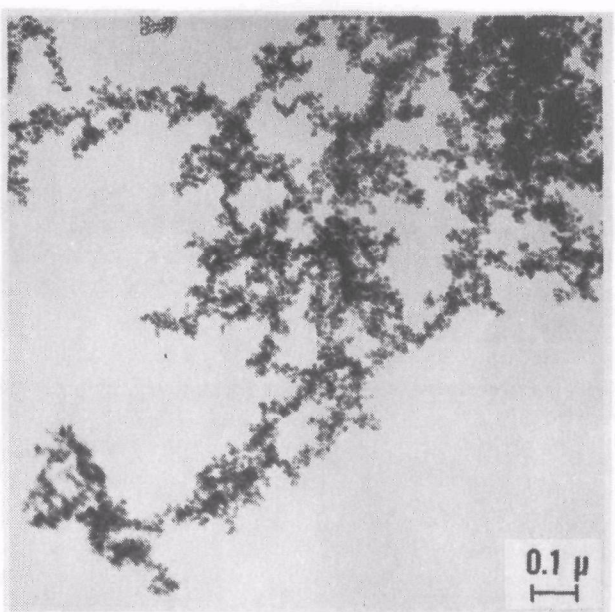

Photograph 8c. Particles from the electric arc furnace simulation aerosol.

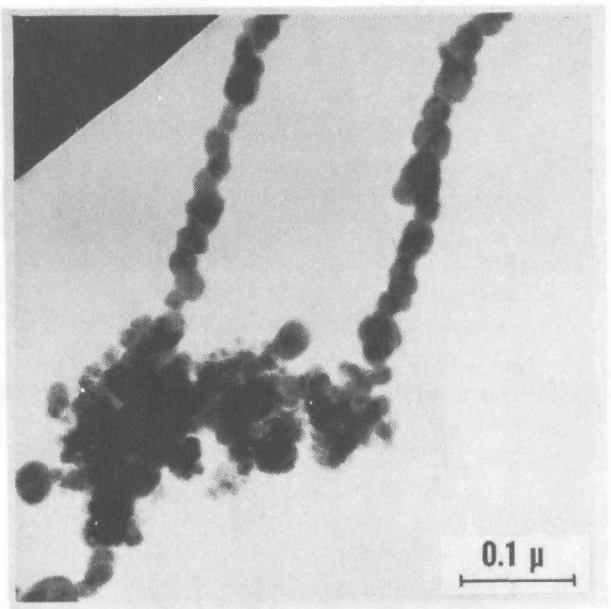

Photograph 8d. Particles from the electric arc furnace simulation aerosol with more magnification.

Figure 6 shows the background particle counts for a typical test with three stage dilution. These counts were recorded prior to burning the solution. To measure a test aerosol, the particle counts in each size range must be high enough so that the background counts can be subtracted to yield a significant difference. On most days the background counts were steady; when they were not, a larger difference between background and burn was required. Since the variability of particle counts increases as the number of particles counted decreases, the ratio of burn counts to background counts must be greater for the larger sized particles. The most likely variable which would reduce the reproducibility of the following aerosol size distribution measurements was a change in the background particle concentration during a test. By carefully controlling this, the reproducibility of the measurements was very good.

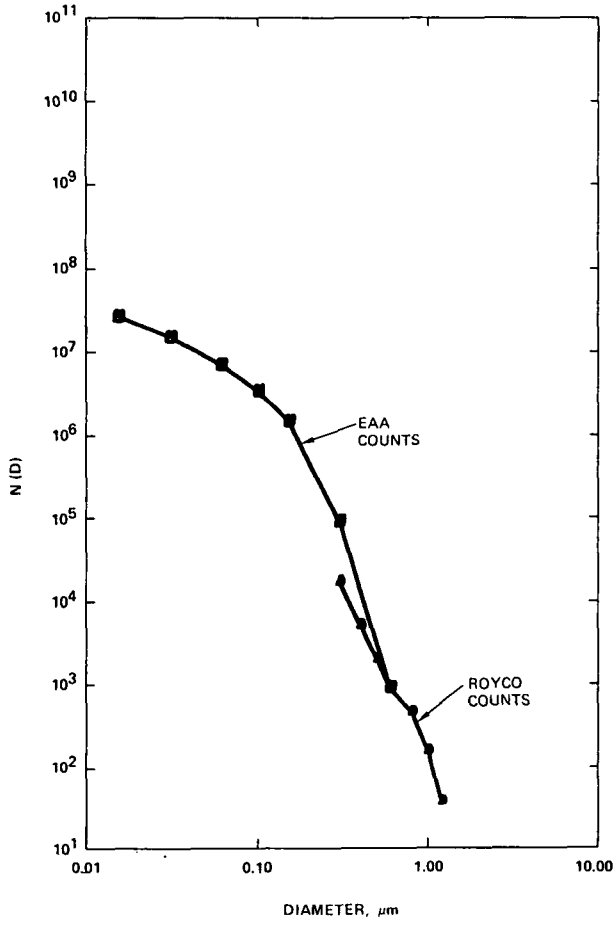

Figure 6. Typical background measurements before aerosol generation. The background measurements shown in this figure are multiplied by 6900 because with three stage dilution the equivalent of 6900 parts of air is mixed with one part of aerosol.

The generated aerosol characteristics depend on the rate at which solution is burned in the generator. The flow rate of solution sprayed into the generator is dependent on the solution viscosity. The viscosity is dependent on the solution temperature at the nozzle; thus, the generated aerosol characteristics depend on the solution temperature at the nozzle. Both the temperature of the solution in the pressure tank and of the air entering the generator affect the solution temperature at the nozzle. The magnitude of this effect was not measured. We believed, however, that this effect was not important for the 26 aerosols generated, measured and described in this report.

For most tests three stage dilution was required to dilute the aerosol particle concentration to prevent Royco and EAA saturation. Three stage dilution reduces the particle concentration by a factor of 6,900. Thus, with three stage dilution, an undiluted aerosol particle concentration of 200 particles per cm^3, is reduced such that less than two particles are counted by the Royco in a 0.3 minute counting time. The concentration of aerosol particles with diameters greater than D_X is roughly inversely proportional to the cube of D_X. With three stage dilution the larger particles had low concentrations. An excessively long time (several minutes) would have been required to count a representative number of them to determine their true concentration. This causes an effective size cut-off. The concentrations of large particles are best measured with two stage dilution.

For some aerosols the particle counts decreased in the size range 0.015 to 0.03 μm and then increased again in the size, range 0.0075 to 0.015 μm. This may have been caused by our using the Whitby-Cantrell data reduction constants.

Because of coincidence counting of particles by the Royco, all Royco counts of diluted aerosol with concentrations in excess of 100 particles/cm^3 were assumed in error (saturated) and are not reported. In some cases, even with three stage dilution, one or both of the instruments was saturated for the smaller sized particles (e.g., Royco 0.3 to 0.5 μm), and additional dilution of the aerosols had to be used. This was accomplished by using smaller orifices at the diluter fume outlet of stages 1 and 2 (see G in Figure 5). This increased dilution is defined as "non-standard three stage dilution". MgO and SiO_2 aerosols were used to determine the increase in dilution. The amount of dilution was found to be a function of particle size; the dilution slowly increased with increasing particle diameter. Average values of dilution were used to convert the instrument particle counts to undiluted aerosol particle concentrations. With non-standard three stage dilution, the average dilution in the EAA size range (0.0075 to 0.3 μm) is 38,700 and in the Royco size range (0.3 to 4 μm) 65,700.

Appendix B has figures showing the size distributions of most of the 26 different aerosols which were generated and measured but not shown in the text. The figures are plotted as N(D) vs D. Appendix C has the particle concentrations and volume percents in each size interval for the 26 different aerosols.

Mass Balances

The solution composition, flow rate, aerosol stack exit velocity and temperature were known for each experiment, therefore the aerosol particle loadings (g/m^3) could be determined by assuming that all of the solid products of combustion were suspended as aerosol particles and an insignificant portion collected onto the flame cone, flame holder and stack. With one exception (the 1.8 g/m^3 basic oxygen furnace simulation aerosol), this assumption is good for all of the aerosols reported. In order to calculate the volume concentrations from the particle loadings, it was necessary to assume particle densities. Handbook values of densities of those compounds identified by X-ray diffraction analysis were used.

The volume concentrations were also determined by using the particle counts from the instruments. To do this, two assumptions were made: first, that the particles counted in the interval $D_x \cdot D_y$ all have a diameter D_G equal to the square root of $D_x D_y$ (geometric mean diameter); second that the particles are all solid spheres. For most of the aerosols these assumptions are in error, especially the second as photographs 6a-8d show.

The Royco and EAA instruments are calibrated with a dilute aerosol of spherical particles. The particle counts from these instruments were used to determine particle volumes and solids loadings of aggregated aerosols. It is not surprising that the volumes and loadings sometimes disagreed by an order of magnitude with the volumes and loadings determined from solution compositions and flow rates (generation rates).

For many of the aerosols, the bulk of the measured volume was contained in particles with diameters less than 0.6 μm (sizes measured by the EAA). For many of these aerosols, the volumes determined from the EAA particle counts were larger than the volumes determined from the generation rates.

Tests were conducted with SiO_2, MgO, ZnO and Fe_2O_3 aerosols to see if the loadings determined from the generation rates and those from the particle counts would be in better agreement at lower particle loadings. Table 8 shows aerosols with two loadings of SiO_2, one with that of the coal fly ash simulation aerosol (0.163 cm^3/m^3), another with a much lower loading (0.004 cm^3/m^3). Table 9 shows MgO, ZnO and Fe_2O_3 at higher and lower particle loadings. Figure 7 shows the particle size distribution of these two SiO_2 aerosols as measured by the EAA. The following points seem to show that the EAA was not saturated at either SiO_2 loading. The maximum current on the EAA was 6.9×10^{-12} amperes on stage 1 for the SiO_2 aerosol containing the higher loading; the EAA did not normally saturate at this current. The ratio of the volume determined from the EAA particle counts to that determined from the generation rates was not reduced at the lower SiO_2 loading; in fact, it increased a little (see Table 8). These observations indicate that instrument saturation is not responsible for the loadings determined from the EAA particle counts being higher than those determined from the generation rates. Lowering particle loadings did not lead to better agreement.

Since the only solid product of combustion of $(CH_3)_2Si(OC_2H_5)_2$ is SiO_2, there is nothing in the chemistry to indicate that the loadings determined

TABLE 8. AEROSOL PARTICLE LOADING (Weight or Volume/Hot Gas Volume) Measured in 0.425 m Stack with Three Stage Dilution

Aerosol Particle Composition	Determined From Generation Rate g/m^3	cm^3/m^3	Determined From EAA & Royco Counts cm^3/m^3	Particle Loading (Counted/ generated)	Particle Density (Handbook Value) g/cm^3	Apparent Maximum Particle Density g/cm^3
SiO_2	0.36	0.16	1.0	6.0	2.2	0.37
SiO_2	0.009	0.0039	0.027	7.0	2.2	0.31
SiO_2 & $Al_2O_3 \cdot 2H_2O$	0.62	0.26	1.4	5.0	2.34	0.47
SiO_2, $Al_2O_3 \cdot 2H_2O$ & Fe_2O_3 & Fe_3O_4*	0.66	0.25	1.1	4.0	2.6	0.65
Same composition as above*	0.66	0.25	1.1	4.0	2.6	0.65
Same as above with Li_2CO_3	0.94	0.39	.55	1.4	2.43	1.7
Fe_2O_3 & Fe_3O_4	0.15	0.029	0.027	0.9	5.17	-
Fe_2O_3 & Fe_3O_4	0.12	.024	.009	0.4	5.17	-
$Al_2O_3 \cdot 2H_2O$, Fe_2O_3 & Fe_3O_4	0.41	0.13	0.08	0.6	3.06	-
$Al_2O_3 \cdot 2H_2O$	0.26	0.1	0.02	0.2	2.55	-

*These aerosols are the coal fly ash simulation aerosol.

TABLE 9. AEROSOL PARTICLE LOADING (Weight or Volume/Hot Gas Volume) Measured in 0.25 m Stack with Three Stage Dilution.

Aerosol Particle Composition	Determined From Generation Rate g/m^3	cm^3/m^3	Determined From EAA & ROYCO Counts cm^3/m^3	Particle Loading (Counted/ Generated)	Particle Density (Handbook Values) g/m^3	Apparent Maximum Particle Density g/cm^3
SiO_2	0.096	0.043	0.544	13	2.2	0.17
MgO	0.62	0.17	3.6	21	3.65	0.17
MgO	0.054	0.015	0.35	24	3.65	0.15
MgO	0.49	0.13	2.9*	22	3.65	0.17
ZnO	0.087	0.016	0.18	11	5.47	0.49
ZnO	0.94	0.17	1.2*	7	5.47	0.78
Fe_2O_3**	0.071	0.014	0.17	12	5.12	0.43
Fe_2O_3**	0.56	0.11	0.89*	8	5.12	0.64
Fe_2O_3**	6.0	1.17	22.*	19	5.12	0.27
Fe_2O_3 & Fe_3O_4	0.78	0.15	0.054	0.36	5.14	-
Mn_3O_4	0.62	0.13	0.11	0.85	4.72	-
Cr_2O_3	0.69	0.13	0.95	7	5.21	0.74
$Ca(OH)_2 \cdot xH_2O$	0.29	0.13	1.1	8	2.24	Hydrated
Ele Arc Sim. Aero.	0.65	0.14	0.054	0.40	4.79	-
Ele Arc Sim. Aero.	1.2	0.24	0.064	0.26	4.79	-
Above w/o Mn	1.0	0.21	0.072	0.34	4.81	-

* Used non-standard 3-stage dilution (see text)

** From $Fe(CO)_5$

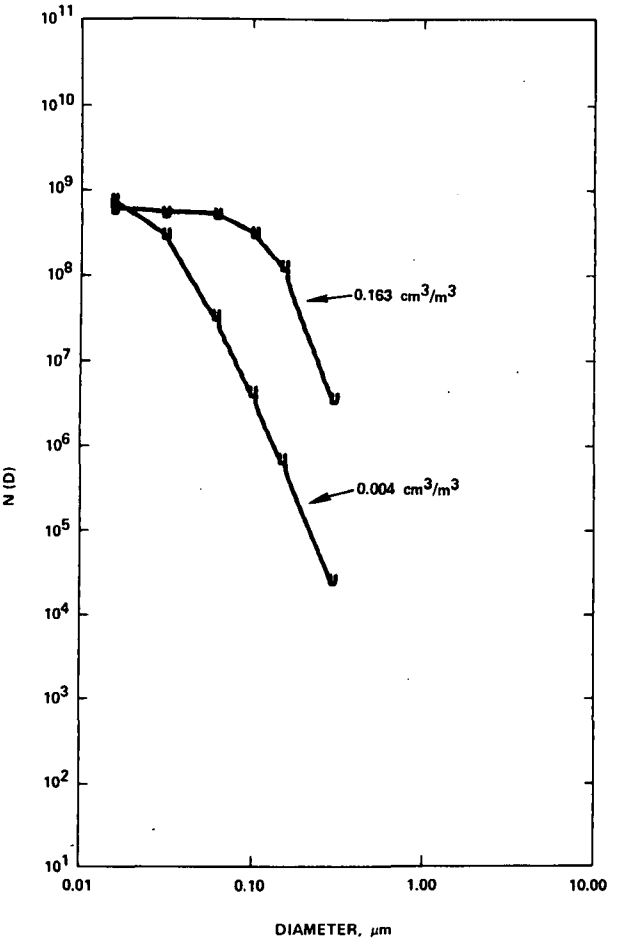

Figure 7. Comparison of measurements with the electrical aerosol analyzer (EAA) of two SiO_2 aerosols, one containing 0.163 cm^3 of SiO_2 per m^3 of aerosol, another containing 0.004 cm^3/m^3. The EAA does not appear to have been saturated.

from the generation rate are in error. When alcohols (methyl, ethyl or propyl) or propane were burned in the generation apparatus with three stage dilution, there was a negligible increase in particle counts over the background counts.

Tables 8 and 9 show several aerosol particle loadings as determined from the generation rates and from the instrument particle counts. The aerosols were generated in the 0.42-m stack (Table 8) and in the 0.25-m stack (Table 9). The "apparent maximum particle density" equates the particle loadings determined from the instrument particle counts (using the assumption that the particles are solid spheres) to those from the generation rates. The apparent maximum particle densities shown in Tables 8 and 9 are equal to the handbook values of densities divided by the counted/generated particle loadings.

Many of the aerosols in Table 9 have nearly constant volume loadings. This was purposely done so that an aerosol of one chemical compound could be compared with an aerosol of another compound. The volume loadings were based on handbook values of densities. The small variation in particle loadings was caused by small variations in the solution flow rates which not only changed the solids generation rates but also the aerosol gas flow rate. This variation in solution flow rates was caused by varying solution viscosities due primarily to the different chemical compositions of the solutions. The volume loadings varied from 0.13 to 0.17 cm^3/m^3. The MgO, ZnO and Fe_2O_3 aerosols were also generated with volume loadings of only 10% of the constant volume (see Table 9). The SiO_2, MgO, ZnO and Fe_2O_3 (from $Fe(CO)_5$) aerosols were measured in much the same manner with the EAA.

CNC vs. EAA Counts

Table 10 shows the total particles counted by the Environment I CNC* and by the EAA and Royco. Since the number of particles counted by the Royco was small compared to the number counted by the EAA, Table 10 essentially shows a comparison of the EAA and CNC counts. For most aerosols the particles counted by the EAA were between 5 and 6 times as great as those counted by the CNC. The average value of the ratio of concentrations (EAA/CNC) is 6.1 with a variance of 3.5. The Fe_2O_3 from $Fe(CO)_5$ and $H_2SO_4 \cdot H_2O$ aerosols were not included in the computation of an average value because they appear to behave differently from the other aerosols. The best agreement between the CNC and EAA was for the aerosol containing $H_2SO_4 \cdot xH_2O$ droplets; perhaps with the other aerosols, particle response as condensation nuclei was slower and growth did not occur on all of the aerosol particles.

EAA vs. Royco Counts

For some aerosols the particle counts from the EAA and Royco in the size range where they overlap ($0.3<D<0.6$ μm) were in good agreement; for other aerosols these instruments counted vastly different numbers of particles in this size range. Both the EAA and Royco are outside of their optimum performance ranges at 0.3-0.6 μm†. Tables 11 and 12 show the EAA and Royco counts for several aerosols. In the best case (Fe_2O_3 and Fe_3O_4, 0.78 g/m^3, Table 12) the particle counts were within 4% of each other; in the worst case (SiO_2, 0.36 g/m^3, Table 11) they differed by a factor of 343! Figures 8 and 9 show $\Delta N/\Delta \log D$ vs. D plots for the Fe_2O_3 and Fe_3O_4 (0.78 g/m^3) aerosol and for the MgO (0.054 g/m^3) aerosol. The Royco and EAA counts are in good agreement for the Fe_2O_3 and Fe_3O_4 aerosol and in poor agreement for the MgO aerosol. These curves are typical of most of the aerosol measurements. The ratio of EAA to Royco counts in the overlapping size range varied from 0.68 to 343. The ratio was a function of the material used to generate the aerosol. For example, with black iron oxide aerosols (mixtures of Fe_2O_3 and Fe_3O_4) generated from hydrated ferric nitrate ($Fe(NO_3)_3 \cdot 9H_2O$) the ratio of EAA to Royco counts was near unity (0.96 to 1.23) while with

*In the Discussion of Results section, the CNC counts are corrected per Liu and Pui (1974).

†Personal communication, G. J. Sem to J. W. Carroz.

TABLE 10. AEROSOL PARTICLE CONCENTRATION (CNC vs EAA)
Measured in 0.25 m Stack Using Three Stage Dilution

Aerosol Particle Composition	Aerosol Generation Rate g/m^3	Particle Concentration From CNC ($\#/cm^3$)	Particle Concentration From EAA ($\#/cm^3$)†	Ratio of Concentrations (EAA/CNC)
SiO_2	0.096	3.4E8	1.9E9	5.6
SiO_2*	0.36	9.3E7	9.4E8	10
MgO	0.62	1.7E8	EAA saturated	-
MgO	0.054	1.3E8	7.3E8	5.6
MgO**	0.49	1.2E8	1.1E9	9.2
ZnO	0.087	2.2E8	1.7E9	7.4
ZnO**	0.94	1.4-1.7E8	7.8E8	5.8
Fe_2O_3	0.071	2.4E8	1.E9	6.3
Fe_2O_3**	0.56	0.2-1.0E9	2.3E9	2.3-12
Fe_2O_3**	6.0	4-30E8	2.2E10	7.3-55
Fe_2O_3 & Fe_3O_4	0.78	2.6E8	7.8E8	3.0
Mn_3O_4	0.62	2.4E8	1.3E9	5.6
Cr_2O_3	0.69	2.1E8	1.0E9	4.8
$Ca(OH)_2$	0.29	3.2E8	1.5E9	4.8
Ele Arc Sim Aero.	0.65	3.0E8	1.5E9	5.0
Ele Arc Sim Aero.	1.2	2.4E8	1.3E9	5.5
Above w/o Mn	1.0	2.8E8	1.3E9	5.4
$H_2SO_4 \cdot xH_2O$	Very low	1.0-1.3E9	2.4E9	2.1
Coal Fly Ash Sim Aero.*	0.66	1.1E8	9.2E8	8.4
Above with Li*	0.94	1.1E8	7.4E8	6.7

† The EAA counts of all particles larger than 0.0075 μm
* Generated in 0.42 m Stack
** Non-standard Three Stage Dilution

TABLE 11. AEROSOL PARTICLE COUNTS. Measured in 0.42 m Stack with Three Stage Dilution

Aerosol Particle Composition	Approximate Aerosol Generation Rate g/m^3	Diameter of Largest Particle Counted (μm)	Particle Volume Median Diameter (μm)	EAA Counts .3<D<.6 (μm)	ROYCO Counts .3<D<.6 (μm)	Ratio of Particle Counts EAA/Royco (.3<D<.6)
SiO_2	0.36	.6	0.2	3.4E6	9.9E3	343
SiO_2*	0.009	0.6**	0.06	2.4E4	-	-
SiO_2, $Al_2O_3 \cdot 2H_2O$	0.62	4	0.2	5.4E6	5.0E4	108
SiO_2, Fe_2O_3 & Fe_3O_4	0.51	3	0.2	2.0E6	3.1E5	6.5
SiO_2, $Al_2O_3 \cdot 2H_2O$ & Fe_2O_3 & Fe_3O_4	0.66	3	0.2	4.7E6	3.6E5	13
Same as above	0.66	8	0.2	3.8E6	4.4E5	8.6
Same as above with Li_2CO_3	0.94	3	0.2	1.7E6	4.5E5	3.8
Fe_2O_3 & Fe_3O_4	0.15	1.5	0.05	at background	4.9E4	-
Fe_2O_3 & Fe_3O_4	0.12	1.5	0.05	1.0E4	8.1E3	1.23
$Al_2O_3 \cdot 2H_2O$, Fe_2O_3 & Fe_3O_4	0.41	8	1.2	4.2E4	6.0E4	0.70
$Al_2O_3 \cdot 2H_2O$	0.26	3	>1.5	1.6E5	5.5E4	2.9

* Both two and three stage dilutions were used.
** 0.1 μm with three stage dilution.

TABLE 12. AEROSOL PARTICLE COUNTS
Measured in 0.25 m Stack with Three Stage Dilution

Aerosol Particle Composition	Aerosol Generation Rate g/m^3	Diameter of Largest Particle Counted (μm)	Particle Volume Median Diameter (μm)	EAA Counts .3<D<.6 (μm)	ROYCO Counts .3<D<.6 (μm)	Ratio of Particle Counts EAA/ROYCO (.3<D<.6)
SiO_2	0.096	0.6	0.15	2.5E5	-	-
MgO	0.62	6	-	2.5E7	4.4E5	58
MgO	0.054	4	0.2	1.6E6	5.9E4	27
MgO	0.49	4*	0.3	2.7E7	6.0E5	45
ZnO	0.087	3	0.1	3.6E5	4.4E4	8.2
ZnO	0.94	4*	0.2	4.2E6	1.8E6	2.3
Fe_2O_3**	0.071	0.6	0.1	2.5E5	8.4E3	30
Fe_2O_3**	0.56	0.8*	0.2	4.5E6	2.7E6	1.7
Fe_2O_3**	6.0	8*	1.05	2.3E7	Saturated	-
Fe_2O_3 & Fe_3O_4	0.78	3	0.3	2.3E5	2.4E5	0.96
Mn_3O_4	0.62	3	0.4	5.5E5	7.0E5	0.79
Cr_2O_3	0.69	10	>4.7	9.7E5	3.5E5	2.8
$Ca(OH)_2 \cdot xH_2O$	0.29	6	>3.6	4.8E5	3.3E5	1.5
Ele Arc Sim. Aero.	0.65	3	0.08	1.4E5	2.1E5	0.68
Ele Arc Sim. Aero.	1.2	4	0.2	2.5E5	3.6E5	0,69
Above w/o Mn	1.0	4	0.3	3.2E5	3.9E5	0.82
$H_2SO_4 \cdot xH_2O$	Very Low	0.06	<0.015	0	0	-

* Used non-standard three stage dilution (see text)
** From $Fe(CO)_5$

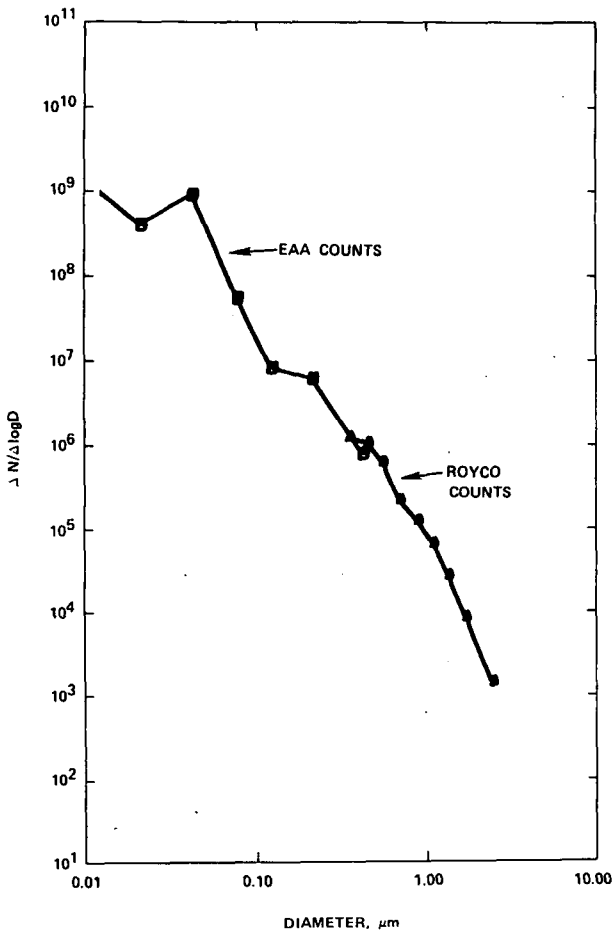

Figure 8. Comparison of measurements with the Royco optical particle counter and the EAA of the 0.78 g/m^3 Fe_2O_3 & Fe_3O_4 aerosol. The measurements with the Royco & EAA are in close agreement.

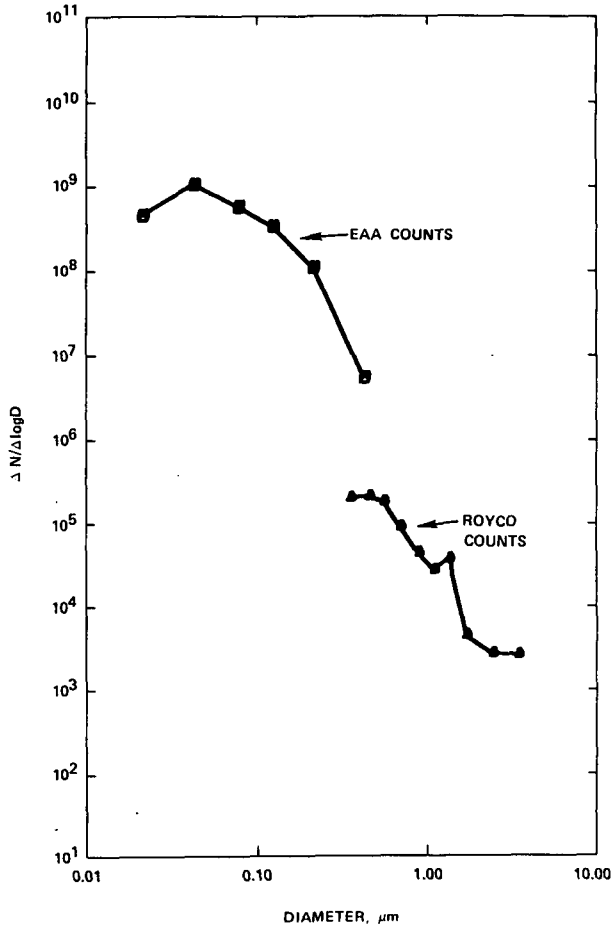

Figure 9. Comparison of measurements with the Royco and EAA of the 0.054 g/m^3 MgO aerosol. The measurements with the Royco and EAA do not agree with each other.

red iron oxide aerosols (Fe_2O_3) generated from iron pentacarbonyl ($Fe(CO)_5$), the ratio was as high as 30. SiO_2 and MgO aerosols had very high ratios of EAA to Royco counts.

The EAA and Royco instruments also did not count the same number of particles in the size range $0.3<D<0.6$ for the background aerosols. Eleven cases were examined for these background aerosols. The ratio of EAA to Royco counts (particles/cm^3) varied from 2.8 to 19.8. Some of the variability was due to the very low background particle concentration (usually about 2 particles/cm^3) and the EAA output was recorded with only one place accuracy. The average ratio of the EAA/Royco counts for the 11 cases was 7.7 with a variance of 25. Figure 6 shows a typical disagreement between the EAA and Royco counts (13 vs. 2.4).

VOLUME DISTRIBUTIONS

Tables 11 and 12 show the diameters of the largest particles counted and the volume median diameters. The SiO_2 aerosols had very few if any particles larger than 0.6 μm. Fe_2O_3 aerosols generated from $Fe(CO)_5$ also had few, if any, particles larger than 0.8 μm except at the very high solids loading (6 g/m^3). Both of these aerosols (SiO_2 and Fe_2O_3) were generated from liquids with high vapor pressures. All of the nitrates decomposed to form aerosols with high enough concentrations of particles larger than a 1 μm to be counted by the Royco with three stage dilution. Even dilute solutions containing nitrates yielded some super μm particles (see the MgO, 0.054 g/m^3 and ZnO, 0.087 g/m^3 aerosols in Table 12).

For most of the aerosols generated, the volume of those particles with diameters between the cut-off (concentrations too low to count) and 10 μm was probably a small amount relative to the measured volume because the volumes of the particles with diameters larger than 1 micron decreased rapidly (see Figure 10). However, the $Al_2O_3 \cdot 2H_2O$, $Ca(OH)_2 \cdot xH_2O$ and Cr_2O_3 aerosols have a large portion of their measured volume contained in large particles (see Figure 11). Volumes contained in particles larger than 10 μm were not measured because the Royco Model 200 does not size particles larger than 10 μm. Also the sample train (diluter and associated plumbing) was not designed for particles larger than about 10 μm.

When 1.8 g/m^3 of Fe_3O_4 with 5% $Ca(OH)_2 \cdot xH_2O$ aerosol was generated, only 10% of the generated volume was accounted for by the instrument particle counts. The volume distribution is shown in Figure 12a. For this aerosol and for some of the others, there was probably a mode in the volume distribution comprised of particles too large to measure with the instruments. This indicates that a limited amount of nitrate can be added to a given volume of ethanol; adding more than this limit results in a significant portion of the generated aerosol particles being too large to qualify as fine particulates. The 1.8 g/m^3 Fe_3O_4 aerosol was probably an example of this.

The 1.8 g/m^3 Fe_3O_4 aerosol was sampled by letting it impact a glass slide coated with adhesive. This method is probably satisfactory for obtaining a representative sample of particles larger than 10 μm if the density of the hollow particles is not too low. Photographs 6b and 7a show SEM photographs of samples of this Fe_3O_4 aerosol. One photograph was used to measure and count 494 particles. The volume distribution from this work is shown in Figure 12b. As is often the case in particle size distributions with less than a few thousand particles counted, not enough large particles were counted. Twenty-nine percent of the volume was contained in two particles, one 42.5 μm and the other 70 μm.

Some of the aerosols had a bimodal volume distribution in the measured size range (0.0075 to 10 μm). Figure 13 shows the bimodal size distribution of the $Al_2O_3 \cdot 2H_2O$, Fe_2O_3 and Fe_3O_4 aerosol (0.41 g/m^3).

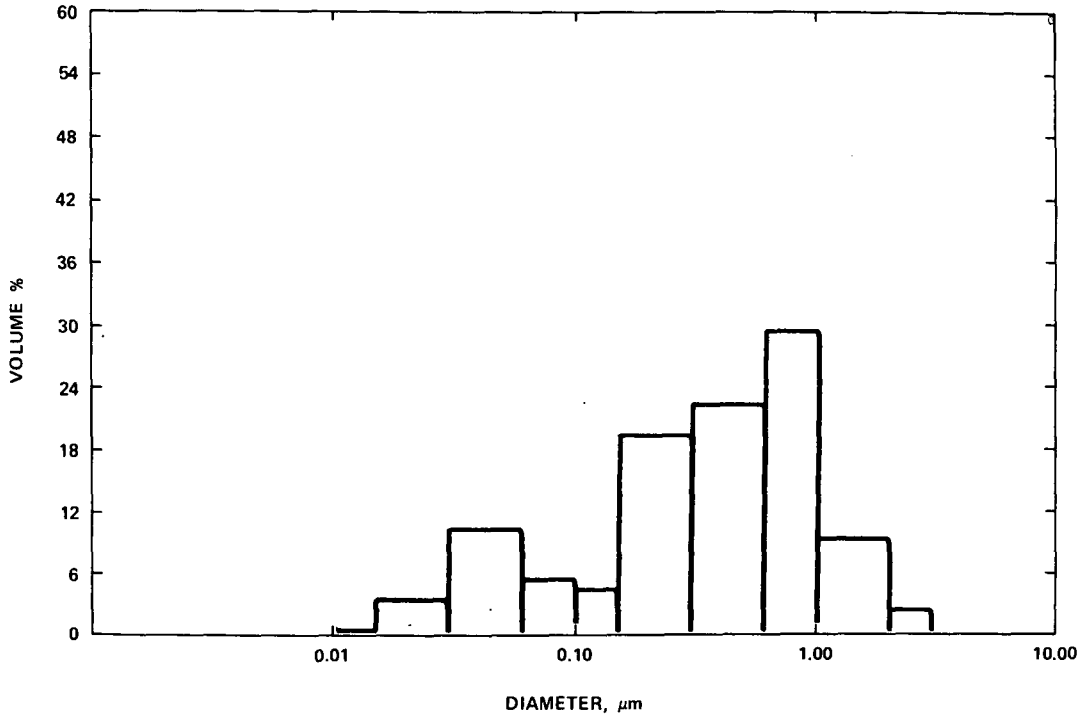

Figure 10. The volume distribution determined from EAA and Royco measurements of the 0.62 g/m^3 Mn_3O_4 aerosol. Most of the volume of aerosol particles appears to be included in the size range measured by the instruments.

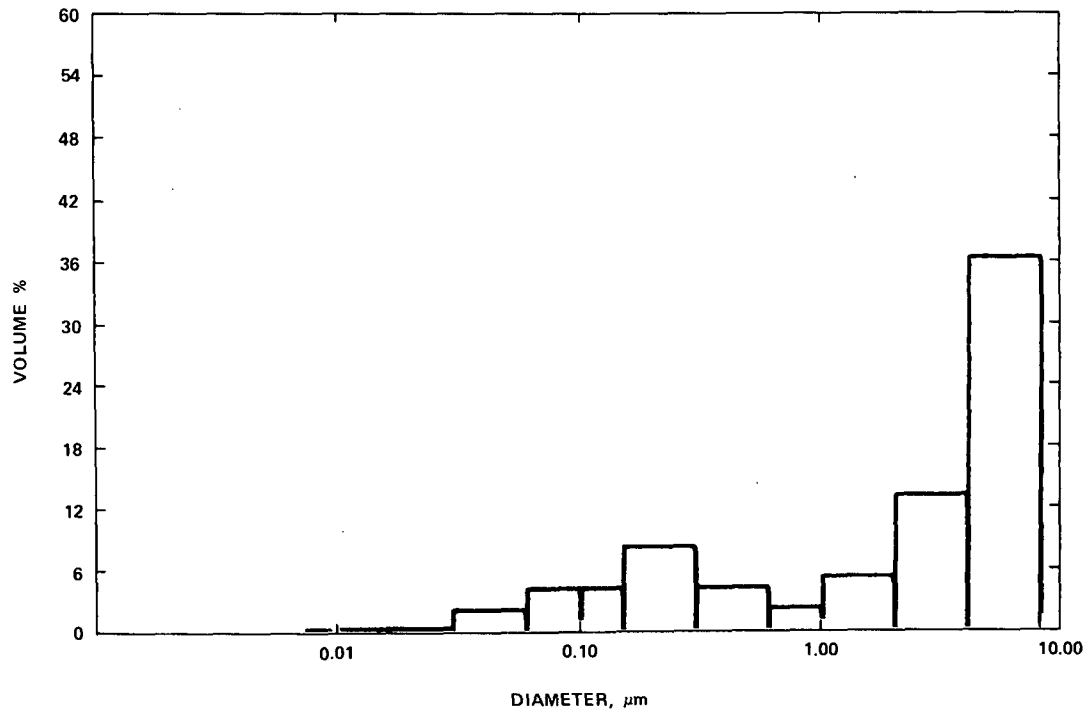

Figure 11. The volume distribution determined from EAA and Royco measurements of the 0.69 g/m^3 Cr_2O_3 aerosol. A significant portion of the volume of aerosol particles probably exists as particles larger than 10 μm.

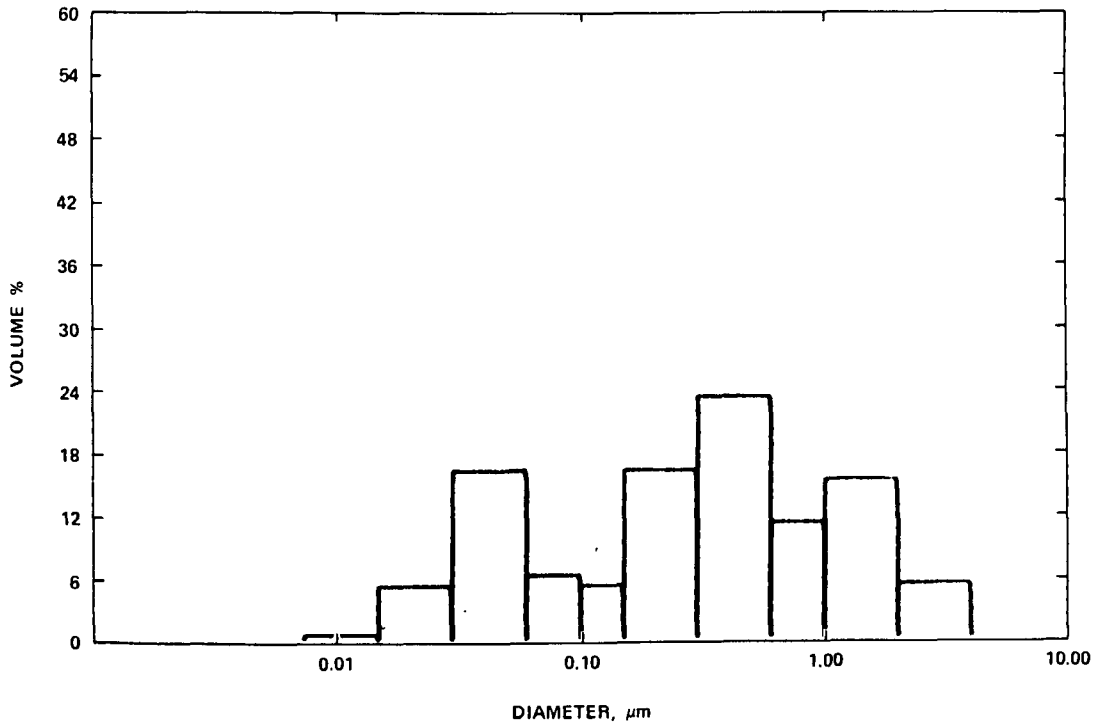

Figure 12a. The volume distribution determined from EAA & Royco measurements of the 1.8 g/m^3 Fe_3O_4 aerosol. This aerosol was found to have a volume mode of larger (D>10 μm) particles.

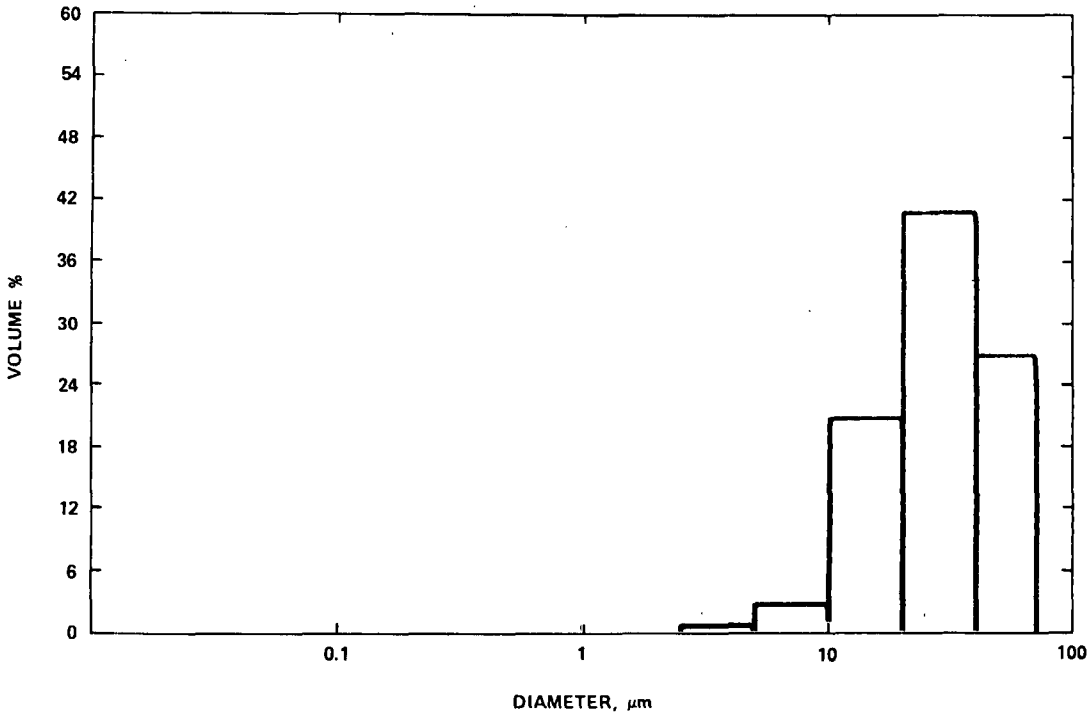

Figure 12b. Fe_3O_4 aerosol 1.8 g/m^3, the volume distribution of some large particles captured on a glass slide. Possibly 80-90% of the aerosol mass existed as large hollow particles.

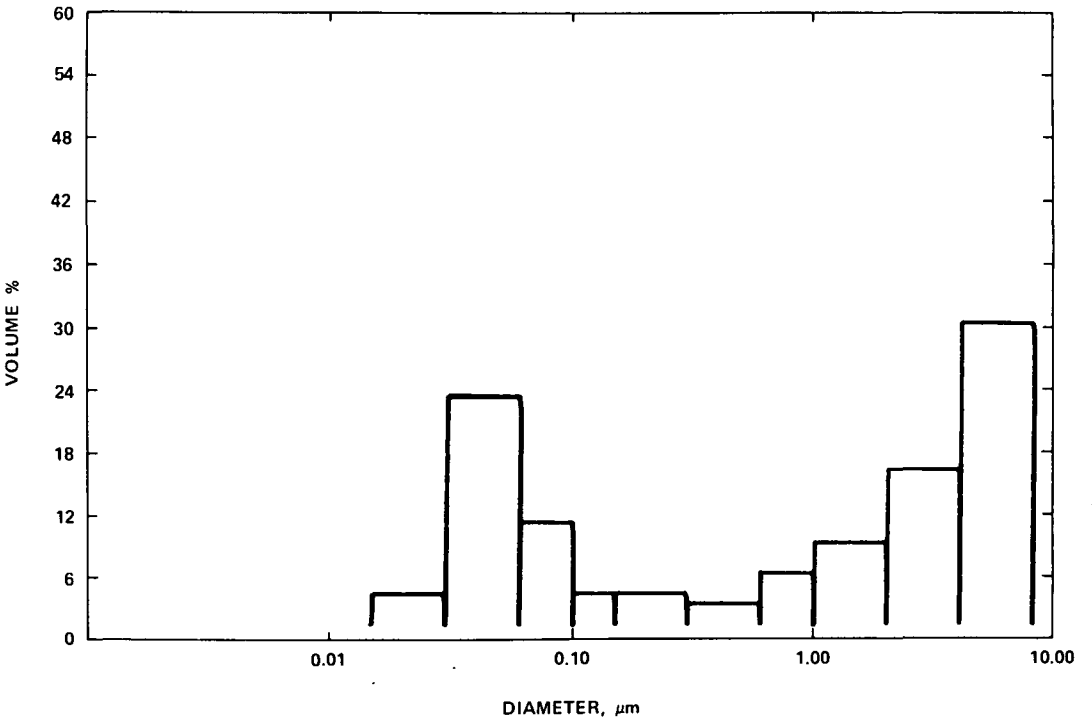

Figure 13. The volume distribution determined from EAA & Royco measurements of the 0.41 g/m^3 Al_2O_3 $2H_2O$, Fe_2O_3 and Fe_3O_4 aerosol. This aerosol has a bimodal distribution.

PARTICLE COMPOSITIONS

Table 13 shows the X-ray diffraction results. Compounds (usually nitrates) were dissolved in alcohol, sprayed and burned. The hot products of combustion rose vertically in the 25.4 cm diameter stack. The solid particles suspended in the fume were collected at the top of the stack by placing the rectangular nickel plated brass plate at a 45^o angle at the top of the stack. The amount of collected material varied from a few milligrams to about a gram. Burn times for collection were about 6 minutes. A part of each sample was immediately sealed in a glass capillary tube to await X-ray diffraction analysis. X-ray diffraction analysis did not yield the composition of those aerosols with amorphous particles.

TABLE 13. PARTICLE COMPOSITION

Compound (grams)	Solvent(s) (liters)	Particle Composition (X-ray diff.)
$Fe(NO_3)_3 \cdot 9H_2O$* 586g	Ethanol 1.5ℓ	Fe_2O_3 with a trace of Fe_3O_4
$Fe(NO_3)_3 \cdot 9H_2O$ 757g $Ca(NO_3)_2 \cdot 4H_2O$ 33g	Ethanol 2ℓ	Fe_3O_4 with some Fe_2O_3 (calcium not detected)
$Mn(NO_3)_2 \cdot 6H_2O$ 111g	Ethanol 1.5ℓ	Mn_3O_4 (hausmannite)
$Cr(NO_3)_3 \cdot 9H_2O$ 160.5g	Ethanol 1.5ℓ	Cr_2O_3
$Mg(NO_3)_2 \cdot 6H_2O$ 400g	Ethanol 2ℓ	Face centered cubic MgO (periclase)
$Mg(NO_3)_2 \cdot 6H_2O$ 200g	Ethanol 2ℓ	Same as above
$Zn(NO_3)_2 \cdot 6H_2O$ 468g	Methanol 2ℓ 40cc water	Hexagonal ZnO (zinkite) plus an unknown organic compound
$Zn(NO_3)_2 \cdot 6H_2O$ 362g	Ethanol 2ℓ	Hexagonal ZnO
$Cd(NO_3)_2 \cdot 4H_2O$ 101g	Methanol 2ℓ 200cc water	CdO plus $Cd(OH)NO_3H_2O$
$VOSO_4 \cdot xH_2O$ 69g	Methanol 1ℓ 100cc water	VO_2, V_2O_4, and V_2O_5
$Cd(NO_3)_2 \cdot 4H_2O$ 50.5g $VOSO_4 \cdot xH_2O$ 69g	Methanol 1ℓ 100cc water	Primarily $CdSO_4$ some CdO, $2CdO \cdot V_2O_5$, and VO_2, V_2O_4, and V_2O_5

*The $Fe(NO_3)_3 \cdot 9H_2O$ was exposed to the ambient air for two days prior to mixing into solution. Both the $Fe(NO_3)_3 \cdot$ crystals and the solution were reddish brown and probably already contained Fe_2O_3.

COAL FLY ASH FUME SIMULATION AEROSOL

Table 14 shows several characteristics of the coal fly ash fume simulation aerosol.

TABLE 14. CHARACTERISTICS OF THE COAL FLY ASH SIMULATION AEROSOL

Stack: Diameter, 0.425m; height, 3.04m

Fume Exit Temperature: 450°K (177°C)

Fume Exit Velocity: 5 m/s

Fume Flow Rate: 0.7 m^3/s, 0.51 kg/s

Particle Loading: 0.66 g/m^3 @ 450°K; 1.1 g/m^3 @ STP

Particle Mass Median Diameter: 1 μm from Celesco impactor;

Volume Median Diameter: 0.2 μm from EAA & Royco

Condensation Nuclei: $1.1x10^8$ particles/cm^3

Nominal Chemical Composition (wt%): 50% SiO_2, 30% Al_2O_3 and 20% Fe_2O_3

Color of Particles: most are pink, some are black

Bulk Density: about 0.3 g/cm^3; packed density: 0.9 g/cm^3

Electrical Resistivity: $2x10^{11}$ - $2x10^{12}$ ohm cm @ ambient temp.

Chemical Analysis

SEM with X-ray Non-Dispersive Analysis

Individual aerosol particles were analyzed using a SEM with an ETEC (Princeton Gamma-Tech) X-ray non-dispersive analysis system to determine if elements Si, Fe and Al existed separate from each other or were bound together in the same particle. Since the beam penetrates about 0.5 μm into the sample or substrate, only particles larger than 0.5 μm diameter could be sampled without having excessive background signal. Ten particles were sampled. One particle contained Si, three contained all three elements, and six of the particles contained Si and Al, but not Fe. This is encouraging since coal fly ash usually contains Si and Al found together as mullite ($3Al_2O_3 \cdot 2SiO_2$). Most of the particles had more Al present than Si; however, the Al to Si ratios were different for each particle. Analysis of an area on the graphite pedestal without any particles visible on the SEM indicated that perhaps there was a fine "coating" of small particles containing Si. These were too small to be seen with the SEM on the graphite substrate. The background signal was high for this measurement. Analysis of a sample which collected on the flame cone and did not flow up the stack showed that the sample contained Al as the major component; next in abundance was Fe; the Si content was about 10% that of Al.

Cyclotron Excitation

The coal fly ash simulation aerosol was sampled for one minute with the Lundgren Impactor (Model 4220 operating at a flow rate of 4.72×10^{-4} m^3sec (4 CFM)) using the first stage of the diluter to cool and dilute the fume. An 0.8 μm Nuclepore filter was located down stream from the Lundgren Impactor. The solids loading on the filter was so high, the flow rate dropped 25% during the sampling time. The collected samples were analyzed by Crocker Nuclear Laboratory (University of Calif., Davis) using cyclotron excitation. Table 15 shows the results. The samples were also examined with an optical microscope. The particle sizes on the stages overlapped each other (see Table 15). Stages 1 and 2 had more uniform particles than stages 3 and 4. Many of the particles on stages 3 and 4 were nonspherical agglomerates of smaller particles. On stages 1-3, there was good separation of the captured particles indicating little likelihood of particle bounce-off. The particles on the Nucleopore filter were stacked on top of one another and it was not possible to determine sizes.

TABLE 15. Cyclotron Excitation Analysis of Lundgren Impactor and Nuclepore Filter Samples of the Coal Fly Ash Simulation Aerosol.

Stage	Theoretical Dia. Range Spheres of Density 2 g/cm³ (μm)	Observed Diameter Range (μm)	Wt. Al ng/cm²	Wt. Si ng/cm²	Wt. Fe ng/cm²	Total Wt. ng/cm²	Wt.%
1	7.2-140	>7	730	140	100	970	0.5
2	3.5-12	2-7	4,500	120	3,600	8,200	4.0
3	1.4-3.5	1-3	3,000	860	2,500	6,400	3.0
4	0.35-1.4	<1-10	2,600	2,500	2,600	7,700	4.0
Filter	<0.35	-	40,000	103,000	21,000	164,000	88.0
Total Wt.			51,000	107,000	30,000	188,000	100
Wt.%			27	57	16		
Wt.% as oxide			30	59	11		
Vol% as oxide*			35**	60	5		
Vol% stages 1-3*			75**	11	14		
Vol% on filter*			31**	65	4		

* Handbook values of the densities were used to calculate particle volumes.

**As $Al_2O_3 \cdot 2H_2O$

Eighty-eight percent of the sample mass was located on the filter indicating the small equivalent aerodynamic diameter of most of the simulation aerosol particles. Some of the Fe_2O_3 appears to be lost in the stack or diluter. The nominal wt% generated, based on the weights of nitrates in the basic solution, is 50% SiO_2, 30% Al_2O_3 and 20% Fe_2O_3; the collected samples had 59% as SiO_2, 30% as Al_2O_3 and 11% as Fe_2O_3. The wt% of oxides on the filter sample was 68% as SiO_2, 23% as Al_2O_3 and 9% as Fe_2O_3.

X-ray Diffraction

X-ray diffraction analysis showed the bulk of the particles to be amorphous. For example, after exposure to X-rays for 48 hours, one sample collected on the flat plate did not yield a pattern. Another sample collected on a 0.6 cm diameter stainless steel rod with its longitudinal axis normal to the flow had a faint pattern believed to be from a mixture of iron oxides. This sample was brown however and the bulk of the aerosol particles are pinkish. When the oxides of each element (Si, Al and Fe) were generated separate from the others, samples of the oxides of Si and Al were amorphous. The iron oxide sample consisted of crystalline Fe_3O_4 and Fe_2O_3.

Because the particles are amorphous, the X-ray diffraction analysis of the coal fly ash simulation aerosol did not conclusively show what compounds the Si, Al and Fe form.

Size Distribution

Figures 14 (plotted as $\Delta N/\Delta \log D$ vs. D) and 15 (plotted as N(D) vs. D) show the size distribution of the coal fly ash simulation aerosol generated on 22 November 1976. Figure 16 shows the size distribution of the coal fly ash simulation aerosol generated again on 3 December 1976. Figures 15 and 16 show the reproducibility when solutions with the same chemical composition are burned under the same conditions on different days. Figures 17 and 18 show the volume distribution of the coal fly ash simulation aerosol (generated on 22 November and on 3 December); again the reproducibility is good.

The particle counts and size distribution were reproducible from run to run, but the volume of particles counted did not agree with the mass of particles generated. The apparent mass determined from the particle counts was four times the generated mass, suggesting the presence of hollow particles, aggregates with densities differing from the handbook values or an instrumental error. Because the EAA and Royco did not count the same number of particles in the diameter range 0.3 to 0.6 μm where their particle counts overlap, there definitely was an instrumental "error" in that size range.

Dr. Raymond L. Chuan (California Measurements Inc., Sierra Madre, CA) came to China Lake and measured the mass distribution. He used a ten stage Celesco C1000 cascade impactor equipped with quartz crystal sensors (Chuan, 1976). Table 16 shows a comparison of his measurements and those of the EAA and Royco. The measured solids loading using the impactor accounted for 42% of the generated solids, which is more reasonable than the 400% obtained with the ROYCO-EAA measurement system. A particle density of 2 g/cm^3 was used to

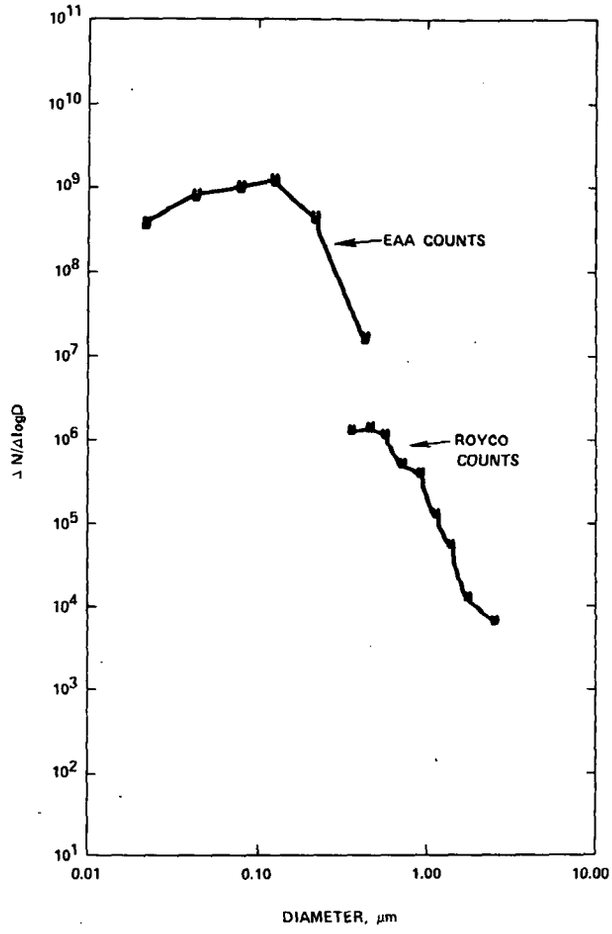

Figure 14. The size-distribution, plotted as $\Delta N/\Delta \log D$ vs. D, from measurements with the EAA and Royco of the coal fly ash simulation aerosol generated 22 November 1976.

determine the particle sizes collected on each impactor stage and to determine the mass of the particles counted by the ROYCO and EAA. The handbook value of density is 2.6 g/cm^3.

An examination of Table 16 shows that the measurements of the Celesco cascade impactor are in fair agreement with the ROYCO optical particle counter but in very poor agreement with the EAA.

Inasmuch as 88% of the aerosol passed through the Lundgren impactor without impacting any of the stages (see Table 15), the EAA and Lundgren measurements agreed with each other.

Table 17 gives a comparison of the measurements of the Celesco and Lundgren impactors. The particle mass median diameter determined from the Lundgren data is less than 0.35 μm; from the Celesco data 1.05 μm (see Figures 19 and 20). The volume median diameter determined from the ROYCO-EAA data is 0.23 μm (see Figure 20).

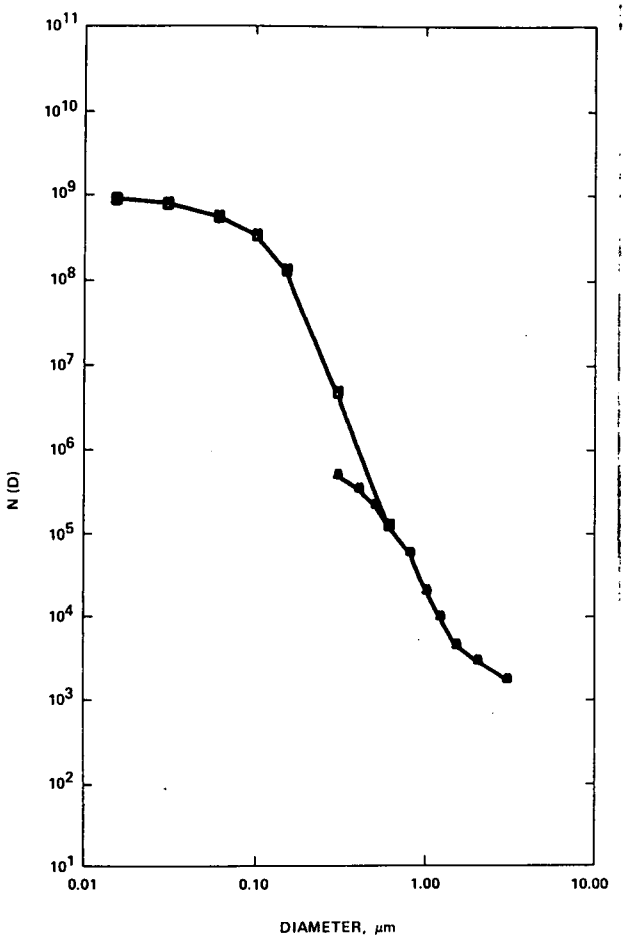

Figure 15. The size distribution from measurements with the EAA and Royco of the fly ash simulation aerosol generated 22 November 1976.

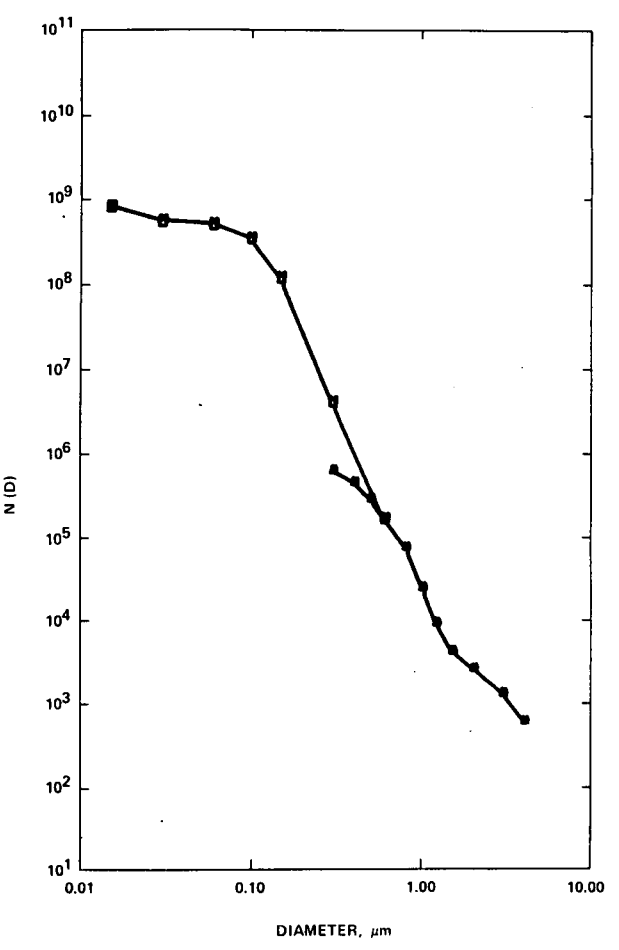

Figure 16. The size distribution from measurements with the EAA and Royco of the fly ash simulation aerosol generated 3 December 1976.

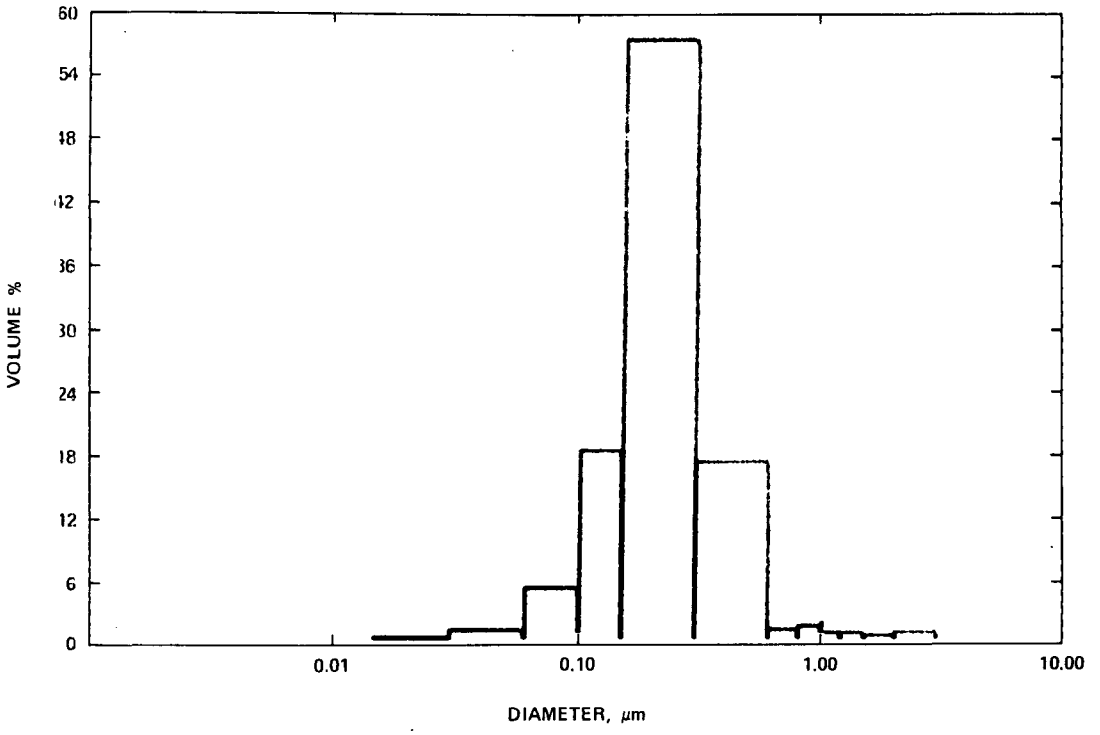

Figure 17. The volume distribution determined from the EAA and Royco measurements of the fly ash simulation aerosol generated 22 November 1976.

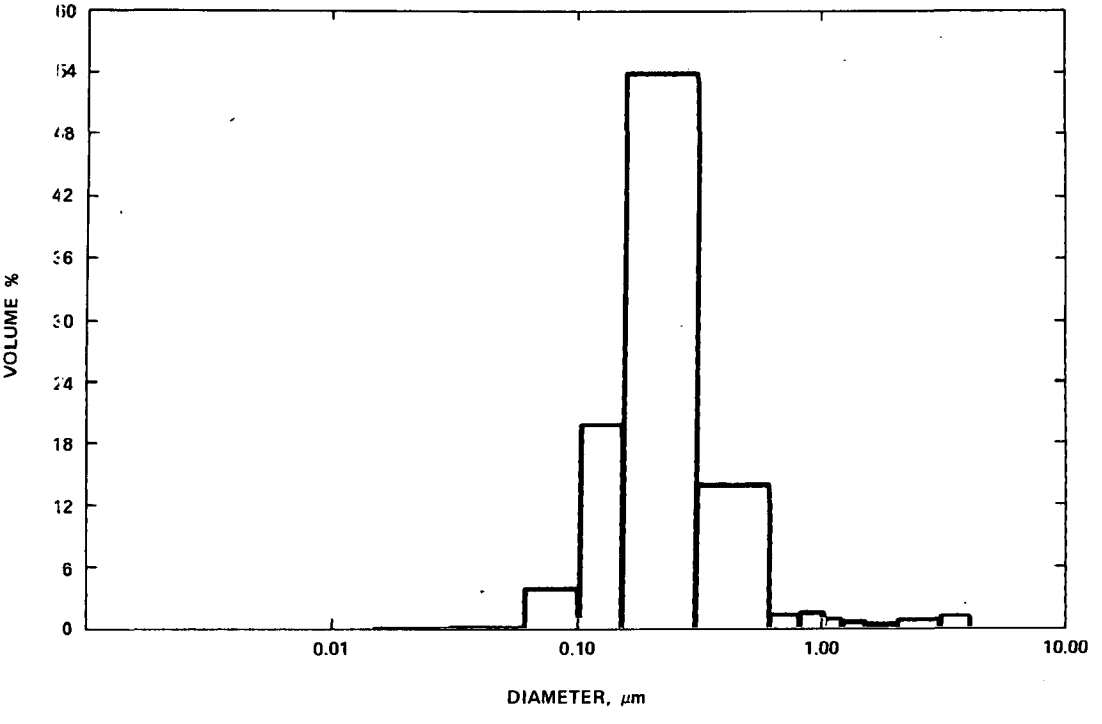

Figure 18. The volume distribution determined from the EAA and Royco measurements of the fly ash simulation aerosol generated 3 December 1976.

TABLE 16. MEASURED MASS DISTRIBUTION OF THE COAL FLY ASH SIMULATION AEROSOL (0.66 g/m^3 of aerosol is generated)

Celesco Cascade Impactor		Whitby Electrical Aerosol Analyzer		Royco Optical Particle Counter	
Diameter Interval μm	Solids Loading g/m^3	Diameter Interval μm	Solids Loading g/m^3	Diameter Interval μm	Solids Loading g/m^3
		0.015			
			0.020		
0.05		0.06			
	0.019		0.110		
0.1		0.1			
	0.027		0.408		
0.2		0.15			
	0.013		1.31		
0.4		0.3		0.4	
	0.050		0.38		0.048
0.8		0.6		0.8	
	0.088				0.053
1.6				1.5	
	0.070				0.024
3.2				3.0	
	0.013				
6.4					
Total Loading	0.28		2.23		0.125

TABLE 17. IMPACTOR DATA (diameter range based on a density of 2 g/cm^3)

Approximate Diameter Range	Wt% in Diameter Range: Celesco Impactor	Wt% in Diameter Range: Lundgren Impactor
0.05-0.4	21	88
0.4-.8	18	4
0.8-1.6	31	3
1.6-6.4	29	4
>6.4	0	0.5

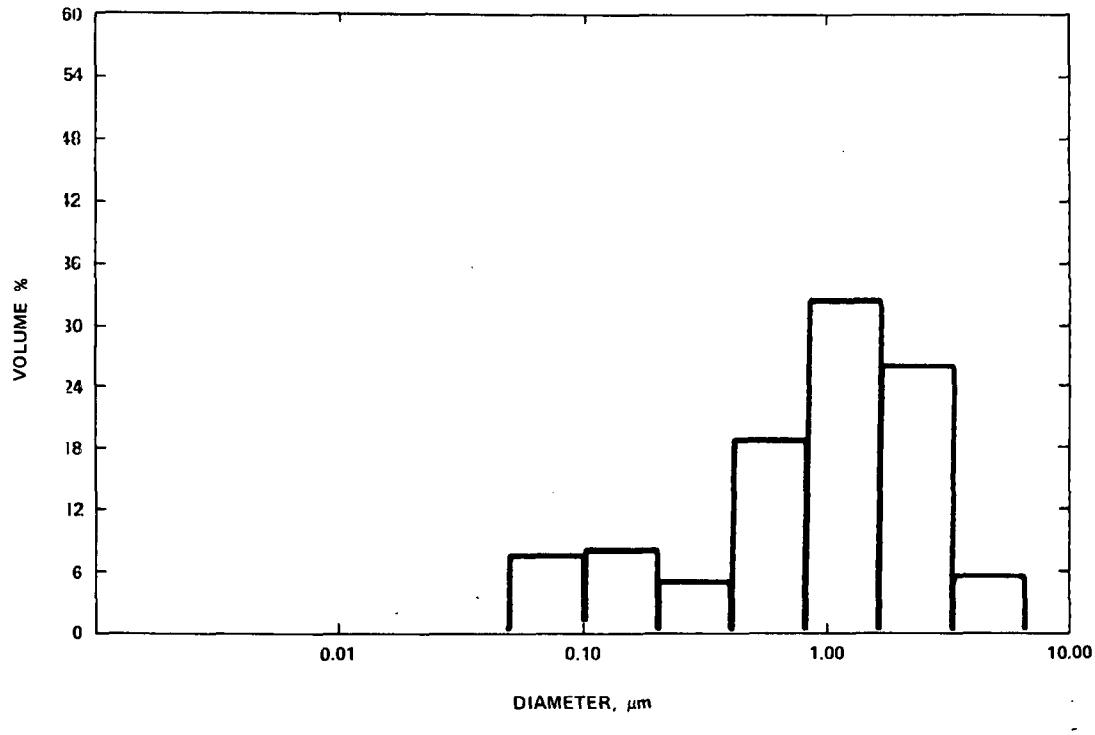

Figure 19. The mass distribution of the fly ash simulation aerosol measured with a Celesco cascade impactor assuming a particle density of 2 g/m^3. (Courtesy of Dr. R. L. Chuan, California Measurements Inc. Sierre Madre, CA. Note how this mass distribution compares with the volume distribution shown in Figs. 17 and 18.

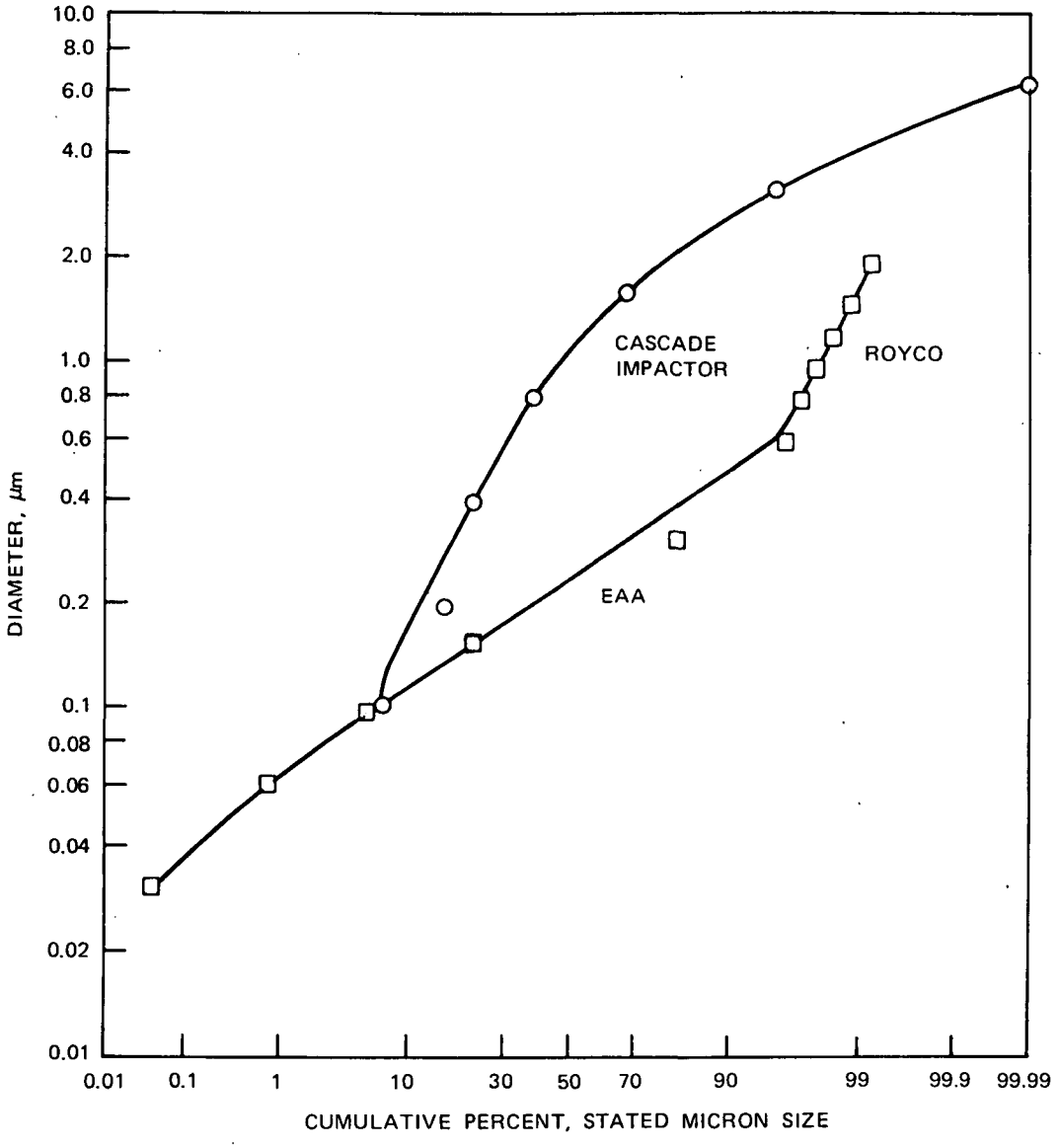

Figure 20. The coal fly ash simulation aerosol size distribution as a function of particle size as determined with a cascade impactor (mass distribution) and with the EAA and Royco (volume distribution).

Particle Resistivity

The particle resistivity has a large effect on the collection efficiency of electrostatic precipitators. Electrostatic precipitators are installed in many coal burning plants. Thus, it is important to have coal fly ash simulation aerosols with various resistivities to conduct all of the necessary precipitator tests. To accomplish this, lithium salts were added to the basic solution (described in Section 4) used to generate the coal fly ash simulation aerosol. $LiNO_3$ and $LiClO_4 \cdot 3H_2O$ are soluble in the solution; on decomposing in the flame they yield Li_2CO_3 and LiCl.

Table 18 shows the particle resistivity of the simulation aerosol with 0.43 grams of Li_2CO_3 per gram of simulation aerosol (SiO_2, Fe_2O_3, Fe_3O_4 and $Al_2O_3 \cdot 2H_2O$) and also another with 0.16 g of LiCl per gram of simulation aerosol.

The resistivities were measured either with samples taken from the flame holder above the flame cone or with samples collected by placing an aluminum screen at the aerosol exit at the top of the stack. Only a small amount of aerosol particles collected on the screen (about 2 grams). With such small quantities, standard procedures for measuring resistivities could not be used. The resistivities shown in Table 18 do, however, show that even with small samples at room temperature and low humidity there is a difference in the particle resistivities when lithium is present in the particles.

A large amount of lithium carbonate (0.43 g/g) was used in the simulation aerosol to measure an extreme case. Smaller amounts of lithium carbonate should be sufficient to adequately alter the particle conductivity. Figures 21 and 22 show the size and volume % distributions of the coal fly ash simulation aerosol with lithium carbonate. Both are close to the measured distributions of the fly ash simulation aerosol without added lithium. The generation rate (as particle volume per m^3 of fume) increased from 0.25 cm^3/m^3 without lithium to 0.39 cm^3/m^3 with lithium. With lithium added, the

Table 18. Particle Resistivity* of Coal Fly Ash Simulation Aerosol ($T=21^{\circ}C$, RH=27%)

Aerosol	Collection Point	Measured Resistivity* (ohm cm)
Simulation aerosol without lithium	Bottom of stack	1×10^{13}
	Top of stack	2×10^{12}
With 0.43g Li_2CO_3 added per g simulation aerosol	Bottom of stack	5×10^{6}
With 0.16g LiCl added per g simulation aerosol	Bottom of stack	2×10^{8}
	Top of stack	2×10^{11}

*These resistivities were measured with small samples of material at room temperature and may not be comparable to standard resistivity measurements.

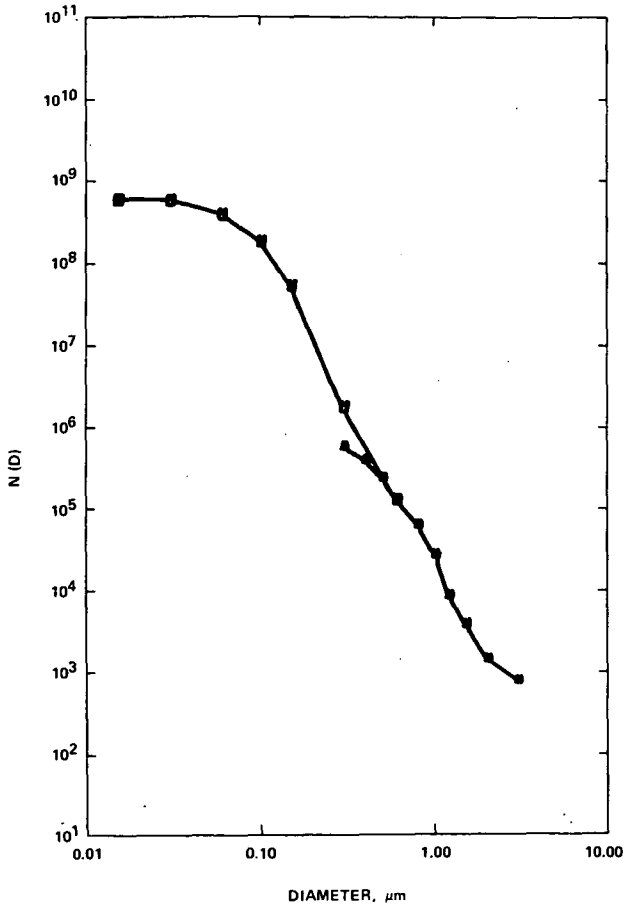

Figure 21. The size distribution of the coal fly ash simulation aerosol with Li_2CO_3 added to increase the particle conductivity. The size distribution is similar to that of the simulation aerosol; adding the Li_2CO_3 had a small effect.

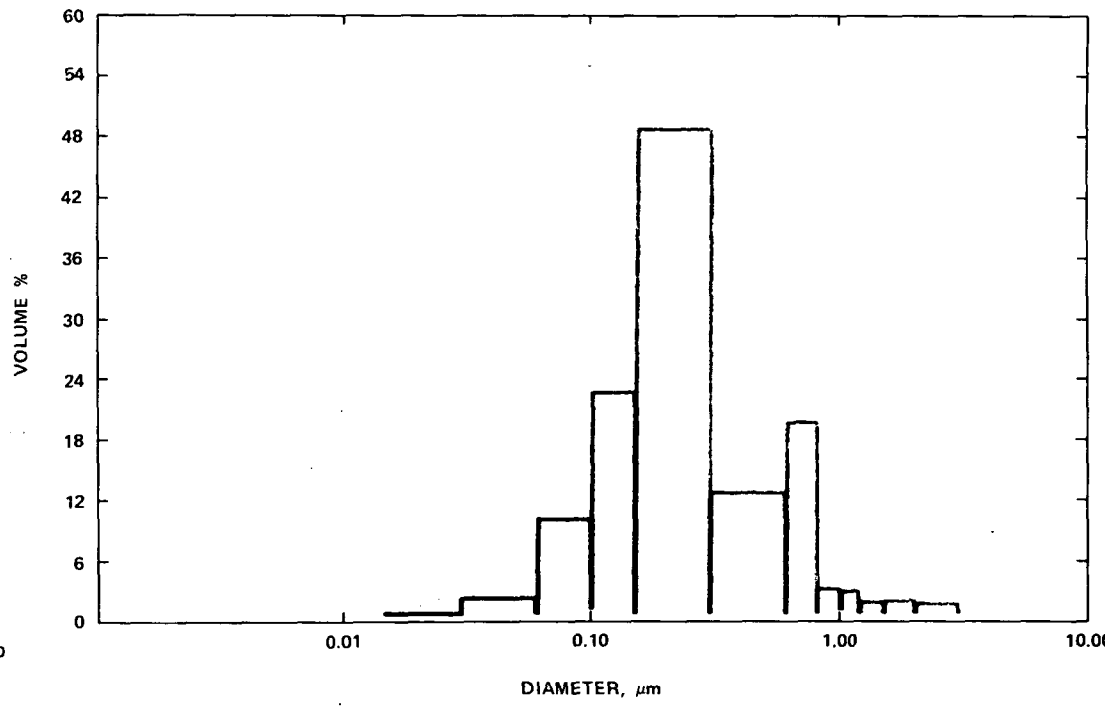

Figure 22. The volume distribution determined from the EAA and Royco measurements of the coal fly ash simulation aerosol with Li_2CO_3 added.

Royco counts were essentially unchanged. There was a reduction in the particle concentration measured by the EAA (compare Figures 15 or 16 with 21). Thus, there was better agreement between the Royco and EAA measurements with added lithium.

Sulfur Dioxide

CS_2 is compatible with the basic solution. Immediately after mixing there is a slight reaction with a few bubbles formed but it does not appear to be a problem. The solution with CS_2 should be usable for a few hours after mixing.

When a solution of CS_2 in ethanol (38 g CS_2 per liter of ethanol) was burned there were some small particles formed. No particles larger than 0.06 μm were detected (see Table 12). After combustion more than 99.8% of the sulfur appeared to exist as SO_2 gas. The remainder (those particles detected) was probably $H_2SO_4 \cdot xH_2O$.

Particle Size Distributions of the Components of the Simulation Aerosol

Since the simulation aerosol is generated by burning the basic solution of 3 solutes [$Al(NO_3)_3 \cdot 9H_2O$, $Fe(NO_3)_3 \cdot 9H_2O$ and $(CH_3)_2Si(OC_2H_5)_2$], in ethanol, simpler aerosols can be made by burning solutions with only one or two solutes. Solutions of all the seven possible combinations (solvent plus 1, 2 or 3 solutes) were burned and the aerosol particle size distributions measured. The weight (per liter of ethanol) of each solute present remained the same as in the basic solution described in Section 4. Figures 15-16 and Appendix B show the size distributions of these aerosols. By laying one figure over another, it was easy to compare the measured size distribution of one aerosol with another. The results of the comparisons follow:

1. The contribution of Fe_2O_3-Fe_3O_4 particles to the coal fly ash simulation aerosol particle counts was very little; burning the basic solution or the basic solution without $Fe(NO_3)_3 \cdot 9H_2O$ resulted in about the same particle counts. This was in agreement with the generation rates; 0.016 cm^3/s as Fe_2O_3-Fe_3O_4 generated vs. 0.16 cm^3/s of the other oxides and also in agreement with the cyclotron excitation analysis results (Table 15) where only 5% of the aerosol volume was Fe_2O_3-Fe_3O_4.

2. The $(CH_3)_2Si(OC_2H_5)_2$ decomposed to form an aerosol which the electrical aerosol analyzer could not measure satisfactorily. Most of the aerosol particle mass was composed of particles too small to be measured by the optical particle counter.

3. When SiO_2 was present in any of the aerosols it completely dominated the particle counts by the electrical aerosol analyzer (EAA); these counts changed little regardless of what else was in the aerosol.

ELECTRIC ARC FURNACE FUME SIMULATION AEROSOLS

Tables 19 and 20 show several of the characteristics of two electric arc furnace (EAF) fume simulation aerosols. EAF aerosol A was generated using the 0.25 m diameter stack without a reducer at the top. EAF aerosol B was generated using the 0.25-m stack with a 0.15-m reducer at the top. The reducer lowers the gas flow thus increasing the aerosol solids loading and exit temperature.

Figures 23-26 show the size and volume distribution of electric arc furnace simulation aerosols A and B. Figure 27 shows the EAA and Royco particle counts of aerosol A plotted as $\Delta N/\Delta \log D$ vs. D. For both aerosol A and B the agreement between the EAA and Royco counts is good. The particle loadings of A and B determined from the EAA and Royco counts agree with the generation rates (see Table 9); the particle loading ratio, counted/generated, was 0.40 and 0.26 for aerosol A and B, respectively. Aerosol B with a higher solids loading has a larger median volume diameter, 0.2 vs. 0.08 μm for A. Figure 28 shows N(D) vs. D for both aerosol A and B. There is not a great deal of difference in these size distributions. Aerosol A has a higher concentration of particles with $D<0.13$ μm and a lower concentration of particles with $D>0.13$ μm. Other details of the particle counts are given in Tables 9, 10, 12 and Appendix C.

TABLE 19. CHARACTERISTICS OF ELECTRIC ARC FURNACE SIMULATION AEROSOL A

Stack: Diameter, 0.25 m; Height, 3.5 m

Fume Exit Temperature: 762°K (489°C)

Fume Exit Velocity: 7.6 m/s

Fume Flow Rate: 0.38 m^3/s; 0.16 kg/s

Particle Loading: 0.65 g/m^3 (1.8 g/m^3 @ STP)

Particle Volume Median Diameter: 0.08 μm*

Condensation Nuclei: 3×10^8 particles/cm^3

Nominal Chemical Composition: 50% Fe_2O_3,
20% Cr_2O_3,
15% MgO,
15% MnO

Nominal Density (Handbook values): 4.8 g/cm^3

Particle Color: Brownish black

*Median of those particles sized and counted

TABLE 20. CHARACTERISTICS OF ELECTRIC ARC FURNACE SIMULATION AEROSOL B

Stack: Exit diameter 0.15 m; Height 3.5 m

Fume Exit Temperature: 931°K (658°C)

Fume Exit Velocity: 12.5 m/s

Fume Flow Rate: 0.21 m^3/s, 0.073 kg/s

Particle Loading: 1.2 g/m^3 (4.0 g/m^3 @ STP)

Particle Volume Median Diameter: 0.2 μm*

Condensation Nuclei 2.4×10^8 particles/cm^3

Nominal Chemical Composition: 50% Fe_2O_3,
20% Cr_2O_3,
15% MgO,
15% MnO

Nominal Density (Handbook values): 4.8 g/cm^3

Particle Color: Brownish black

*Median of those particles sized and counted

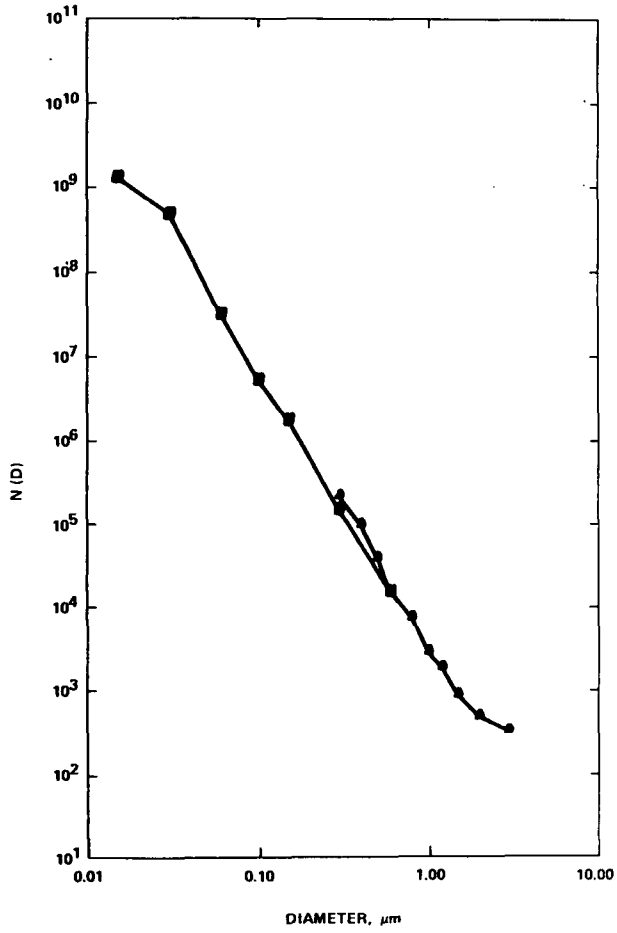

Figure 23. Electric arc furnace simulation aerosol A (0.65 g/m^3) size distribution from measurements with the EAA and Royco.

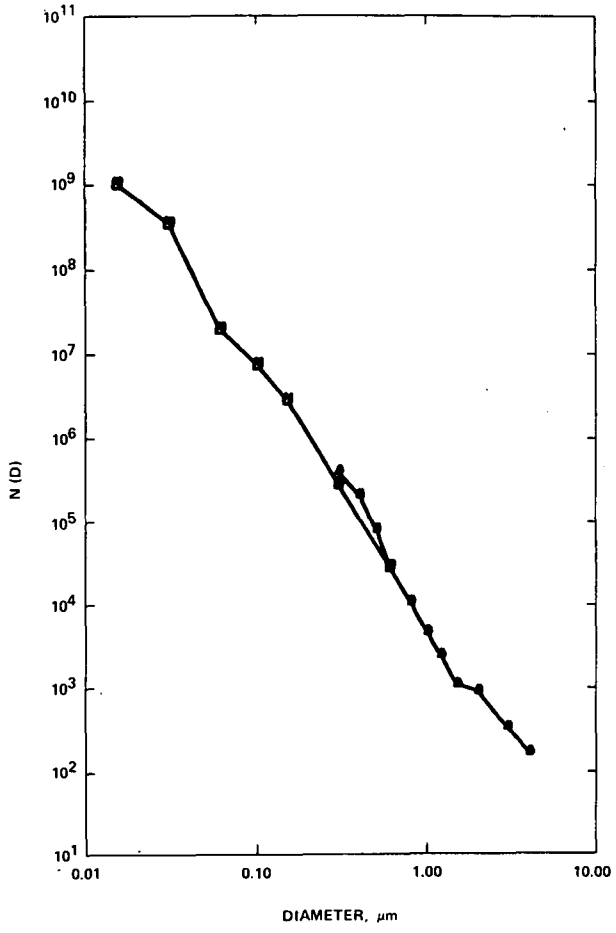

Figure 24. Electric arc furnace simulation aerosol B (2.1 g/m^3) size distribution from measurements with the EAA and Royco.

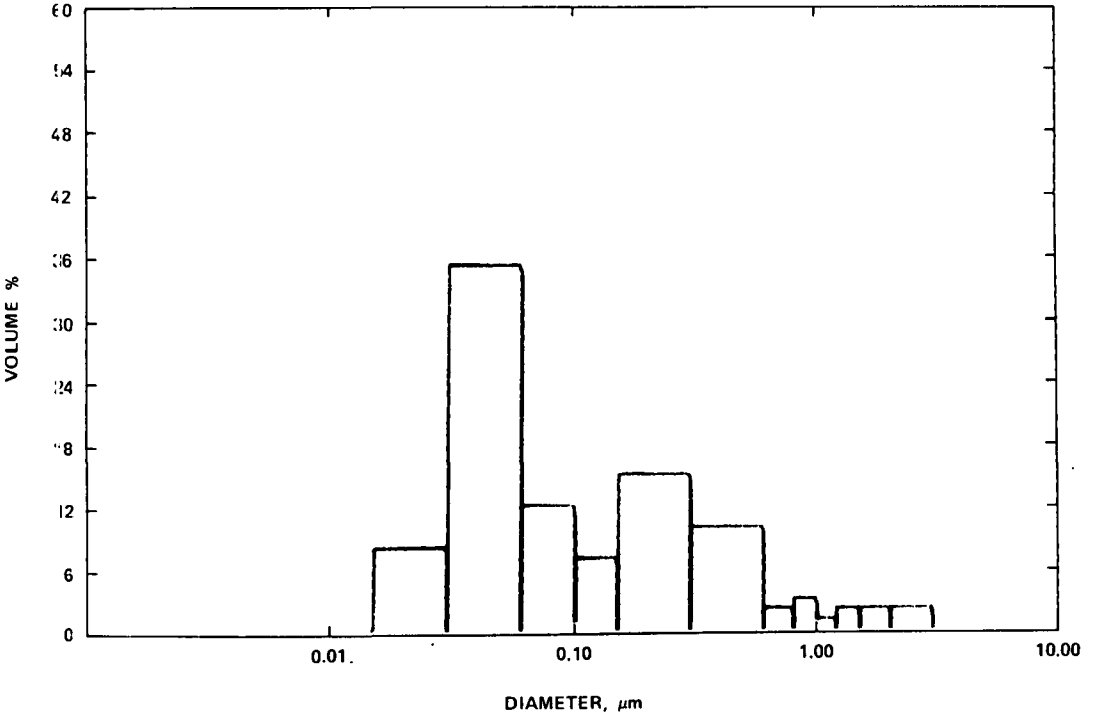

Figure 25. The volume distribution determined from EAA and Royco measurements of electric arc furnace simulation aerosol A (0.65 g/m^3).

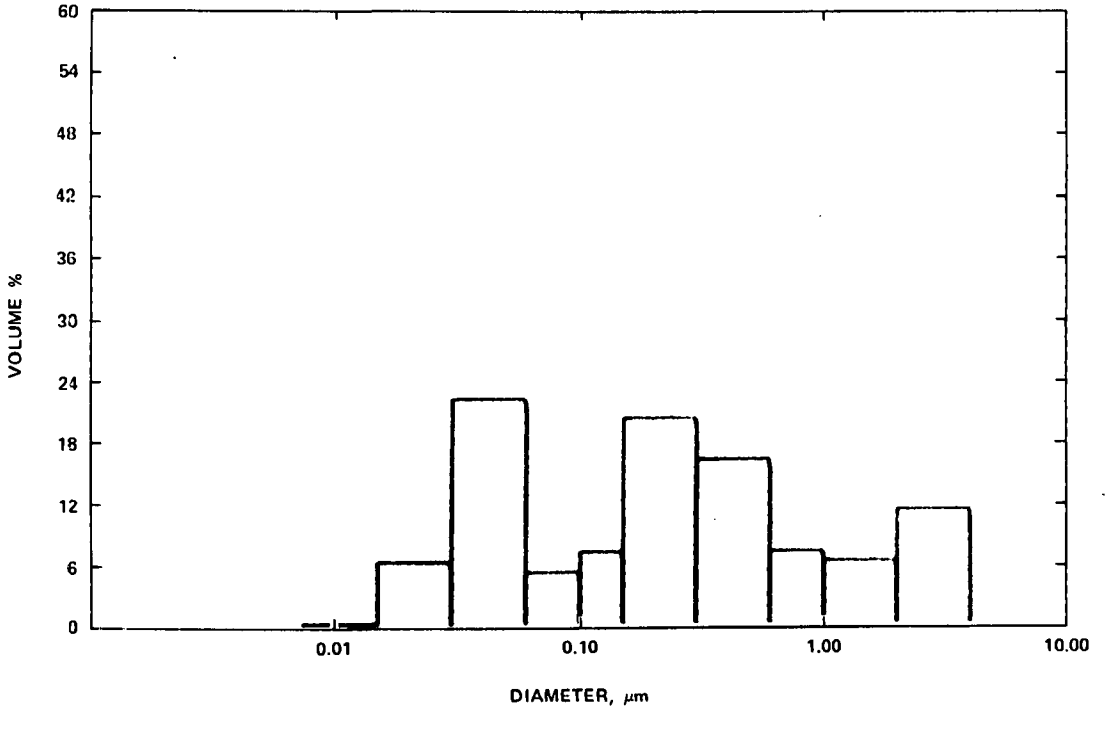

Figure 26. The volume distribution determined from EAA and Royco measurements of electric arc furnace simulation aerosol B (1.2 g/m^3).

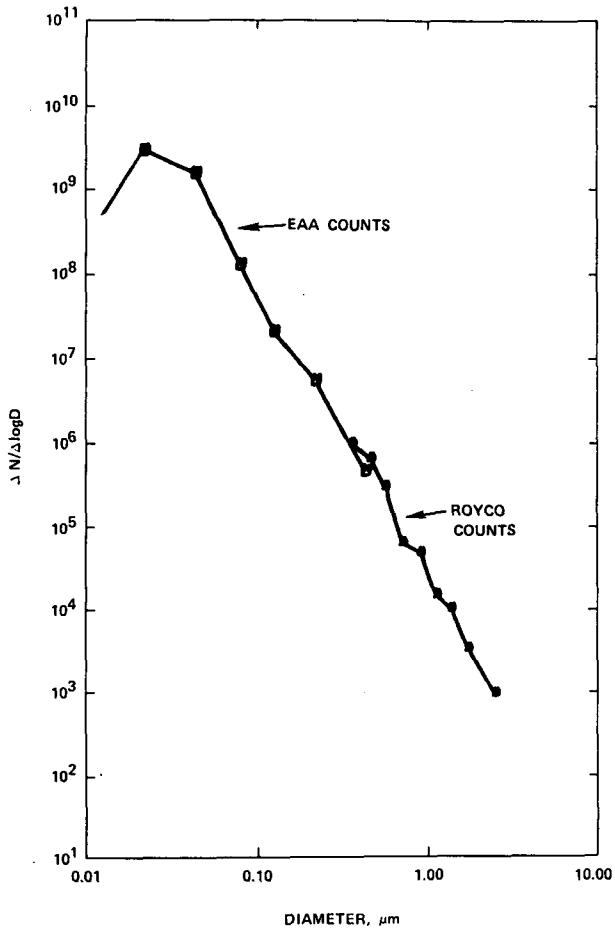

Figure 27. Electric arc furnace simulation aerosol A (0.65 g/m^3) size distribution, plotted as $\Delta N/\Delta \log D$ vs. D.

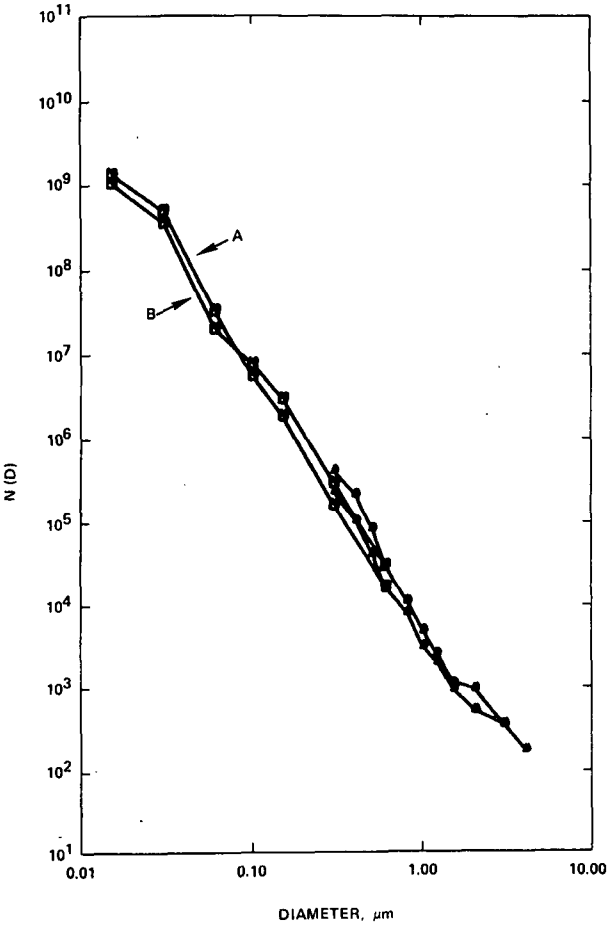

Figure 28. The measured size distributions of the electric arc furnace simulation aerosols A and B are nearly the same.

BASIC OXYGEN FURANCE FUME SIMULATION AEROSOLS

Tables 21 and 22 show several of the characteristics of two basic oxygen furnace fume simulation aerosols. Simulation aerosol AA (Table 21) has a very high particle loading (6 g/m^3 hot, 16.8 g/m^3 @ STP) of red Fe_2O_3; 95% of the particle volume was contained in particles with diameters between 0.15 and 3 μm. Simulation aerosol AA was generated from a solution of $Fe(CO)_5$ in acetone (see Section 4). Simulation aerosol BB (Table 22) was primarily Fe_3O_4 with some Fe_2O_3 and $Ca(OH)_2 \cdot xH_2O$; it had a large portion of the particle mass in particles with diameters greater than 10 μm. It was generated from a solution of $Fe(NO_3)_3 \cdot 9H_2O$ and $Ca(NO_3)_2 \cdot 4H_2O$ in ethanol (see Section 4). Lowering the concentration of solutes will reduce the particle loading but will also reduce the portion of large particles.

TABLE 21. CHARACTERISTICS OF BASIC OXYGEN FURNACE FUME SIMULATION AEROSOL AA

Stack: Exit diameter, 0.15 m; Height, 3.5 m

Fume Exit Temperature: $764^{o}K$ ($491^{o}C$)

Fume Exit Velocity: 10 m/s

Fume Flow Rate: 0.17 m^3/s; 0.073 kg/s

Particle loading: 6 g/m^3 (16.8 g/m^3 @ STP)

Particle Volume Median Diameter: 1.05 μm

Condensation Nuclei: 3.9 - $29x10^8$ particles/cm^3

Nominal Chemical Composition: 100% Fe_2O_3

Nominal Density (Handbook values): 5.12 g/cm^3

Particle Color: Red

TABLE 22. CHARACTERISTICS OF BASIC OXYGEN FURNACE FUME SIMULATION AEROSOL BB

Stack: Exit diameter, 0.15 m; Height, 3.5 m

Fume Exit Temperature: $913^{o}K$ ($640^{o}C$)

Fume Exit Velocity: 12.7 m/s

Fume Flow Rate: 0.21 m^3/s; .076 kg/s

Particle Loading: 1.8 g/m^3 (6.0 g/m^3 @ STP)

Particle Volume Median Diameter: 0.3 μm*

Nominal Chemical Composition: 95% Fe_2O_3, 5% CaO

Nominal Density (Handbook values): 4.8 g/cm^3

Particle Color: Black

Magnetic Properties: Highly magnetic

*Median of only those particles sized and counted with the EAA and Royco

Figures 29-31 show the size and volume % distribution of aerosol AA. The measurements were only approximate because only one reading was taken for each size range. The instruments were then shut off to prevent damage. Even with the 38,700 dilution factor too many particles entered the sample train and most surfaces of the instruments in contact with the diluted aerosol were left with a coating of red Fe_2O_3. The particle counts of sizes between 0.6 and 1.2 μm were estimated because the Royco was saturated. The Royco counted high background counts (e.g., 40 particles/cm^3 with D>2 μm) for several hours after the test. The EAA appeared to operate satisfactorily until this experiment was completed; however, it would not function properly for several days thereafter. Other details of the particle counts of aerosol AA are given in Tables 9, 10, 12 and Appendix C.

Figures 12a and 12b show the volume distribution of aerosol BB.

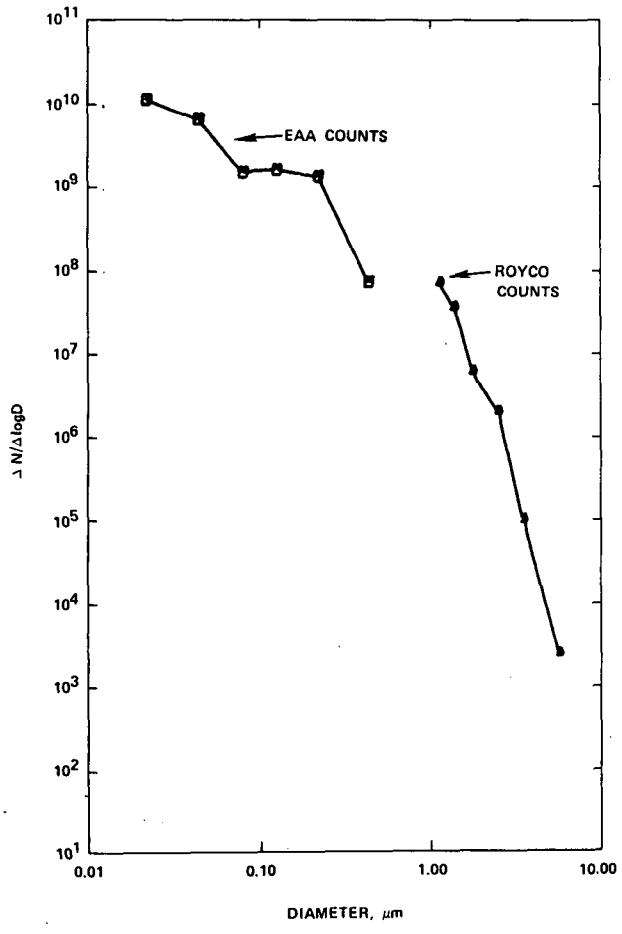

Figure 29. Basic oxygen furnace simulation aerosol AA (Fe_2O_3 6 g/m^3) size distribution plotted as ΔN/Δ logD vs. D.

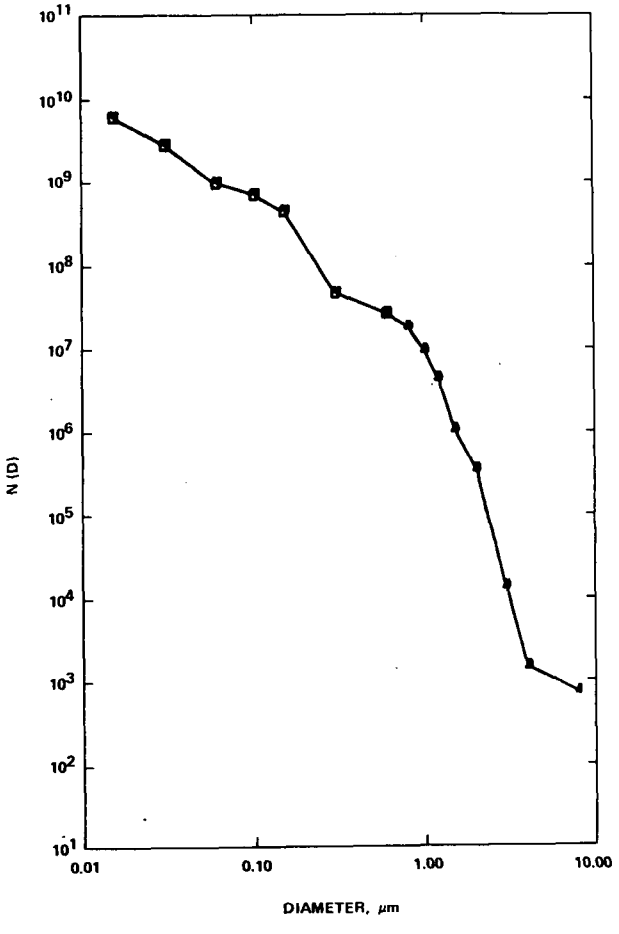

Figure 30. Basic oxygen furnace simulation aerosol AA (Fe_2O_3 6 g/m^3) size distribution from measurements with the EAA and Royco.

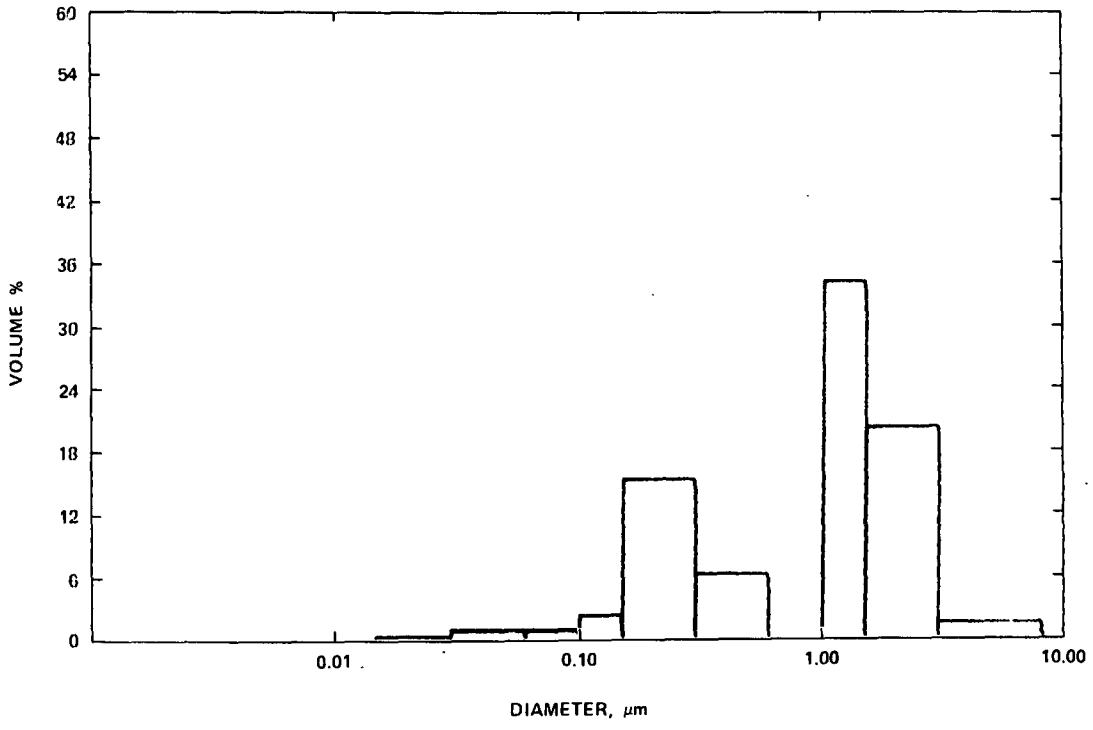

Figure 31. The volume distribution determined from EAA and Royco measurements of the basix oxygen furnace simulation aerosol AA. Ninety-five percent of the particle volume was contained in particles with diameters between 0.15 and 3 μm.

ZINC SMELTER FUME SIMULATION AEROSOL

Table 23 shows several of the characteristics of the ZnO(0.94 g/m^3) aerosol described also in Tables 9, 10, 12 and Appendix C. This aerosol can be used to simulate zinc smelter effluents. It was generated by burning a solution containing 159 g of (73% pure) zinc nitrate per liter of methanol. Ethanol can be used in place of methanol; with ethanol the exit fume temperature rises. The basic solution for generating simulated zinc smelter effluent shown in the Section 4 can also be used. Because of the toxicity of CdO, this solution was not used in particle size measurement experiments. ZnO (1.3 g/m^3) fumes generated by burning solutions consisting of 234 g of (73% pure) zinc nitrate per liter of methanol also had volume median diameters of 0.2 μm. Figures 32-34 show the size and volume % distribution of the ZnO(0.94 g/m^3) fume.

TABLE 23. CHARACTERISTICS OF THE ZINC SMELTER FUME SIMULATION AEROSOL

Stack: Diameter, 0.25 m; Height, 3.5 m

Fume Exit Temperature: 579°K (306°C)

Fume Exit Velocity: 5.8 m/s

Fume Flow Rate: 0.29 m^3/s; 0.16 kg/s

Particle Loading: 0.94 g/m^3 (2 g/m^3 @ STP)

Particle Volume Median Diameter: 0.2 μm

Condensation Nuclei: 1.4-1.7x10^8 particles/cm^3

Nominal Density (Handbook values): 5.47 g/cm^3

Particle Color: white

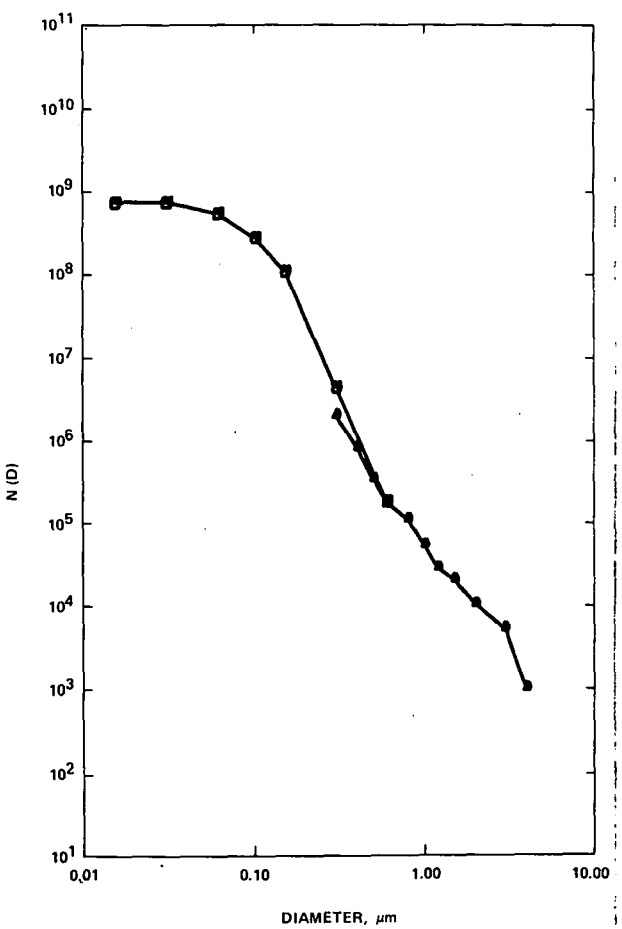

Figure 32. ZnO (0.94 g/m^3) aerosol size distribution from measurements with the EAA and Royco.

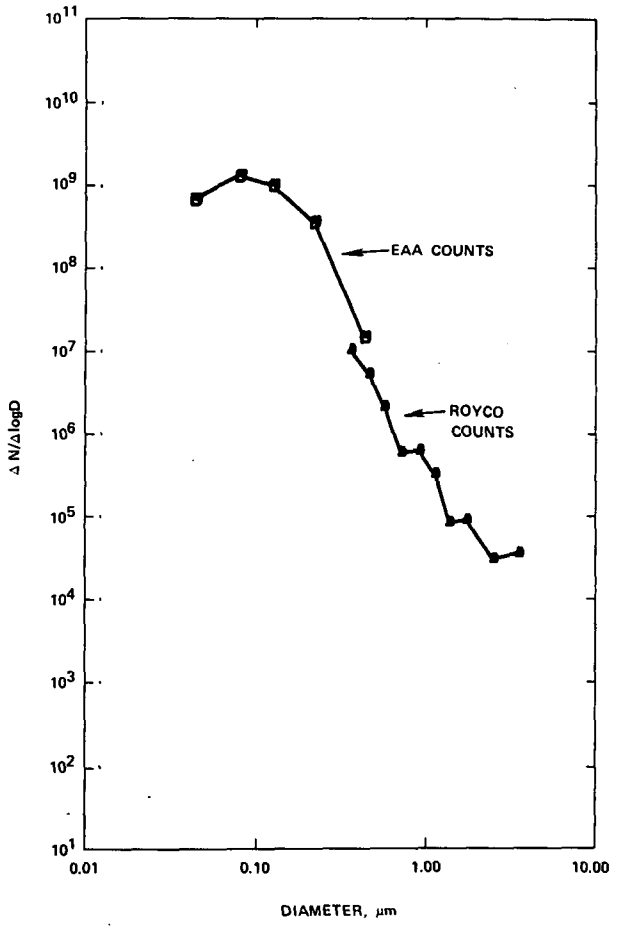

Figure 33. ZnO (0.94 g/m^3) aerosol size distribution plotted as ΔN/ΔlogD.

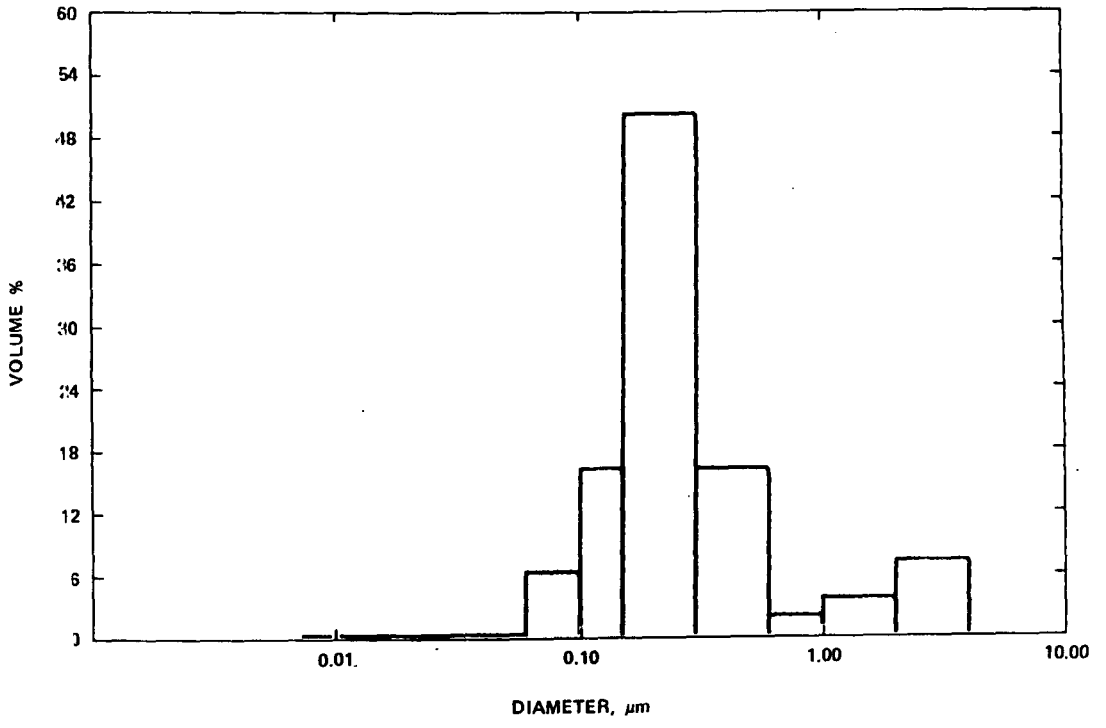

Figure 34. The volume distribution determined from EAA and Royco measurements of the ZnO (0.94 g/m^3) aerosol.

SECTION 7

COST OF RAW MATERIALS

Table 24 shows the materials cost for generating 45 kg (100 pounds) of the various simulation aerosol particulates. Forty-five kg is a large amount of aerosol. (i.e., The coal fly ash simulation aerosol has a particle loading of 0.66 g/m^3; therefore, 68,200 m^3 (2.4×10^6 ft^3) of aerosol would have to be generated to contain 45 kg of particles.)

The materials cost for a simulation aerosol for the zinc smelter is much less if a pure ZnO aerosol is used. It would cost $1112 to generate 45 kg of the pure ZnO (0.94 g/m^3) aerosol shown in Table 23 versus $2512 to generate 45 kg of the zinc smelter aerosol shown in Table 24.

TABLE 24. Estimated cost of ingredients to generate 45 kg (100 pounds) aerosol particles to simulate the fine particulate effluent from the following industrial sources.

Ingredient	Amount	Cost/lb $	Cost $
	PULVERIZED COAL COMBUSTION		
$(CH_3)_2Si(OC_2H_5)$	51 kg (112 lbs)	$7.30	$818
$Al(NO_3)_3 \cdot 9H_2O$	91 kg (200 lbs)	1.90	380
$Fe(NO_3)_3 \cdot 9H_2O$	42 kg (92 lbs)	1.95	179
C_2H_5OH	454ℓ (120 gal)	1.95/gal	234
		TOTAL COST	$1,611
	ELECTRIC ARC FURNACE		
$Fe(NO_3)_3 \cdot 9H_2O$	114 kg (251 lbs)	1.95	489
$Cr(NO_3)_3 \cdot 9H_2O$	47 kg (103 lbs)	1.47	151
$Mg(NO_3)_2 \cdot 6H_2O$	43 kg (95 lbs)	2.00	190
51% $Mn(NO_3)_2$ in H_2O	33 kg (72 lbs)	2.60	187
CH_3CH_2OH	989ℓ (261 gal)	1.95/gal	509
		TOTAL COST	$1,526
	BASIC OXYGEN FURNACE (AEROSOL AA)		
$Fe(CO)_5$	112 kg (246 lbs)	17/lb	4,182
CH_3COCH_3	183ℓ (48 gal)	11/gal	528
		TOTAL COST	$4,710
	BASIC OXYGEN FURANCE (AEROSOL BB)		
$Fe(NO_3)_3 \cdot 9H_2O$	218 kg (480 lbs)	1.95	936
$Ca(NO_3)_2 \cdot 4H_2O$	9.5 kg (21 lbs)	1.70	36
CH_3CH_2OH	863ℓ (228 gal)	1.95	445
		TOTAL COST	$1,417
	ZINC SMELTER		
$Zn(NO_3)_2 \cdot 4H_2O$	86 kg (189 lbs)	2.02	382
$Cd(NO_3)_2 \cdot 4H_2O$	32 kg (71 lbs)	10.87	772
$VOSO_3 \cdot xH_2O$	8 kg (18 lbs)	60.00	1,080
CH_3OH	540ℓ (143 gal)	1.95/gal	278
		TOTAL COST	$2,512

SECTION 8

DISCUSSION OF RESULTS

The program objective of developing reproducible stable sources of well-characterized solid particulate, fine particle aerosols for laboratory pilot plant tests of pollution abatement equipment was accomplished. Methods were developed for generating fine particle aerosols which have chemical compositions typical of four industrial effluents. The SO_2 content of the carrier gas can be regulated at any desired concentration. Particle resistivities can be lowered by adding lithium salts. The volume median diameter of the particles can be varied from 0.06 to 5 μm by adjusting solution compositions, concentrations or the stack exit diameter. Aerosol particle loadings can be varied from less than 0.01 g/m^3 to 6 g/m^3. Magnetic, non-magnetic, sticky, not sticky, highly resistive, water soluble, hydroscopic and hydrophobic aerosols were generated.

All twelve of the metal nitrates and other compounds (excluding $VOSO_4$ in H_2O and CH_3OH which are probably incompatible with $(CH_3)Si(OC_2H_5)_2$) used in these programs are believed to be compatible in solution with each other. Thus, aerosols consisting of several thousand different combinations of chemical compounds can be generated. An infinite number of weight ratios can be formulated. There are also several other metal nitrates and chlorides which are soluble in ethanol and/or methanol. They could be used to generate aerosols of other metal oxides and chlorides. The most useful aerosols, however, will probably be those comprised of a single compound.

When an aerosol is generated such that all of its particles consist of a single compound and crystal type (e.g., face centered cubic MgO), then all of the particles will have most, if not all, of the same properties such as density, resistivity, permitivity, etc. It should be possible to determine any remaining size dependent properties using the current knowledge of solid state physics. By using several different simple aerosols, properly chosen to have a wide range of properties, it should be possible to obtain data which will lead to the determination of basic theories, as opposed to empirical findings, of the important parameters of specific pollution abatement equipment. This knowledge could then be used in models to predict which particle sizes of particular compounds in industrial effluents would not be collected by various pollution abatement equipment. Tests conducted with simple aerosols of a single compound and crystal type will simplify the analysis and will yield less ambiguous results. When using a simple aerosol, the analytical costs will be much less than when using a complex aerosol; and the confidence of the analysis will be higher.

Complex aerosols consisting of several chemical compounds usually have particles with differing compositions and properties. These aerosols probably would not be as useful in determining basic pollution abatement equipment parameters because of the analytical difficulties. The characterization of the coal fly ash simulation aerosol showed that the average chemical composition of the particles was a function of size (see Table 15, cyclotron excitation analysis) and that in a given size range the chemical composition varied from particle to particle (see the X-ray Non-dispersive Analysis Section). These are properties typical of real fly ash and other industrial effluents (see Section 3). Based on these findings one would expect that the particles might have varying properties depending on their composition. They also may have surface compositions which are different from the bulk particle compositions. It would be difficult to determine all of the various aerosol particle properties and to determine whether each is due to the bulk or surface compositions. For example, a 0.2 μm Fe_2O_3 particle with hundreds of 0.01 μm SiO_2 particles coating its surface would probably have a resistance comparable to SiO_2 not Fe_2O_3.

Use of single compounds is safer than using complex compounds. Toxic materials could be avoided. Once the basic principles are better known, the important properties of materials such as CdO probably can be simulated by other non-toxic materials and the abatement equipment tests could be performed with a non-toxic material.

The make-up of the surface of a particle determines many of the physical properties of the particle. The flame method used to generate particles with fresh surfaces is superior to resuspension of old materials. It closely duplicates the actual effluent sources. As particles age, the surface properties change. It is also unlikely that submicron sized long chain aggregates can be collected then resuspended so that they duplicate the long chain aggregates contained in industrial effluents.

Many trace elements condense onto the surface of effluent particles (Davison, 1974; Pueschel 1976). The particle's surface properties will often be a function of this surface coating, not the bulk composition. In order to adequately simulate these effluents, it may be necessary to generate simulation aerosols with particle composition different from the bulk effluent particle compositions.

The plots of size distributions and Tables 11 and 12 show that the EAA and Royco particle counts are in good numerical agreement for some aerosols and in poor agreement for others. The instrument particle counts given in the Results Section were not, however, corrected for specific aerosols properties (e.g., optical properties). The Royco Model 200 optical particle counter has a right angle optical system and the particle light scattering to the detector is a function of the particle shape and refractive index. Table 25 shows the optical properties of several of the generated aerosol materials. Cooke and Kerker (1975) showed the strong dependence of the Royco Model 200 optical particle counter response to both the refractive index and adsorption coefficient of a particle.

TABLE 25. OPTICAL PROPERTIES

Compound	Refractive Index (λ=0.589 μm)	Adsorption Coefficient	Particle Count ratio EAA/Royco 0.3<D<0.6 μm
SiO_2	1.5	~0	343
MgO	1.74	~0	27-58
ZnO	2.01	~0	2.3-8.2
Fe_3O_4	2.42	0.55-0.57	0.96
Mn_3O_4	2.15-2.46	0.5-1(Est.)*	0.79
Cr_2O_3	2.55	-	2.8
Fe_2O_3	3.01-3.46	0.97-1.07	2-30

*Estimated values

If the assumption is made that the particles in the size range the Royco is measuring (0.3<D<10 μm) are single spheres, then the size distribution indicated by the Royco could be corrected for those aerosols whose optical properties are known. A realistic measure of the size distribution should result. Since the Royco was calibrated with latex spheres (m=1.59), a particle refractive index greater than 1.59 will cause particles larger than 0.8 μm to be sized larger than they are and a particle adsoprtion coefficient greater than zero will cause particles larger than 0.3 μm to be sized smaller than they are (Cooke, 1975). Whitby (1967) showed that the Royco underestimates the size of India Ink aerosols by a factor of 2.5(D=1 μm) to 5(D>2 μm). The India Ink particles were shown to be spheres with rough surfaces. Gebhart (1976) states that for particles smaller than the wavelength of light, scattering becomes more and more a volume effect and depends only on the optical properties. As long as light scattering is a volume effect, the scattering cross-section of a particle becomes mainly a function of its volume and less of its shape. Consequently, a light-scattering device used for particles smaller than the wavelength of the light measures the equivalent volume diameter of a non-spherical particle.

Since the Royco counts of the background laboratory air were normally lower than the EAA counts by a factor of 7.7 and since the particles in the laboratory air should have typical optical properties, there appears to be a systemmatic error in at least one of the instruments. The EAA was calibrated with a Model 3030 EAA and the particle counts of both instruments in the size range 0.3<D<0.6 μm were in good agreement ($\pm$10%). Thus, either the Royco or both EAA's appear to be in error in this size range for the background counts. For those aerosols where the EAA and Royco agreement is very

good, the refractive index must have caused the Royco to "over size" and the resulting agreement was coincidental.

The poorest agreement between the EAA and Royco was with SiO_2 particles which were transparent and with the MgO particles which are white. Since the concentration of particles decreases roughly in proportion to the cube of the diameter, under or over sizing has a large effect on the number of particles counted in a size range. For SiO_2 aerosols the particle concentration in the size range $0.3<D<0.6$ μm decreases even more rapidly than D^3, thus a greater error would have occurred. The optical properties of SiO_2 and MgO are close to that of latex (see Table 25) and they could not be responsible for causing the Royco to indicate such gross sizing errors (Cooke 1975). The EAA and Royco counts are significantly different for the SiO_2 and MgO aerosols even if the Royco counts are increased by a factor of 7.7 which is equal to the average EAA/Royco count ratio for the background. Since the particle shape should not be important for the Royco in the overlap size range $0.3<D<0.6$ μm (Gebhart 1976), the EAA counts in this size range must be in error for the SiO_2 and MgO aerosols. For these aerosols, the equivalent sphere diameters measured by the EAA appear to be significantly larger than the equivalent volume diameters measured by the Royco.

For many aerosols the loadings determined from the EAA and Royco counts are greater than those determined from the generation rates (see Tables 8 and 9). Aerosol particle loadings determined from the uncalibrated instrument counts could be in error for several reasons. The equivalent sphere diameters measured by the EAA could be significantly larger than the equivalent volume diameters. Many of the compounds generated had optical properties which were significantly different from those of latex; thus the equivalent light scattering diameter measured by the Royco was not equal to the geometric diameter. For particles larger than the wavelength of light the shape of the particles has a significant effect on the light scattering, thus the sizing of non-spherical particles larger than about 5 μm by the Royco can be in serious error. Whitby (1967) found that for particles larger than 5 μm, the particle shape and surface characteristics seemed to effect the Royco sizing. Another source of error is that particles with light scattering diameters larger than 10 μm were not sized. After aerosol dilution the size cut-off was even less than 10 μm (see Tables 11 and 12). For the SiO_2, MgO, ZnO and Fe_2O_3 aerosols most of the counted particle volume was less than 0.3 μm. Thus it is the EAA counts which are responsible for most of the determined particle loading (see Appendix C). Because of this, it appears that the equivalent sphere diameters counted by the EAA were larger than the equivalent volume diameters not only for the SiO_2 and MgO aerosols but also for the ZnO and Fe_2O_3 (generated from $Fe(CO)_5$) aerosols.

The particle counts of the Cr_2O_3 aerosol indicated a relatively large number and thus volume % of particles larger than 5 μm. If these particles were not smooth spheres, the uncalibrated Royco size measurements would have been in serious error. Another possible explanation for the Cr_2O_3 particle loadings determined from the Royco counts being greater than the loadings determined from the generation rates is hollow aerosol particles. Hydration of the $Ca(OH)_2 \cdot xH_2O$ aerosol particles could have caused the high particle loadings.

Table 10 shows aerosol particle concentrations measured by the Environment/One condensation nuclei counter (CNC) and by the EAA. Dividing these concentrations by the dilution (6,900, for three stage and 38,700 for non-standard three stage) converts the aerosol concentrations to the instrument counts of the diluted aerosols. Liu and Pui (1974) compared the Environment/One and EAA at several NaCl particle concentrations. They showed that the Environment/One CNC had a linear response at concentration levels up to 52,000 particles/cm^3 (indicated concentration) but the indicated concentration was lower than the true concentration by a factor of 2.5. At higher concentrations the instrument response was nonlinear; at 140,000 particles/cm^3 indicated, the indicated concentration was lower than the true concentration (600,000) by a factor of 4.3. These findings of Liu and Pui were used to correct the CNC measurements shown in Table 10. After correction, the EAA counts (see Table 10) of the total particle concentrations were higher than the corrected CNC measurements by a factor of 2.45. For the $H_2SO_4 \cdot xH_2O$ droplet aerosol the EAA counts of the particle concentrations were lower than the corrected CNC measurements by a factor of 2.1.

Tables 26-29 summarize comparisons of the effluents and the simulants. The zinc smelter effluent can also be simulated by the simulation aerosol generated from the basic zinc smelter solution shown in Section 4. This aerosol consists of ZnO and CdO with some VO_2, V_2O_4, V_2O_5, $ZnSO_4$, $CdSO_4$, and $2CdO \cdot V_2O_5$.

TABLE 26. COMPARISON OF COAL FLY ASH EFFLUENTS WITH SIMULANT

	Effluents	Simulant
Temperature ^oC	121-157	177
Particle Loading (g/m^3)	2.3-12.8	1.1
Mass or Volume Median Diameter (μm)	~15 μm	0.2-1
Particle Density (g/cm^3)	0.6-3	2.6
Bulk Density	0.5-0.8	0.3-0.9
Electrical Resistivity (ohm cm)	10^8-10^{13}	$5x10^6$-$2x10^{12}$
Particle Composition	SiO_2	SiO_2
	Fe_2O_3	Fe_2O_3
	Al_2O_3	Fe_3O_4
	CaO	$Al_2O_3 \cdot xH_2O$
	MgO	
	Na_2O	

TABLE 27. COMPARISON OF ELECTRIC ARC FURNACE EFFLUENTS WITH SIMULANTS

	Effluents	Simulants
Temperature (^{o}C)	100-1650	489-658
Particle Loading (g/cm^3)	0.2-5	1.8-4
Mass or Volume Median Diameter (μm)	0.3-5.4	0.08-0.2
Particle Density (g/cm^3)	3.8-3.9	4.8
Electrical Properties (ohm cm^3)	$6x10^5$-$7x10^{13}$	Not Measured
Particle Composition	Fe_2O_3, FeO,	Fe_2O_3
	Cr_2O_3, SiO_2,	Fe_3O_4
	Al_2O_3, CaO,	Cr_2O_3
	MgO, MnO,	MgO
	ZnO, CuO,	MnO
	NiO, PbO,	
	C, S, P,	
	Alkalies	

TABLE 28. COMPARISON OF BASIC OXYGEN FURNACE EFFLUENTS WITH SIMULANTS

	Effluents	Simulants
Temperature (^{o}C)	290-1650	491-640
Particle Loading (g/cm^3)	4.6-23	6-16.8
Mass or Volume Median Diameter (μm)	0.095	0.3-1.05
Particle Density (g/cm^3)	3.44	4.8-5.1
Particle Composition	Fe_2O_3	Fe_2O_3
	FeO	or
	MnO	Fe_3O_4
	SiO_2	Fe_2O_3
	Al_2O_3	$Ca(OH)_2 \cdot xH_2O$
	CaO	
	MgO	

TABLE 29. COMPARISON OF ZINC ROASTER AND SINTERING MACHINE EFFLUENTS WITH SIMULANT

	Effluents	Simulants
Temperature (^{o}C)	160-482^{o}C	306
Particle Loading (g/cm^3)	0.9-150	2
Mass or Volume Median Diameter (μm)	0.4-15	0.2
Particle Density	-	5.47
Particle Composition	ZnO	ZnO
	PbO	
	CdO	

These simulation aerosols appear to have characteristics similar to those of the effluents and should suffice for many pollution abatement equipment tests.

REFERENCES

1. Brakhnova, I. T. Environmental Hazards of Metals, Consultants Bureau, New York, 1975, 277 pp.

2. Carroz, J. W. and R. C. Noles. A new ground based solution burner for cloud seeding and production of atmospheric tracer materials. Third Conference on Weather Modification, Am. Met. Soc., June 26-29, 1972, pp. 37-39.

3. Cavin, D. C., W. A. Klemm and G. Burnet. Analytical methods for characterization of fly ash. AEC Ames Laboratory, Ames, Iowa, 1974, 19 pp., IS-M-14.

4. Chuan, R. L. Rapid measurement of particulate size distribution in the atmosphere. Fine Particles edited by B.Y.H. Liu, Academic Press, N.Y., 1976, pp. 763-775.

5. Cooke, D. D. and Milton Kerker. Response calculations for light-scattering aerosol particle counters. Applied Optics, 14(3), March 1975, pp. 734-739.

6. Davison, R. L., D. F. S. Natusch, J. R. Wallace, C. A. Evans Jr. Trace elements in fly ash. Environ. Sci. Tech., 8(13), Dec. 1974, pp. 1107-1113.

7. Drehmel, D. C. Primary fine particle control technology. 69th Annual Meeting of the Air Pollution Control Association, Portland, Oregon, June 27-July 1 1976, 14 pp.

8. Drehmel, D. C. and D. E. Black. Particulate control in energy processes: a status report. J. Air Pollution Control Assoc., 26(12), December 1976, pp. 1141-1143.

9. Gebhart, J. J., Heyder, C. Roth, W. Stahlhofen. Optical aerosol size spectrometry below and above the wavelength of light - a comparison. Fine Particles edited by B.Y.H. Liu, Academic Press, N.Y., 1976, pp. 793-815.

10. Harvey, R. D. Petrographic and mineralogical characteristics of carbonate rocks related to sulfur dioxide sorption in flue gases. Illinois State Geological Survey, July 1971, 93 pp., PB 206-487.

11. Harris, D. B., D. C. Drehmel. Fractional efficiency of metal fume control as determined by Brink impactor. Presented at 66th Annual Meeting APCA Chicago, Ill., June 24-28, 1973, 26 pp.

12. Liu, B.T.H. and D.Y.H. Pui. A submicron aerosol standard and the primary, absolute calibration of the condensation nuclei counter. J. of Colloid and Interface Science, 47 (1), April 1974, pp. 155-171.

13. Luke, W. I. Nature and distribution of particles of various sizes in fly ash. T. R. 6-583, Corps of Engineers, Vicksburg, Mississippi, Nov. 1961, 21 pp, AD-731-654.

14. Pueschel, R. F. Aerosol formation during coal combustion: condensation of sulfates and chlorides on fly ash. Geophysical Research Letters, 3 (11),November 1976, pp. 651-653.

15. Sem, G. H. Submicron particle sizing experience on a smoke stack using the electrical aerosol size analyzer. Presented at the Seminar on In-Stack Particle Sizing for Particulate Control Device Evaluations, Environmental Protection Agency, National Environmental Research Center, Research Triangle Park, N.C., December 3-4, 1975.

16. Shen, T. T., et al. Characterization of differences between oil-fixed and coal-fired power plant emissions. To be presented at the International Clean Air Congress, Tokyo, Japan, May 1977.

17. Vandegrift, A. E., et al. Particulate pollutant system study. Vol. III - Handbook of Emission Properties. Midwest Research Institute, 1 May 1971, 607 pp., PB-203-522.

18. Whitby, K. T. and R. A. Vomela. Response of single particle optical counters to nonideal particles. Environ. Sci. Tech., 1 (10), October 1967, pp. 801-814.

19. Yakowitz, H., M. H. Jacobs, and P. D. Hunneyball. Analysis of urban particulates by means of combined electron microscopy and X-ray microanalysis. Micron, 3: pp. 498-505, 1972.

20. Author unknown. Engineering and cost study of the Ferroalloy Industry. EPA, Research Trinagle Park, North Carolina, EPA 450/2-74-008, May 1974, pp. D20-D28.

APPENDIX A

OPERATING SPECIFICS

OPERATING PROCEDURE

This operating procedure is to be used with the generation apparatus described in the text.

The procedure for safe operation of the generation apparatus consists of two important points.

1. Do not use any system for pressurizing the pressure tank which will cause the tank pressure to rise above 200 psi, also keep a pressure relief valve on the tank in good operating order.

2. Do not expose people to dangerous levels of toxic chemicals. Mix, spray and burn the chemicals described in the final report only with adequate protection.

The generation of reproducible aerosols requires the use of "good" solutions. With one possible exception, the solutions described in Section 4 of the final report should be mixed just prior to use. They will degrade within several hours after mixing. The stability of iron pentacarbonyl in acetone was not measured. However, all of the nitrates, except for ferric nitrate, are stable for months when dissolved in ethanol. Ferric nitrate in ethanol forms a significant amount of insoluble material within 24 hours. When chromic and ferric nitrate are in solution together an insoluble compound forms within several hours. Many of the other nitrate compounds named in Section 4 of the final report are probably compatible and stable for long periods of time when dissolved in ethanol. Until the stability of a particular solution has been tested, it should be used within a few hours after mixing.

After generating aerosol, the hardware should be washed several times with water, the nozzle should be disassembled and then washed. Some of the nitrates are very corrosive. Other operating parameters and a description of the apparatus are given in Section 4 of the final report. They include using 200 psi solution pressure and a WDB 4.0, 30^{o} Delavan nozzle.

DILUTER DESCRIPTION

Parts List (All dimensions in English Units to aid in construction)

1. Fume Intake Tube: 1/2 inch stainless steel tubing with 7/16 inch ID.

2. Porous Metal Tube: 2 Inch OD, 9 inches long, 1/8 inch wall thickness, grade F-30 sintered brass (Pacific Sintered Metals Co., 16120 So. Figueroa St., Gardena, Calif. 90247).

3. Brass T: 10 inches long, 3 1/2 inch OD. brass tube. Dilution air intake tube has a 4 inch long, 2 1/8 inch OD copper arm 2 inches from fume intake end. Copper arm is made from 2 1/8 inch OD, 1 31/32 inch ID, Standard "2 inch" copper pipe.

4. Phenolic End Piece: 2 inches thick, OD is machined to fit ID of brass T. Also machined to hold fume intake probe and porous metal tube (see Figure 5).

5. Brass End Piece: 1 1/4 inches thick, OD is machined to fit inside brass T and to hold porous metal tube and copper pipe.

6. Copper pipe: 24 inches long, copper pipe (Std. "2 inch pipe", 2 1/8 inch OD, 1 31/32 inch ID).

7. Mixer: 2(ea) thin (0.030 inch) brass disks. OD of upstream disk = 2 1/16 inch; OD of downstream disk = 1 15/16 inch; each disk has 6(ea) 1/2 inch holes punched in it (see Figure 2E). Disks held together with 2 3/8 inch long piece of 1/4 inch copper tubing.

8. Elbow: Std. copper 90^{o} elbow with standard "1/2 inch" copper pipe soldered in so to be coaxial with the 2 inch copper pipe (see Figure 2 G).

9. Other Metal Parts: Standard 1/2 inch and 2 inch pipe and 90^{o} elbows are used to complete the set up. Standard 1/2 inch copper pipe has a .52 inch ID. All fittings are fastened together with duct tape. Standard copper sweat fitting reducers are used at B and G for "orifices". At C and E paper washers are used.

10. Fan: Model HH33 Quick-Air blower-suction unit operated at low speed. Inlet blocked with 31/32 inch ID orifice, outlet blocked with 15/16 inch ID orifice to reduce fan suction (Clements Mfg. Co., 6650 S. Narragansett Ave, Chicago, Ill. 60638).

Orifice Sizes (All dimensions in English Units to aid in construction)

Diluters 3(ea) (see Figure 4)

1. First Stage Diluter (see Figure 5)

   (a) Fume intake (see Plate 4)
   (b) Orifice ID @ B = 1/4 inch
   (c) No orifice @ C, ID = 1 31/32 inches
   (d) Orifice ID @ G = 3/8 inch
   (e) Orifice ID @ I = 3/4 inch

2. Second Stage Diluter (see Figure 5)

   (a) Intake at G in Stage 1
   (b) No orifice @ B, ID = 1/2 inch
   (c) Orifice ID @ C = 1 1/4 inches
   (d) Orifice ID @ G = 3/8 inch
   (e) Orifice ID @ I = 1 inch

3. Third Stage Diluter (see Figure 5)

   (a) Intake at G in stage 2
   (b) No orifice @ B, ID = 1/2 inch
   (c) Orifice ID @ C = 1 1/16 inches
   (d) Orifice ID @ G = 3/8 inch
   (e) No orifice @ I, ID = 1 31/32 inches

APPENDIX B

AEROSOL SIZE DISTRIBUTIONS

The figures contained in this appendix show size distributions, not shown in the text, of most of the aerosols which were generated and measured. The figures are plotted as N(D) vs. D.

Refer to Tables 8 through 12 in text for additional information on these aerosols.

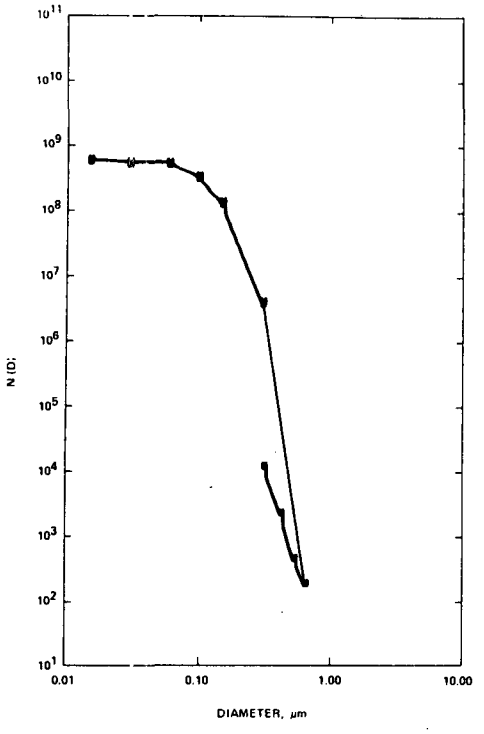

B-1. SiO_2(0.36g/m^3)

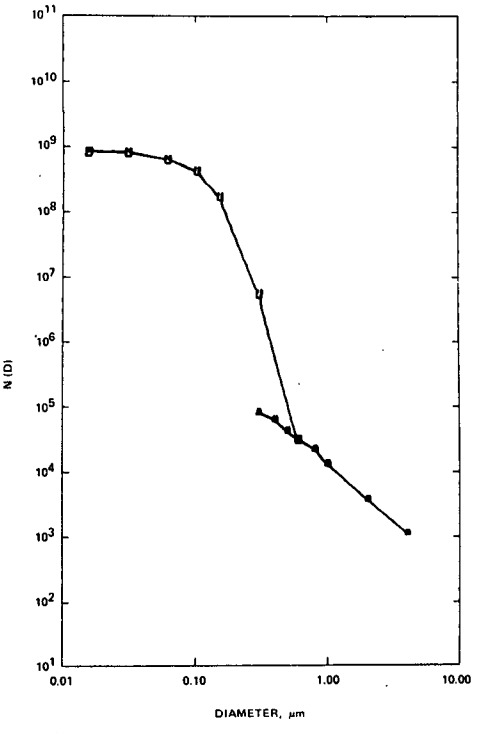

B-2. SiO_2 & $Al_2O_3 \cdot 2H_2O$(0.62g/m^3)

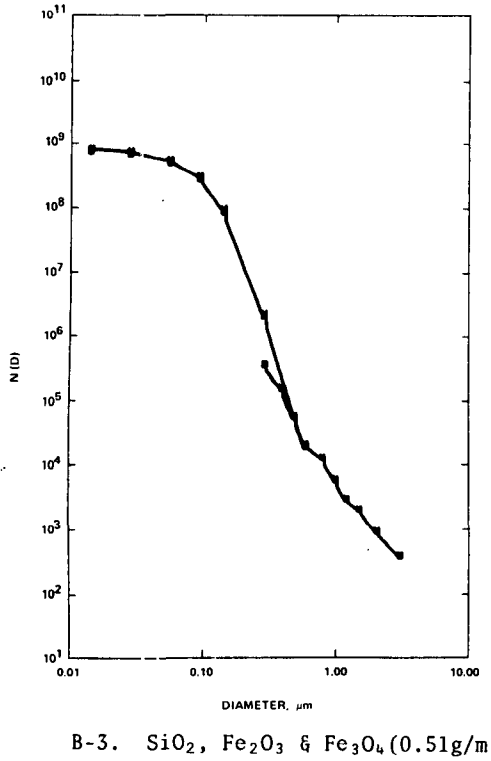

B-3. SiO_2, Fe_2O_3 & Fe_3O_4(0.51g/m^3)

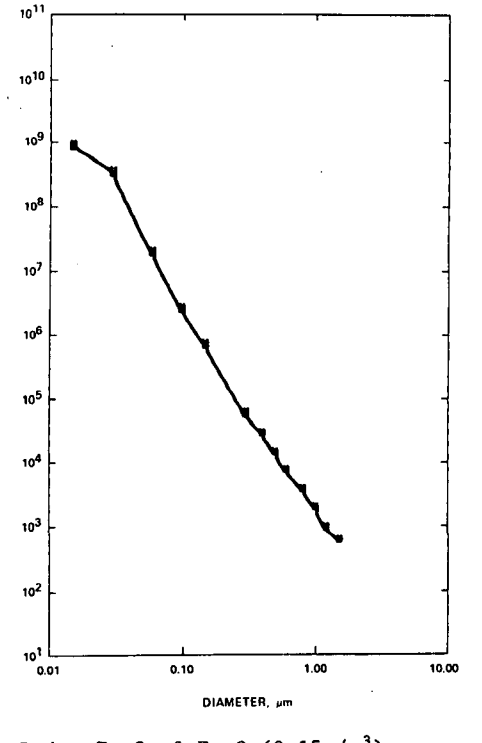

B-4. Fe_2O_3 & Fe_3O_4(0.15g/m^3) used reduced pressure.

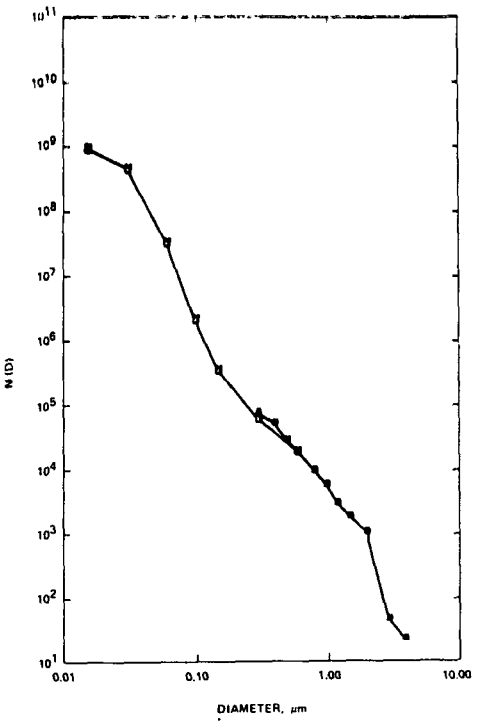

B-5. $Al_2O_3 \cdot 2H_2O, Fe_2O_3$ & Fe_3O_4 ($0.41 g/m^3$)

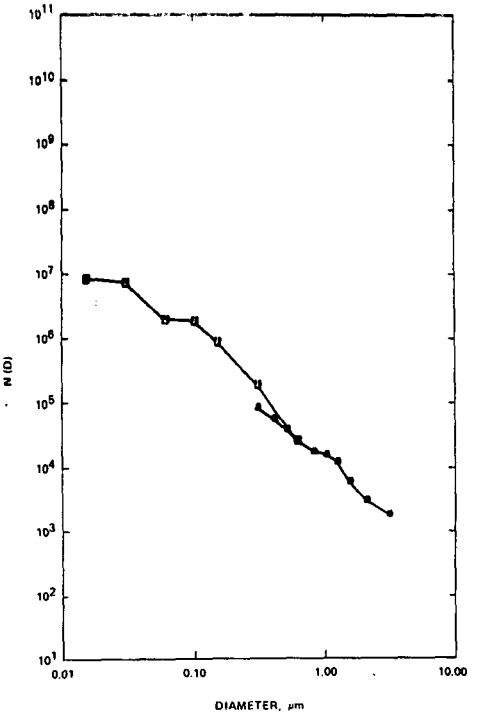

B-6. $Al_2O_3 \cdot 2H_2O (0.26 g/m^3)$

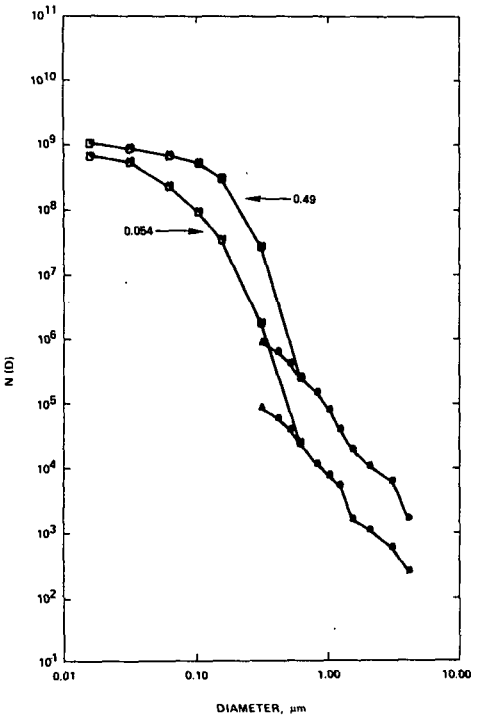

B-7. MgO(0.054 & $0.49 g/m^3$)

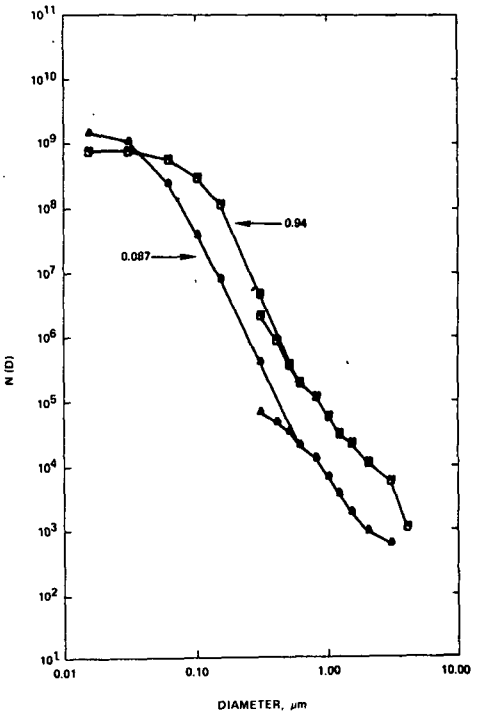

B-8. ZnO(0.087 & $0.94 g/m^3$)

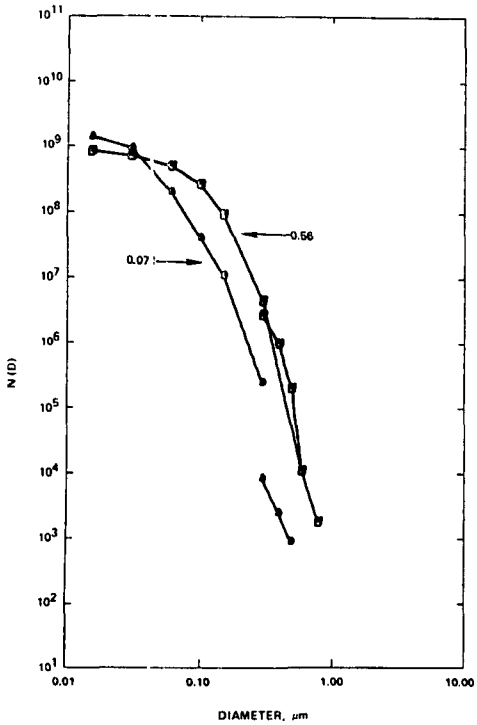

B-9. Fe_2O_3(0.071 & 0.56 g/m^3)

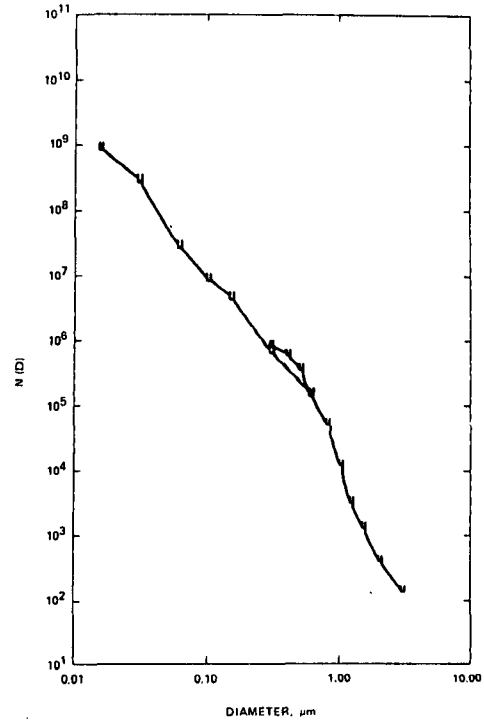

B-10. Mn_3O_4(0.62g/m^3)

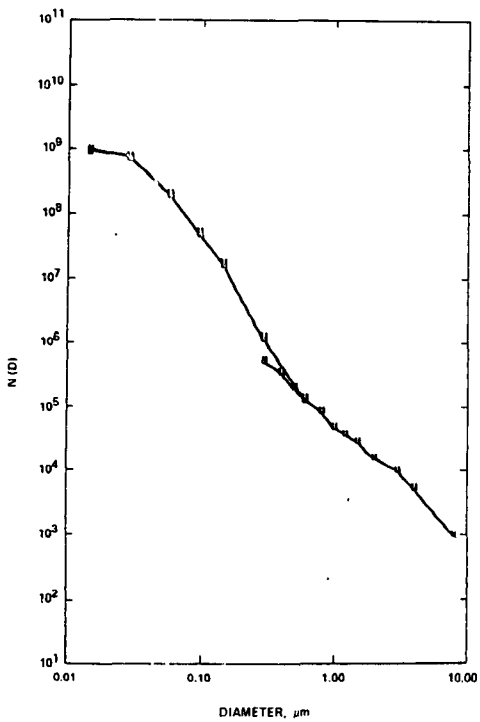

B-11. Cr_2O_3(0.69g/m^3)

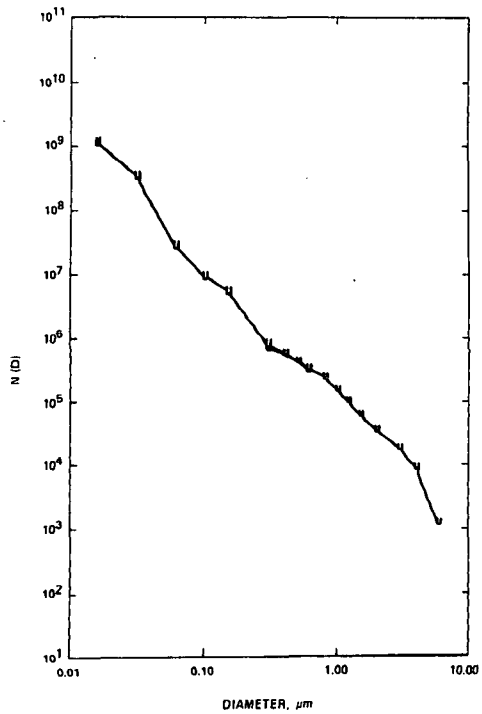

B-12. $Ca(OH)_2$(0.29g/m^3)

APPENDIX C

PARTICLE CONCENTRATIONS AND VOLUME PERCENTS

This appendix shows the particle concentrations and the resulting volume percents for 26 different aerosols. The diameter intervals are shown at the top of each page, the aerosols are described by their particle composition followed in parenthesis by the particle loading (g/m^3). The dilution each aerosol underwent before measurement is given in Tables 11 and 12 in the text. To convert aerosol concentrations back to the counts measured by the instruments divide the concentrations shown in this appendix by 6900 for standard three stage dilution and 256 for two stage dilution. For non-standard three stage dilution divide the concentrations derived from the EAA counts by 38,700 and the concentrations derived from the Royco counts by 65,700.

The following Whitby-Cantrell constants were used to convert the EAA outputs to particle counts: The original data reduction constants given in the instrument manual are also shown.

Diameter	Constant	Original Constant
.0075	1.5E5	9.1E5
.015	8.8E4	2.3E5
.03	5.9E4	6.2E4
.06	1.5E4	2.2E4
.1	1.2E4	1.2E4
.15	8.8E3	6.8E3
.3	3.3E3	3.3E3
.6		

PARTICLE CONCENTRATIONS AND VOLUME PERCENTS

	.0075	.015	.03	.06	.1	.15	.3	.6	.3	.4	.5	.6	.8	1.0	1.2	1.5	2.0	3.0	4.0	8.0
SiO_2(0.36)	3.6E8	6.1E7	2.0E7	2.0E8	1.8E8	1.2E8	3.4E6		8.2E3	1.5E3	2.3E2									
	-	.03	.8	5	18	63	14													
SiO_2(0.009)	4.9E7	1.9E8	2.3E8	2.6E7	2.8E6	6.1E5	2.4E4		Not above background											
	.1	4	40	27	12	13	4													
SiO_2,$Al_2O_3 \cdot 2H_2O$(0.62)		3.0E7	1.8E8	2.2E8	2.5E8	1.6E8	5.4E6		1.8E4	2.1E4	1.1E4	9.2E3	9.2E3		9.1E3			2.6E3		
		.01	.5	4	18	59	16		.03	.07	.07	.1	.2		1			2		
SiO_2,Fe_2O_3,Fe_3O_4(0.51)		9.7E7	1.1E8	2.3E8	2.0E8	8.5E7	2.0E6		1.9E5	9.1E4	3.2E4	7.1E3	6.0E3	2.5E3	8.4E2	9.2E2	4.6E2			
		.1	.6	7	25	55	11		.5	.6	.4	.2	.3	.2	.1	.3	.5			
Coal Fly Ash Simulation	0	1.1E8	2.4E8	2.3E8	2.1E8	1.3E8	4.7E6		1.5E5	1.2E5	9.0E4	6.0E4	3.6E4	9.5E3	5.0E3	1.5E3	1.1E3			
Aerosol(0.66)		.05	.8	5	18	57	17		.3	.5	.7	.9	1	.6	.6	.3	.7			
Coal Fly Ash Simulation	0	2.9E8	4.7E7	1.8E8	2.3E8	1.2E8	3.8E6		1.7E5	1.6E5	1.1E5	9.1E4	4.8E4	1.4E4	4.7E3	1.5E3	1.2E3	6.1E2	4.8E2	
Aerosol(0.66)		.1	.2	4	20	54	14		.3	.7	.9	1	2	.9	.6	.4	.8	1	4	
Same as above with	1.1E8	9.7E6	2.1E8	2.2E8	1.3E8	5.3E7	1.7E6		1.9E5	1.5E5	1.1E5	6.2E4	3.6E4	1.8E4	4.8E3	2.4E3	6.1E2			
Li_2CO_3(0.94)		.009	1.5	9	22	48	12		.7	1	2	2	2	2	1	1	.9			
Fe_2O_3,Fe_3O_4(0.15)		5.9E8	3.3E8	1.6E7	1.8E6	6.1E5	-		3.0E4	1.3E4	6.1E3	3.4E3	1.6E3	9.2E2	3.1E2					
		11	49	14	6	11	-		2	2	2	2	2	2	1.5					
Fe_2O_3,Fe_3O_4(0.12) +		4.2E8	1.1E8	5.2E6	3.8E5	1.3E5	1.0E4		4.4E3	2.7E3	9.6E2	4.7E2	1.3E2	6.8E1	4.3E1					
		22	47	13	4	7	4		1	1	.9	.8	.5	.5	.6					
$Al_2O_3 \cdot 2H_2O$, Fe_2O_3,		5.0E8	4.4E8	3.2E7	1.8E6	3.0E5	4.2E4		2.6E4	2.4E4	1.0E4	9.4E3	4.2E3	3.0E3	1.3E3	8.4E2	6.1E2	2.3E2	2.5E2	
Fe_3O_4(0.41)		3	22	10	3	3	2		.7	1	1	2	3	2	2	4	5	10	29	
$Al_2O_3 \cdot 2H_2O$(0.26)		1.2E6	5.3E6	1.0E5	9.2E5	6.6E5	1.6E5		2.7E4	1.7E4	1.1E4	7.7E3	1.9E3	3.4E3	5.2E3	2.8E3	1.0E3			
		.02	.7	.1	3	11	20		2	3	3	4	2	8	2	24	26			
SiO_2(0.096)	4.0E8	2.7E8	7.1E8	3.6E8	1.6E8	4.4E7	1.4E6		Not above background											
		.3	5	16	28	40	10													
MgO(0.62)	(EAA saturated all stages $\leq$6)								1.5E5	1.5E5	1.3E5	1.0E5	8.0E4	3.6E4	2.6E4	1.2E4	7.3E3	2.8E3	*	*
									1	2	3	5	8	6	9	9	14	16		

+ Solution pressure reduced to 0.7 MPa (100 psi)

* MgO(0.62): ΔN=1.3E3, Vol%=16 (4<D<5), ΔN=5.7E2, Vol%=13 (5<D<6)

PARTICLE CONCENTRATIONS AND VOLUME PERCENTS

	.0075	.015	.03	.06	.1	.15	.3	.6	.3	.4	.5	.6	.8	1.0	1.2	1.5	2.0	3.0	4.0	8.0	10.0
MgO(0.054)	4.5E7	1.5E8	3.2E8	1.3E8	5.9E7	3.2E7	1.6E6		2.5E4	2.0E4	1.4E4	1.1E4	4.2E3	2.1E3	3.6E3	5.4E2	4.6E2	3.1E2			
		.2	4	9	16	46	19		.2	.3	.3	.5	.5	.4	1	.4	1	2			
MgO(0.49)	0	1.9E8	2.0E8	1.6E8	2.2E8	2.7E8	2.6E7		2.4E5	2.1E5	1.5E5	9.8E4	6.6E4	3.7E4	1.9E4	8.4E3	4.0E3	4.4E3			
	0	.03	.3	1	7	47	36		.2	.4	.4	.6	.8	.9	.9	.8	1	3			
ZnO(0.087)	2.1E8	4.1E8	8.5E8	2.0E8	3.0E7	7.1E6	3.6E5		1.9E4	1.3E4	1.2E4	6.5E3	6.1E3	2.8E3	1.6E3	8.8E2	3.1E2				
		1	19	28	17	20	8		.2	.4	.6	.6	1	1	1	1	1				
ZnO(0.94)	0	0	2.1E8	2.8E8	1.8E8	1.1E8	4.2E6		1.2E6	4.9E5	1.5E5	7.1E4	5.7E4	2.4E4	7.7E3	1.0E4	4.9E3	4.1E3			
	0	0	.8	6	16	50	16		2	1	.7	.7	1	.9	.5	2	2	5			
Fe_2O_3(0.071)**	3.4E7	4.8E8	8.3E8	1.7E8	3.2E7	1.0E7	2.5E5		5.9E3	1.6E3	8.8E2										
		1	20	24	18	31	6		.08	.05	.05										
Fe_2O_3(0.56)**	1.4E9	1.4E8	2.3E8	2.5E8	1.8E8	9.2E7	4.5E6		1.7E6	8.4E5	1.9E5	9.3E3									
	.1	.08	1	7	20	52	20		4	5	2	.2									
Fe_2O_3(6)**	1.5E10	3.7E9	2.1E9	3.5E8	3.0E8	4.4E8	2.3E7		saturated			9.0E6	8.9E6	5.7E6	3.4E6	7.7E5	3.6E5	1.2E4	7.2E2		
	.07	.1	.6	.6	2	15	6					-	-	16	18	9	11	1	.3		
Fe_xO_y(0.78)	3.6E8	1.2E8	2.8E8	1.2E7	1.4E6	1.8E6	2.3E5		1.5E5	1.0E5	4.7E4	2.6E4	1.2E4	5.0E3	2.5E3	1.0E3	2.3E2				
	.4	1	21	5	3	17	17		6	9	8	8	8	6	6	5	3				
Mn_3O_4(0.62)	3.7E8	6.5E8	2.8E8	2.1E7	4.3E6	4.1E6	5.5E5		2.4E5	2.5E5	2.0E5	1.0E5	3.9E4	8.8E3	1.9E3	9.1E2	2.6E2				
	.2	3	10	5	4	19	22		5	11	16	16	13	5	2	2	2				
Cr_2O_3(0.69)	5.0E7	2.3E8	5.7E8	1.5E8	3.4E7	1.5E7	9.7E5		1.6E5	1.3E5	5.7E4	4.9E4	3.2E4	1.0E4	8.0E3	1.1E4	4.6E3	3.8E3	3.6E3	5.7E2	
		.1	2	4	4	8	4		.4	.7	.5	1	1	1	1	3	4	9	36	23	
$Ca(OH)_2$(0.29)	3.0E8	8.7E8	3.2E8	2.0E7	3.8E6	4.7E6	4.8E5		9.3E4	1.4E5	1.0E5	8.5E4	8.3E4	5.1E4	4.1E4	2.7E4	1.7E4	8.9E3	*		
	.02	.4	1	.4	.3	2	2		.2	.5	.8	1	3	3	5	7	13	18			
Ele. Arc Aerosol(0.65)	1.1E8	9.0E8	4.8E8	2.8E7	3.7E6	1.6E6	1.4E5		1.2E5	6.1E4	2.3E4	7.5E3	4.4E3	1.1E3	9.2E2	3.9E2	1.5E2				
	.1	8	35	12	7	15	10		5	5	4	2	3	1	2	2	2				
Ele. Arc Aerosol(1.2)	1.8E8	7.7E8	3.5E8	1.2E7	4.6E6	2.6E6	2.5E5		1.9E5	1.2E5	5.1E4	1.6E4	6.0E3	2.1E3	1.3E3	1.5E2	5.4E2	1.5E2			
	.02	6	22	5	7	20	16		6	9	7	4	3	2	3	1	6	5			
$H_2SO_4 \cdot xH_2O$	2.5E9	4.0E7	1.8E7	nil																	
	63	8	29																		

* $Ca(OH)_2$(0.29): ΔN=7.5E3, Vol%=43(4<D<6)

** From $Fe(CO)_5$

TECHNICAL REPORT DATA *(Please read Instructions on the reverse before completing)*		
1. REPORT NO. EPA-600/2-77-132	2.	3. RECIPIENT'S ACCESSION NO.
4. TITLE AND SUBTITLE Generation of Fumes Simulating Particulate Air Pollutants		5. REPORT DATE July 1977 6. PERFORMING ORGANIZATION CODE
7. AUTHOR(S) J.W. Carroz, F.K. Odencrantz, and W.G. Finnegan		8. PERFORMING ORGANIZATION REPORT NO.
9. PERFORMING ORGANIZATION NAME AND ADDRESS Research Department Naval Weapons Center China Lake, California 93555		10. PROGRAM ELEMENT NO. 1AB012; ROAP 21ADM-031 11. CONTRACT/GRANT NO. EPA Interagency Agreement IAG-D5-0669
12. SPONSORING AGENCY NAME AND ADDRESS EPA, Office of Research and Development Industrial Environmental Research Laboratory Research Triangle Park, NC 27711		13. TYPE OF REPORT AND PERIOD COVERED Final; 1/75-4/77 14. SPONSORING AGENCY CODE EPA/600/13
15. SUPPLEMENTARY NOTES IERL-RTP project officer for this report is Dennis C. Drehmel, Mail Drop 61, 919/541-2925.		

16. ABSTRACT The report describes techniques developed for generating large quantities of reproducible, stable, inorganic, fine-particle aerosol fumes. These fumes simulated particulate air pollutants emitted from power generation, basic oxygen furnaces, electric arc furnaces, and zinc smelting. The aerosols were generated by burning flammable solutions containing appropriate soluble compounds (e.g., nitrates) of the desired elements. In the flame, these compounds decomposed to oxides. Particle size determinations were made using scanning and transmission electron microscope (SEM and TEM) photographic analysis of captured particles, as well as Whitby and Royco aerosol analyzers. The generated aerosol flow rates were as high as 42 cu m per min (148 cfm); particle loadings were as high as 16.8 g per cu m at STP. For most aerosols the aerosol particle and condensation nuclei concentrations were of the order of 10 to the 9th power particles per cu cm. The aerosol volume median diameters varied from less than 0.015 to greater than 4.7 micrometers and were primarily a function of the solution ingredients. Methods were developed to vary the SO2 concentration and particle resistivities.

17. KEY WORDS AND DOCUMENT ANALYSIS		
a. DESCRIPTORS	b. IDENTIFIERS/OPEN ENDED TERMS	c. COSATI Field/Group
Air Pollution, Dust Control, Measurement Particles, Combustion Products Flue Gases, Fly Ash, Oxides Inorganic Compounds, Fumes, Simulation Electric Power Generation Basic Converters, Oxygen Blown Converters Zinc Industry, Smelting	Air Pollution Control Stationary Sources Fine Particles Condensation Nuclei	13B -- 14B 21B -- -- -- 07B -- -- -- 10A 11F -- -- 13H
18. DISTRIBUTION STATEMENT Unlimited	19. SECURITY CLASS *(This Report)* Unclassified 20. SECURITY CLASS *(This page)* Unclassified	21. NO. OF PAGES 97 22. PRICE

EPA Form 2220-1 (9-73)